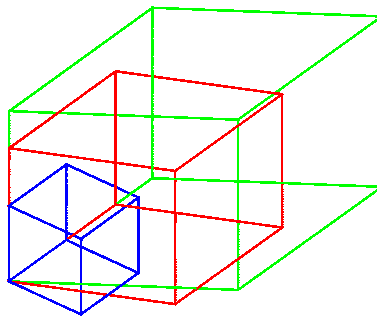ulm university universität
uulm

Institute of Theoretical Physics
Ulm University
Albert-Einstein-Allee 11
D-89069 Ulm
Germany

# Topics in Quantum Gravity

**Dissertation**
zur Erlangung des Doktorgrades Dr. rer. nat.
der Fakultät für Naturwissenschaften Universität Ulm

vorgelegt von

**Raphaël Lamon**
aus Caracas, Venezuela

**Ulm, 2010**

Erstgutachter: **Prof. Dr. Frank Steiner**
Zweitgutachter: **Prof. Dr. Wolfang Arendt**

Amtierender Dekan: **Prof. Dr. Joachim Ankerhold**

Tag der Promotion: **29. Juni 2010**

# Abstract

Quantum gravity is an attempt to unify general relativity with quantum mechanics which are the two highly successful fundamental theories of theoretical physics. The main difficulty in this unification arises from the fact that, while general relativity describes gravity as a macroscopic geometrical theory, quantum mechanics explains microscopic phenomena. As a further complication, not only do both theories describe different scales but also their philosophical ramifications and the mathematics used to describe them differ in a dramatic way. Consequently, one possible starting point of an attempt at a unification is quantum mechanics, i.e. particle physics, and try to incorporate gravitation. This pathway has been chosen by particle physicists which led to string theory. On the other hand, loop quantum gravity (LQG) chooses the other possibility, i.e. it takes the geometrical aspects of gravity seriously and quantizes geometry.

The first part of this thesis deals with a generalization of loop quantum cosmology (LQC) to toroidal topologies. LQC is a quantization of homogenous solutions of Einstein's field equations using tools from LQG. First the general concepts of closed topologies is introduced with special emphasis on Thurston's theorem and its consequences. It will be shown that new degrees of freedom called Teichmüller parameters come into play and their dynamics can be described by a Hamiltonian. Several numerical solutions for a toroidal universe will be presented and discussed. Following the guidlines of LQG this dynamics will be rewritten using the Ashtekar variables and numerical solutions will be shown. However, in order to find a suitable Hilbert space a canonical transformation must be performed. On the other hand this transformation makes the quantization of geometrical quantities less tractable such that two different ways will be presented. It will be shown that in both cases the spectrum of such geometrical operators depends on the initial value problem. Furthermore, we will succeed in solving the quantum Gauss constraint.

In the second part of the thesis we will introduce some aspects of phenomenological quantum gravity and their possible detectable signatures. The goal of phenomenological quantum gravity is to derive conclusions and make predictions from expected characteristics of a full theory of quantum gravity. One possibility is an energy-dependent speed of light arising from a quantized space such that the propagation time of two photons differs. However, the amount of these corrections is very small such that only cosmological distances can be considered. Gamma-ray bursts (GRB) are ideal candidates as they are short but very luminous bursts of gamma-rays taking place at distances billions of light-years away. We shall study GRBs detected by the European satellite INTEGRAL and develop a new method to analyze unbinned data. A $\chi^2$-test will provide a lower bound for quantum gravity corrections, which will be nevertheless well below the Planck mass. Then we shall study the sensibility of NASA's new satellite Fermi Gamma-ray Space Telescope and conclude that it is well suited to detect corrections. This prediction has just been confirmed when Fermi detected a very energetic photon emanating from GRB 090510 which highly constrains models with linear corrections to the speed of light. However, as will be shown at the end

of this thesis, more bursts are needed in order to definitely falsify such models.

# Zusammenfassung

Der Schwerpunkt der vorliegenden Arbeit liegt im Bereich der Quantengravitation. Das Ziel der Quantengravitation ist, die beiden grossen physikalischen Theorien des 20. Jahrhunderts, nämlich die Quantentheorie und die allgemeine Relativitätstheorie, zu vereinigen. Während die allgemeine Relativitätstheorie die Gravitation und somit die makroskopische Welt beschreibt, kümmert sich die Quantentheorie um Vorgänge im atomaren und subatomaren Bereich. Da sich beide Theorien sowohl mathematisch als auch physikalisch und philosophisch stark unterscheiden, ist es trotz der Vielfalt der Ansätze bis jetzt noch nicht gelungen, eine vollständige Quantengravitationstheorie zu finden. Zum Beispiel startet die String-Theorie mit der Annahme, dass die Quantenmechanik bzw. Teilchenphysik fundamentaler ist, und versucht, die Gravitationskraft in diesem Rahmen zu behandeln. Auf der anderen Seite liegt die Schleifenquantengravitation (loop quantum gravity), welche die Deutung der Gravitation als gekrümmte Geometrie ernst nimmt und diese zu quantisieren versucht.

Im ersten Teil dieser Arbeit wird die Schleifenquantenkosmologie auf toroidale Topologien erweitert. Die Schleifenquantenkosmologie ist eine Quantisierung homogener Lösungen der Einsteinschen Feldgleichungen mit den Methoden der Schleifenquantengravitation. Als Erstes wird das Konzept der geschlossenen Topologien allgemein behandelt, wobei speziell Gewicht auf das Theorem von Thurston und dessen Folgerungen gelegt wird. Dabei entstehen neue Freiheitsgrade, die sogenannten Teichmüller-Parameter, deren zeitliche Entwicklung mit Hilfe der Hamiltonschen Dynamik beschrieben wird. Numerische Resultate im Falle eines toroidalen Universums werden vorgelegt und besprochen. Diese Dynamik wird dann mit Hilfe der Ashtekar-Variablen neu formuliert und auch numerisch untersucht. Um den Torus à la Schleifenquantengravitation quantisieren und einen Hilbertraum finden zu können, wird eine kanonische Transformation der Ashtekar-Variablen durchgeführt. Dies erschwert allerdings die Quantisierung der geometrischen Operatoren, wobei zwei Quantisierungsmöglichkeiten beschrieben werden. Wie es sich herausstellen wird, ist das Spektrum dieser Operatoren vom Anfangswertproblem abhängig. Da die allgemeine Relativitätstheorie ein vollständig eingeschränktes System ist, müssen die Constraints gelöst bzw. der Kern der Constraint-Operatoren gefunden werden. Dies ist im Falle des Gauss-Constraint sowohl klassisch wie auch quantenmechanisch gelungen, allerdings konnte der Kern des Hamiltonschen Operators nicht gefunden werden.

Der zweite Teil der Arbeit beschäftigt sich mit der phänomenologischen Quantengravitation und deren möglichen experimentellen Beobachtungen. Die phänomenologische Quantengravitation vertritt die Ansicht, dass mögliche Folgerungen von erwarteten Eigenschaften des Raums untersucht werden können, obwohl noch keine vollständige Quantengravitation verfügbar ist. Zum Beispiel könnte eine quantisierte Raumzeit eine energieabhängige Lichtgeschwindigkeit verursachen, so dass Korrekturen zur Flugzeit von Photonen eingerechnet werden müssten. Da diese Korrekturen aber sehr klein sind, werden nur kosmo-logische Distanzen in Betracht gezogen. Dank der kosmologischen Entfernung der Gamma-ray Bursts

(GRB) sind diese die besten Kandidaten, um Abweichungen in den Flugzeiten zu messen. Ein GRB ist ein kurzzeitiger, aber gewaltiger Energieausbruch im Universum, der eine grosse Menge an Gammastrahlen produziert. Als Erstes werden Bursts untersucht, die vom europäischen Satelliten INTEGRAL aufgespürt wurden, und eine neue Methode eingeführt, um ungebinnte Daten zu analysieren. Mit Hilfe eines $\chi^2$-Tests konnte eine untere Grenze für diese Korrekturen gegeben werden, die allerdings weit unterhalb der Planck-Energie liegt. Dann wird die Sensibilität des neuen NASA Satelliten Fermi Gamma-ray Space Telescope untersucht und festgestellt, dass dieser in der Lage ist, eindeutige Aussagen über lineare Korrekturen zur Lichtgeschwindigkeit zu machen. Dies wurde auch vor Kurzem bestätigt, als allein schon ein sehr energiereiches Photon genügte, um solche Modelle in Schwierigkeiten zu bringen. Wie aber aus dieser Doktorarbeit ersichtlich wird, müssen allerdings mehrere Bursts aufgespürt werden, um diese Modelle definitiv zu falsifizieren.

# Contents

# Introduction

Two major advances in theoretical physics have revolutionized our understanding of Nature. On the one hand the devolpment of quantum mechanics began over a century ago by Max Planck and was put on a solid mathematical foundation in 1931 by John von Neumann. This theory is extraordinarily successful in describing all microscopic phenomena such as atomic spectra. On the other hand the theory of general relativity was published by Albert Einstein in 1915 as a unification of Newton's law of universal gravitation and Einstein's special relativity theory. The predictions of this theory range from the perihelion advance of Mercury to the existence of black holes and have been tested and confirmed to an incredible precision. But general relativity is more than just a theory of gravity or, as particle physicists would say, a spin-2 interaction theory as it revolutionized the concept of space-time and devoided the meaning of coordinates. The underlying principle (or symmetry) is general covariance which states that the form of physical laws should be invariant under arbitrary differentiable coordinate transformations.

In sum we have two theories which are very successful in their respective domains. This shouldn't be much of a problem as their domains do not overlap, even in the most powerful particle accelerators. However, when considering domains where both quantum mechanics and gravity play an important role such as black holes or the big bang, both theories loose their predictability and hence their validity. As such they have to be replaced by a more fundamental theory which reduces to quantum mechanics in the limit of weak gravity and to general relativity in the limit of large actions. This theory is called quantum gravity and is the 'holy grain' of modern theoretical physics. One of the main difficulties in finding it is the fundamental and conceptual difference of quantum mechanics and Einstein's gravitation theory. While in quantum mechanics space-time is a fixed entity on top of which particles live and interact, general relativity is a theory of space-time itself as described by Einstein's field equations.

The very fact that a unification of two very different theories is sought has led to two approaches to quantizing gravity. On the one hand the viewpoint of string theory is that we should build up on the highly successful unification process that has led to the Standard Model of particle physics and try to incorporate gravity as a spin-2 particle living on a fixed background. On the other hand loop quantum gravity (LQG) takes the concepts of general relativity seriously and quantizes gravity in a background independent way. However, since both approaches are still incomplete a third possibility has been developed, called phenomenological quantum gravity, which consists in deriving consequences of expected features of quantum gravity.

One of the jewels of LQG is loop quantum cosmology (LQC) which is a quantization of homogeneous solutions of Einstein's field equations using tools from LQG. As such, it is not the cosmological sector of the full theory but only an application of it. One of the most striking results of LQC is the resolution of gravitational singularities. For example the big bang singularity is replaced by a 'big bounce' which explains the formation of our

universe as a result of a previously collapsing universe. Moreover LQC provides naturally a possible mechanism for cosmic inflation or resolves the Schwarzschild singularities.

This thesis is divided into two parts. The first one generalizes the standard open and flat topology usually used in loop quantum gravity to a toroidal topology. We shall first introduce the general tools such as Hamiltonian general relativity and mathematical methods of differential geometry and topology. We shall also explain the differences arising from a closed topology by explaining the main constructions of LQC on a Euclidean space. However, we would like to stress that we won't give a self-contained introduction to the mathematics behind this construction or to LQC but rather refer to the available literature for further details. The second part deals with empirical signatures of one subtopic of phenomenological quantum gravity which is an energy-dependent speed of light. We shall study a possible Lorentz violation by using bright flashes at cosmological distances known as gamma-ray bursts.

# Part I

# Loop Quantum Cosmology

# Chapter 1

# Introducing General Relativity

Since there are many good books and reviews on both general relativity [97, 108] and loop quantum gravity [12, 91, 104] we will only give a short introduction. Furthermore mathematical tools used in this chapter such as differential geometry and fiber bundle theory can be found in [74, 75].

## 1.1   Canonical General Relativity

Let us consider a four-dimensional, Lorentzian manifold $(M, g_{\mu\nu})$, where the metric tensor field $g_{\mu\nu}$ has the Lorentzian signature $(-, +, +, +)$ and $\mu, \nu = 0, \ldots, 4$. The propagation of the metric is described by the Einstein-Hilbert action given by $(c \equiv 1)$

$$S_{\text{E--H}}[g] = \frac{1}{2\kappa} \int_M *R[g], \tag{1.1}$$

where $R$ is the Ricci scalar (see e.g. [97]), $\kappa = 8\pi G$ the gravitational constant and $* : \Lambda^p(M) \to \Lambda^{4-p}(M)$ the Hodge star operator defined by

$$*(dx^{\mu_1} \wedge \ldots \wedge dx^{\mu_p}) \mapsto \frac{\sqrt{|g|}}{(4-p)!} \epsilon^{\mu_1 \ldots \mu_p}{}_{\nu_{p+1} \ldots \nu_4} dx^{\nu_{p+1}} \wedge \ldots \wedge dx^{\nu_4},$$

where $\Lambda^p(M)$ is the space of $p$-forms (see e.g. [74, 97] for details) and $\epsilon_{\mu_1 \ldots \mu_4}$ the totally anti-symmetric tensor. In order to derive a canonical form of the action (1.1) we make the assumption that $M$ has the topology $M \cong \mathbb{R} \times \Sigma$, where $\Sigma$ is a three-dimensional manifold of arbitrary topology with metric $h_{ab}$, $a, b = 1, \ldots, 3$. Thus, $M$ admits a foliation into hypersurfaces $\Sigma_t$, for all $t \in \mathbb{R}$ (see Fig. 1.1). The standard parametrization of a vector field $T^\mu$ is given by

$$T^\mu(x, t) = N(x, t)n^\mu(x, t) + N^\mu(x, t),$$

where $x$ are local coordinates on $\Sigma$, $n^\mu$ is a unit vector normal to $\Sigma_t$, $N$ the lapse and $N^\mu$ the shift vector. The metric can then be recast into the form

$$ds^2 = (-N^2 + h_{ab}N^aN^b)dt^2 + 2h_{ab}N^b dt dx^a + h_{ab}dx^a dx^b.$$

In terms of Hamiltonian mechanics the metric $h_{ab}$ represents the configuration variables. The conjugate momenta are given by the extrinsic curvature $K_{ab}$ which represents the changes in the spatial slice and is given by

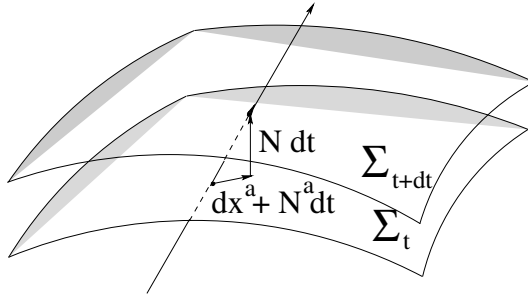$$K_{ab} = \frac{1}{2N}(\dot{h}_{ab} - (\mathcal{L}_{\vec{N}}h)_{ab}), \tag{1.2}$$

Figure 1.1: Foliation of the manifold $M$ into spacelike hypersurface. $N^a$ is the shift vector and $N$ the lapse.

where the dot is the time derivative and $\mathcal{L}_{\vec{N}}$ the Lie derivative along $\vec{N}$ [74]:

$$(\mathcal{L}_{\vec{N}} h)_{ab} = N^c \partial_c h_{ab} + (\partial_a N^c) h_{cb} + (\partial_b N^c) h_{ac}.$$

A Legendre transform of the Einstein-Hilbert action w.r.t these canonical variables yields the ADM action [7]. However, due to the lack of mathematical understanding of the space of metrics or equivalently of the space of extrinsic curvature tensors alternative variables had to be found. This was done by Ashtekar [8, 9] using a triad formulation.

### 1.1.1 Non-coordinate Bases

In the coordinate basis the tangent space $T_p\Sigma$ of $\Sigma$ at the point $p \in \Sigma$ is spanned by $\partial_a$ and the cotangent space $T_p^*\Sigma$ by $dx^a$. However it is possible to find an alternative choice by considering linear conbinations such that

$$e_i := e_i^a \partial_a, \quad \{e_i^a\} \in GL(3, \mathbb{R}) \quad \text{and} \quad \det e_i^a > 0.$$

The coefficients $e_i^a$ are called triads or dreibeins where $a = 1, \cdots, 3$ are space tangent indices and $i = 1, \cdots, 3$ 'internal' indices in $\mathbb{R}^3$. We further require that the basis $\{e_i\}$ be orthonormal w.r.t. $h$, i.e.

$$h_{ab} e_i^a e_j^b = \delta_{ij}.$$

All the spatial information is contained in these triads and the inverse metric is given by

$$h^{ab} = \delta^{ij} e_i^a e_j^b.$$

It is clear from the last equation that the triads can be rotated without changing the metric,

$$e_i^a \to e_i'^a = O_i^j e_j^a, \quad (O)_{ij} \in SO(3)$$

leaves the metric invariant. Moreover it is invariant under a reflection, i.e. a change of the orientation of the triad. Classically this does not pose a problem because both sectors are separated by a degenerate configuration where the metric is singular. Since the classical evolution breaks down at such points these sectors cannot be connected.

In the sequel we shall use the group $SU(2)$ instead of $SO(3)$. The reason is that the adjoint representation of $SU(2)$ spanned by $(T_i)_{kl} = \epsilon_{ijk}$, where $\epsilon_{ijk}$ is the structure constants of $SU(2)$, corresponds to the fundamental representation of $SO(3)$. In other words there is an isomorphism $\mathbb{R}^3 \to su(2); v^i \to v^i \tau_i$, where $\tau_i$ are the generators of $SU(2)$[1]. We can thus view $e_a^i$ as an $su(2)$-valued one-form via $e = e_a^i \tau_i dx^a$.

---

[1] We use the convention that the generators of the Lie algebra $su(2)$ are given by $\tau_j = \frac{1}{2i}\sigma_j$, where $\sigma_j$ are the Pauli matrices such that $\tau_i \tau_j = \frac{1}{2}\epsilon_{ijk}\tau_k - \frac{1}{4}\delta_{ij}$.

## 1.2 Ashtekar Variables

In this section we write general relativity in terms of Ashtekar variables. We first need this definition:

**Definition 1.** *Let $(M, g)$ be a Riemann manifold and $T_p(M)_s^r$ the set of tensors of rank $(r, s)$ defined on the tangential space $T_p(M)$ of $M$ at the point $p \in M$. An element $(\sqrt{|\det(g)|})^w t \in T_p(M)_s^r$ is called a tensor field of density weight $w \in \mathbb{R}$.*

The Ashtekar representation uses a triad with density weight $+1$ which takes values in the dual of the Lie algebra $su(2)$:

$$E_i^a = \frac{e_i^a}{|\det e_j^b|}$$

related to the spatial metric by

$$\eta^{ij} E_i^a E_j^b = h^{ab} \det h, \tag{1.3}$$

where $\eta_{ij}$ is the three-dimensional Minkowski metric. The densitized triad has the same properties concerning gauge rotations and its orientation as the triad $e_i^a$. It is canonically conjugated to the extrinsic curvature coefficients

$$K_a^i := K_{ab} e_i^b,$$

where $K_{ab}$ is given by Eq. (1.2), such that[2]

$$\{K_a^i(x), E_j^b(y)\} = \kappa \delta_a^b \delta_j^i \delta(x, y).$$

The Ashtekar connection $A = A_a^i \tau_i dx^a$ is a one-form, which takes values in $su(2)$, given by

$$A_a^i = \Gamma_a^i + \gamma K_a^i, \tag{1.4}$$

where $\gamma > 0$ is the Barbero-Immirzi parameter [50, 54] and the spin connection defined by [104]

$$\Gamma_a^i = -\epsilon^{ijk} e_j^b (\partial_{[a} e_{b]}^k + \frac{1}{2} e_k^c e_a^l \partial_{[c} e_{b]}^l), \tag{1.5}$$

where the square brackets stand for $\partial_{[a} e_{b]} := \frac{1}{2}(\partial_a e_b - \partial_b e_a)$. As explicitly shown in, e.g., [104], the derivation of the above expression starts with the metric compatibility condition $D_a h_{bc} = 0$, such that

$$D_a E_j^a = \partial_a E_j^a + \epsilon_{jkl} \Gamma_a^k E_l^a = 0.$$

The Ashtekar connection can be seen as (the pull-back to $\Sigma$ by local sections of) a connection on an $SU(2)$ fiber bundle. If $\Sigma = \mathbb{R}^3$ or $\Sigma = \mathbb{T}^3$ the bundle $P$ is even trivial such that $P = \Sigma \times SU(2)$ globally. As such it transforms under a local gauge transformation $g : \Sigma \to SU(2)$ (i.e. transformations between two sections of the principal bundle $P(M, SU(2))$) in the following way:

$$A \mapsto A' = g^{-1} A g + g^{-1} dg, \tag{1.6}$$

---

[2]Loosely speaking, we can define the Poisson brackets as

$$\{f(x), g(y)\} = \kappa \sum_{k,c=1}^{3} \int_M \left( \frac{\delta f(x)}{\delta K_c^k(z)} \frac{\delta g(y)}{\delta E_k^c(z)} - \frac{\delta g(y)}{\delta K_c^k(z)} \frac{\delta f(x)}{\delta E_k^c(z)} \right) d^3 z.$$

For a mathematically rigorous formulation see [104].

where $d : \Lambda^p(M) \to \Lambda^{p+1}(M)$ is the exterior derivative whose action on a $p$-form is defined by

$$d\omega = d\left(\frac{1}{p!}\omega_{\mu_1\dots\mu_p}dx^{\mu_1}\wedge\dots\wedge dx^{\mu_p}\right) = \frac{1}{p!}(\partial_\nu\omega_{\mu_1\dots\mu_p})dx^\nu\wedge dx^{\mu_1}\wedge\dots\wedge dx^{\mu_p}$$

with the property $d^2 = 0$. On the other hand the densitized triad transforms according to

$$E \mapsto E' = g^{-1}Eg. \tag{1.7}$$

The new phase space is spanned by the mutually conjugated variables $A_a^i$ and $E_i^a$ such that

$$\{A_a^i(x), E_j^b(y)\} = \kappa\gamma\delta_a^b\delta_j^i\delta(x,y),$$

which is similar to that of a Yang-Mills theory with $SU(2)$ as structure group[3]. The Ashtekar representation can be used to perform the Legendre transformation of the Einstein-Hilbert action. This lengthy calculation can be found in [104] and the result is a fully constrained system given by

$$S = \frac{1}{2\kappa}\int_{\mathbb{R}}dt\int_\Sigma d^3x\left(2\dot{A}_a^i E_i^a - [\Lambda^j G_j + N^a H_a + N\mathcal{H}]\right), \tag{1.8}$$

where $G_j$ is the Gauss constraint, $H_a$ the diffeomorphism (or vector) constraint, $\mathcal{H}$ the Hamiltonian and $\Lambda^j$, $N^a$, $N$ are Lagrange multipliers. The Gauss constraint is given by the covariant derivative of $E_i^a$ w.r.t. the connection $A_a^i$, i.e.

$$G_i = \mathcal{D}_a E_i^a = \partial_a E_i^a + \epsilon_{ijk}A_a^j E_k^a \tag{1.9}$$

stems from the fact that gravity has to be invariant under $SO(3)$-rotations of the triad $E_i^a \to O_i^j E_j^a$, where $O_i^j \in SO(3)$. The diffeomorphism constraint (modulo Gauss constraint) originates from the requirement of independence from any spatial coordinate system or background and is given by

$$H_a = F_{ab}^i E_i^b, \tag{1.10}$$

the curvature two-form $F := dA + A \wedge A$ of the connection $A$ is given by

$$F_{ab}^i = \partial_a A_b^i - \partial_b A_a^i + \epsilon_{jk}^i A_a^j A_b^k. \tag{1.11}$$

Finally the Hamiltonian constraint tells us that gravity must be invariant under a reparametrization of the coordinate time and is given by

$$\mathcal{H} = e^{-1}\left(\epsilon_{ijk}F_{ab}^i E^{aj} E^{bk} - 2(1+\gamma^2)K_{[a}^i K_{b]}^j E_i^a E_j^b\right), \tag{1.12}$$

where $e = \text{sgn}(\det E)\sqrt{|\det E|}$. The components of the extrinsic curvature in Eq. (1.12) are functions of the Ashtekar connection $A_a^i$ and the densitized triad $E_i^a$ because of the dependence of the spin connection $\Gamma_a^i$ on the triad $e_i^a$ (see Eq. (1.5)).

---

[3]One of the main difference is the dynamics. For a Yang-Mills theory there is a true dynamics determined by Eq. (2.1) whereas in the case of general relativity the system is fully constrained with no dynamics.

### 1.2.1 Hamiltonian Constraint for Flat Topologies

In the case where the three-dimensional spatial manifold is flat the spin connection $\Gamma_a^i$ vanishes such that $K_a^i = \gamma^{-1} A_a^i$. Moreover the curvature (1.11) of the Ashtekar connection simplifies to

$$F_{ab}^i = \epsilon_{jk}^i A_a^j A_b^k.$$

The first term in Eq. (1.12) can be rewritten as

$$\epsilon_{ijk} F_{ab}^i E^{aj} E^{bk} = \epsilon_{ijk} \epsilon_{ilm} A_a^l A_b^m E^{aj} E^{bk} = (\delta_{jl}\delta_{km} - \delta_{jm}\delta_{lk}) A_a^l A_b^m E^{aj} E^{bk} = 2 A_{[a}^j A_{b]}^k E_j^a E_k^b.$$

In the flat case the second term in Eq. (1.12) is given by

$$-2(1+\gamma^2) K_{[a}^i K_{b]}^j E_i^a E_j^b = -2(1+\gamma^{-2}) A_{[a}^i A_{b]}^j E_i^a E_j^b$$

such that

$$\mathcal{H} = -\gamma^{-2} \epsilon_{ijk} F_{ab}^i \frac{E^{aj} E^{bk}}{e}. \tag{1.13}$$

In the next few chapters we shall extensively use this last expression as we will consider only topologies with a flat geometry.

# Chapter 2

# Toroidal Cosmology in Ashtekar Variables

The Einstein field equations are local equations in the sense that they only describe the local geometry of the spacetime. For example the Robertson-Walker metric explicitly contains the parameter $k$ which gives an account of the intrinsic spatial curvature. Using the Friedmann equations this parameter can be determined experimentally since it is directly related to the density parameter $\Omega_{\text{tot}}$ and the Hubble parameter $h$. Recent measurements of the energy density of the universe tend to slightly favor a positively curved universe [61], yet a flat curvature lies within the 1-$\sigma$ range. The simplest assumption is that the spatial topology of the universe is just $\mathbb{R}^3$ which is the assumption of the $\Lambda$CDM model. Nevertheless in the mathematical literature it is well known that a flat space does not mean that its topology is necessarily $\mathbb{R}^3$, in fact there are 18 possible topologies with a flat space. Since the Einstein field equations are not sensitive to topology every possibility has to be considered as a possible candidate for the global geometry of our universe until it is ruled out by experiment. In order to do so we first note that the spectrum of the Laplace operator sensitively depends on the topology. For example, the eigenvalue problem for $\triangle$ on $\mathbb{T}^3$ is given by $(\triangle + E_{\vec{n}})\Psi_{\vec{n}} = 0$, $\vec{n} \in \mathbb{Z}^3$, and on $S^3$ by $\triangle\Psi_{\beta,l,m} = (\beta^2 - 1)\Psi_{\beta,l,m}$, where $\beta \in \mathbb{N}$, $0 \leq l \leq \beta - 1$ and $|m| \leq l$. The implication of a solution of the form $\Psi_{\vec{n}}$ is the existence of a wave function $\Psi_{\vec{n}}$ with a maximal length corresponding to, e.g., the length of the edges of the torus. Since the departure from a continuous solution is biggest for large wavelengths we have to look for large-scale structures of the universe in order to distinguish between cosmic topologies. The best way to do so is to measure the inhomogeneities of the cosmic microwave background (CMB), expand these in multipole moments and compare the low multipoles with the predictions from theory. It can be shown that in certain closed topologies a suppression in the power spectrum of the low multipoles is expected because of the existence of a largest wavelength. Since such a suppression is present in the CMB several studies compared the theoretical predictions for various topologies with the data. While most analyzed topologies can already be ruled out, three of them describe the data even better than the infinite $\Lambda$CDM model, namely the torus [16, 17, 20], the dodecahedron [19, 35] and the binary octahedron [18] (see also references therein). While the last two topologies are spherical the torus is the simplest model of a closed flat topology.

However, we know that standard cosmology cannot be the final answer as its predictability breaks down at the big bang. A quantization of the Friedmann equations à la Wheeler-DeWitt does not improve this behavior either. This situation has changed thanks to a new model called loop quantum cosmology (LQC) developed over the last few years which removes the initial singularity. LQC [11, 13, 14, 25, 26, 27, 28, 29, 30] is the approach

motivated by loop quantum gravity (LQG) [12, 91, 104] to the quantization of symmetric cosmological models. The usual procedure is to reduce the classical phase space of the full theory to a phase space with a finite number of degrees of freedom. The quantization of these reduced models uses the tools of the LQG and is therefore called LQC but it does not correspond to the cosmological sector of LQG. The results of LQC not only provide new insights into the quantum structure of spacetime near the big bang singularity but also remove this singularity by extending the time evolution to negative times.

In summary, on the one hand we have hints from observation that our universe may have a closed topology, on the other hand we have a very successful loop quantization of various cosmologies. Thus, starting from these two motivations, we would like to study LQC with a torus topology. But contrary to the works on the CMB we don't want to restrict the analysis to a cubical torus. To do so we construct a torus using Thurston's theorem and find that the most general torus has six degrees of freedom which consist of e.g. three lengths and three angles. We will study its dynamics by numerically solving the Hamiltonian coupled to a scalar field. After rewriting this Hamiltonian in terms of Ashtekar variables we will see that the quantization of such a torus leads to a product between the standard Hilbert spaces of LQC and the Hilbert spaces over the circle. Moreover, we will find two ways to quantize the components of the triad and show that both (generalized) eigenfunctions are not normalizable in this Hilbert space.

As a side remark we would like to point out that the consequences of putting a non-abelian gauge theory into a box with periodic boundary conditions have been studied in e.g. [99]. The motivation behind this idea is an attempt to explain the quark confinement in QCD without explicitly breaking gauge invariance. To simplify the analysis the $su(N)$-valued gauge field is chosen to be pure gauge, i.e. $A = U^{-1}dU$ with $U \in SU(N)$, such that the holonomy around a closed curve $C$ only depends on the topological property of $C$. Since general relativity written in terms of Ashtekar variables is also a (constrained) Yang-Mills theory it may be tentalizing to use the methods developed for QCD in a box to LQC of a torus universe. However, we will derive an Ashtekar connection for the homogeneous torus which is not pure gauge so that the holonomies along $C$ also depend on the length of $C$. This may not be surprising in view of the fact that the Hilbert space of LQC on $\mathbb{R}^3$ is spanned by almost periodic functions with an arbitrary length parameter $\mu$.

## 2.1 The Role of Topology

As an illustrative example let us consider electrodynamics on the Minkowski space $\mathbb{R}^{3+1}$ with metric $\eta = \text{diag}(-1, 1, 1, 1)$, the details of this section can be found in [21, 74]. The corresponding principal bundle is given by $P(\mathbb{R}^{3+1}, U(1))$, where $U(1)$ is the gauge group of electromagnetism. Since the base space is contractible to a point the bundle $P$ is trivial, i.e. $P$ has a section. We are thus able to find a global connection

$$\mathcal{A} = \mathcal{A}_\mu dx^\mu \in \Lambda^1(\mathbb{R}^{3+1}) \otimes u(1),$$

usually called the gauge potential, which differs from the usual vector potential $A$ by the Lie algebra factor $i$, i.e. $\mathcal{A}_\mu = iA_\mu$. The exterior derivative of this one-form defines a two-form $\mathcal{F} := d\mathcal{A} = \frac{1}{2}\mathcal{F}_{\mu\nu}dx^\mu \wedge dx^\nu$ called the field strength satisfying the Bianchi identity $d\mathcal{F} = 0$. This is ensured by Poincaré's lemma because the four-dimensional Minkowski spacetime is contractible to a point, meaning that we are able to find a vector potential $\mathcal{A}$ such that $\mathcal{F} = d\mathcal{A}$ is exact, which also implies that $d\mathcal{F} = d^2\mathcal{A} = 0$ because $d^2 = 0$. The

Maxwell action is then given by

$$S_M[\mathcal{A}] = -\frac{1}{4} \int_{\mathbb{R}^{3+1}} \mathcal{F} \wedge *\mathcal{F}. \tag{2.1}$$

A variation of this action w.r.t $\mathcal{A}$ yields the vacuum Maxwell equations

$$d\mathcal{F} = 0 \quad \text{and} \quad d*\mathcal{F} = 0.$$

We can identify the components of $\mathcal{F}_{\mu\nu}$ with the electric field $\mathbf{E}$ and the magnetic field $\mathbf{B}$ as

$$E_i = -i\mathcal{F}_{i0}, \quad \text{and} \quad B_i = -\frac{i}{2}\epsilon_{ijk}\mathcal{F}_{jk}.$$

We could now ask ourself what happens if we remove a single point from $\mathbb{R}^3$, i.e. we would like to know to what extent the theory of electromagnetism changes on $\mathbb{R}^3 - \{0\}$. We could argue naively that the only thing that changes would be that the field strength $\mathcal{F}$ is only defined on $\mathbb{R}^3 - \{0\}$ (assuming for simplicity that everything is time independent). From calculus we know the integral of a function over an interval does not change if we remove single points. The implication would be that the Maxwell action $S_M[\mathcal{A}]$ would not change, leading to the same Maxwell equations. However this consideration is erroneous because removing a point from the base manifold changes the topology. In short, there is *no* scalar potential and *no* vector potential on $\mathbb{R}^3 - \{0\}$. How is this possible? After all, only a single point was removed.

The construction derived at the beginning of this subsection relied heavily on the contractibility of the base manifold $\mathbb{R}^{3+1}$. This is not the case anymore when the origin has been removed since $\mathbb{R}^3 - \{0\}$ is of the same homotopy type as the two-sphere $S^2$ [74]. The relevant bundle is now $P(S^2, U(1))$ which is not trivial because $S^2$ is not contractible. Two charts are needed to cover $S^2$:

$$U_N := \{(\theta, \phi) | 0 < \theta < \frac{1}{2}\pi + \epsilon\} \quad \text{and} \quad U_S := \{(\theta, \phi) | \frac{1}{2} - \epsilon < \theta < \pi\},$$

leading to two local gauge potentials $\mathcal{A}_N$ and $\mathcal{A}_S$. On $U_N \cap U_S$ they are equal up to a gauge, i.e.

$$\mathcal{A}_N = \mathcal{A}_S + id\varphi,$$

where $\varphi : S^1 \to \mathbb{R}$ is a gauge transformation. The technical reason is that the transition functions on $U_N \cap U_S$ define a map from $S^1$ to $U(1)$ which is classified by the fundamental group $\pi_1(U(1)) = \mathbb{Z}$. Using Stoke's theorem the total magnetic flux $\Phi$ is given by

$$\Phi = \int_{U_N} d\mathcal{A}_N + \int_{U_S} d\mathcal{A}_S = \int_{S^1} \mathcal{A}_N - \int_{S^1} \mathcal{A}_S = 4\pi g,$$

where $g$ is the strength of the monopole. Technically the integer $2g$ is the homotopy class of the bundle $P$. Further details on the Dirac monopole can be found in [21, 74, 75].

The conclusion we reach is that gauge theories are very sensible to the topology of the base manifold. Passing from $\mathbb{R}^3$ to $\mathbb{R}^3 - \{0\}$ changes electrodynamics in a dramatic way. Since gravity in Ashtekar variables is closely related to an $SU(2)$ Yang-Mills theory we have to be careful when deriving the equations of loop quantum cosmology in a torus.

## 2.2 Compact Homogeneous Spaces

The purpose of this chapter is to introduce the concepts of compact three-dimensional topologies which heavily relies on Thurston's geometrization conjecture (or theorem) which was proposed in 1982 by William Thurston [105]. He was only able to give a partial proof for a subclass of manifolds, a sketch of the proof of the full conjecture came in 2003 from Grigori Perelman using the Ricci flow [82, 83, 84]. Despite the fact that there exist eight Thurston geometries we shall primarily concentrate on the Euclidean geometry, further details can be found in [106].

### 2.2.1 Mathematical Preliminaries

Let $\tilde{\Sigma}$ be a simply connected smooth manifold and $S$ a Lie group acting on $\tilde{\Sigma}$ by means of a map $\sigma : \tilde{\Sigma} \times S \to \tilde{\Sigma}$. Furthermore this action is **transitive** if $\forall\, x, y \in \tilde{\Sigma}\ \exists\, g \in S$ such that $\sigma(x, g) = y$ and **free** if $\sigma(p, g) = p$ for some $p \in \tilde{\Sigma}$, then $g$ must be the unit element $e$ of $S$. The simplest example is the action of the translation group $T^3$ which acts freely and transitively on $\mathbb{R}^3$.

The **isotropy group** of $x \in \tilde{\Sigma}$ is a subgroup of $S$ defined by

$$S_x = \{g \in S | \sigma(x, g) = x\},$$

sometimes also called the stabilizer. By definition, whenever $\sigma$ acts freely the isotropy group contains only the identity.

**Definition 2.** *A geometry is a pair $(\tilde{\Sigma}, S)$ where $\tilde{\Sigma}$ is a simply connected manifold and $S$ a Lie group acting transitively on $\tilde{\Sigma}$ with compact isotropy subgroup. A geometry $(\tilde{\Sigma}, S')$ is a subgeometry of $(\tilde{\Sigma}, S)$ if $S'$ is a subgroup of $S$. A geometry $(\tilde{\Sigma}, S)$ is called maximal if it is not a subgeometry of any geometry and minimal if it does not have any subgeometry.*

Thurston further requires that there should exist at least one compact manifold modeled on $(\tilde{\Sigma}, S)$ [106]. A metric on a manifold $\tilde{\Sigma}$ is **homogeneous** if the isometry group acts transitively on $\tilde{\Sigma}$ and **locally homogeneous** if $\forall p, q \in \tilde{\Sigma}$ there exist neighborhoods $U, V$ and an isometry $(U, p) \to (V, q)$.

### 2.2.2 Relation between a compact manifold and its covering

In this subsection we would like to elucidate the construction of homogeneous manifolds. Let $(\tilde{\Sigma}, \tilde{g})$ be a homogeneous Riemann manifold, $(\Sigma, g)$ a compact homogeneous Riemann manifold, $\mathrm{Isom}^+\tilde{\Sigma}$ the orientation preserving isometry group of $\tilde{\Sigma}$ and $\Gamma$ a subgroup of $\mathrm{Isom}^+\tilde{\Sigma}$. We would like to know how to construct a homogeneous covering from $\Sigma$ and a compact homogeneous manifold from $\tilde{\Sigma}$. In order to do that we will need a map

$$\pi : \tilde{\Sigma} \to \Sigma \tag{2.2}$$

called the covering map.

We are now ready to quote the theorem of Thurston:

**Theorem 1.** *Any maximal, simply connected three-dimensional geometry $(\tilde{\Sigma}, S)$ which admits a compact quotient $\Sigma$ is equivalent to the geometry $(X, \mathrm{Isom} X)$ where $X$ is one of $\mathbb{E}^3$, $\mathbb{H}^3$, $S^3$, $S^2 \times \mathbb{R}$, $\mathbb{H}^2 \times \mathbb{R}$, $\widetilde{SL}(2, \mathbb{R})$ Nil or Sol.*

$\tilde{\Sigma}$ homogeneous Riemann manifold $\qquad\qquad$ $\Sigma$ compact homogeneous Riemann manifold

$\downarrow$ $\qquad\qquad\qquad\qquad\qquad\qquad\qquad\qquad$ $\downarrow$ $\Sigma$ arcwise connected

$\Sigma := \tilde{\Sigma}/\Gamma$ locally homogeneous $\qquad\qquad$ $\Sigma$ has unique covering $\tilde{\Sigma}$ (up to diffeos)

$\qquad\downarrow$ $\Gamma$ discrete subgroup of $\mathrm{Isom}^+\tilde{\Sigma}$ $\qquad\qquad$ $\downarrow$ $\pi : \tilde{\Sigma} \to \Sigma$

$\Sigma$ Hausdorff $\qquad\qquad\qquad\qquad\qquad\qquad\qquad$ $\tilde{g} := \pi_* g$ locally homogeneous

$\qquad\downarrow$ $\Gamma$ acts freely on $\tilde{\Sigma}$ $\qquad\qquad\qquad\qquad$ $\downarrow$ Thm. of Singer[96]

$(\Sigma, g)$ compact homogeneous Riemann manifold $\quad$ $(\tilde{\Sigma}, \tilde{g})$ homogeneous Riemann manifold
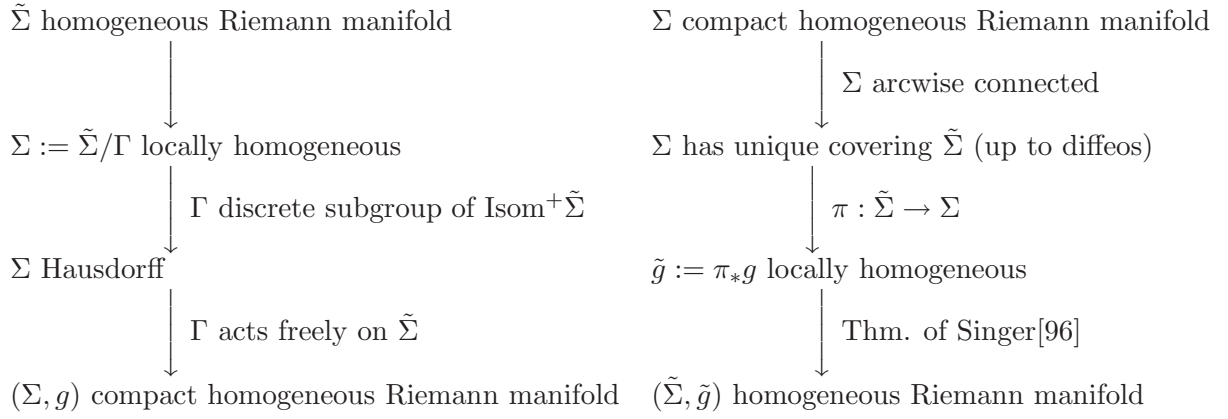
$\mathbb{E}^3$ is the three-dimensional flat Riemannian manifold, $S^2$ resp. $S^3$ the unit two-dimensional resp. three-dimensional sphere and $\mathbb{H}^2$ resp. $\mathbb{H}^3$ the two-dimensional resp. three-dimensional hyperbolic manifold. Nil is the group of matrices of the form

$$\begin{pmatrix} 1 & x & z \\ 0 & 1 & y \\ 0 & 0 & 1 \end{pmatrix},$$

Sol the three-dimensional group with the following multiplication rule:

$$\begin{pmatrix} a \\ b \\ c \end{pmatrix} \begin{pmatrix} x \\ y \\ z \end{pmatrix} = \begin{pmatrix} a + e^{-c}x \\ b + e^c y \\ c + z \end{pmatrix}$$

and $\widetilde{SL}(2, \mathbb{R})$ the universal covering group of $SL(2, \mathbb{R})$.

The meaning of Thm. 1 is that there are only eight homogeneous geometries which can be supported by closed 3-manifolds. Thus, if we assume that our universe is locally homogeneous and closed we automatically know which classes of topology and geometry it can have. The drawback of this theorem applies only to maximal geometry $(\tilde{\Sigma}, S)$. However, given a nonmaximal geometry $(\tilde{\Sigma}, S')$ we know that $S' \subset S$. If this geometry admits a compact quotient there is a discrete freely acting subgroup $\Gamma'$ of $S'$ such that $\tilde{\Sigma}/\Gamma'$ is compact. If follows that $\Gamma'$ is also a subgroup of $S$ such that the maximal geometry $(\tilde{\Sigma}, S)$ also admits a compact quotient. Thm. 1 ensures that $(\tilde{\Sigma}, S)$ is equivalent to one of the eight Thurston geometries, proving that $(\tilde{\Sigma}, S')$ is a subgeometry of one of the eight Thurston geometries.

Let $I(S_x)$ be the component of the isotropy group $S_x$ containing the identity and $(X, S)$ be a maximal geometry. Then $I(S_x)$ must be either $SO(3)$, $SO(2)$ or the trivial group [93]. If $I(S_x) = SO(3)$ then the space $X$ has constant curvature and the geometry is equivalent to either $S^3$, $\mathbb{E}^3$ or $\mathbb{H}^3$.

**The case of $\mathbb{E}^3$**

$\mathbb{E}^3$ is the three-dimensional flat Riemann manifold with metric

$$ds^2 = dx^2 + dy^2 + dz^2.$$

An isometry of $\mathbb{E}^3$ is given by the action of the group $IO(3, \mathbb{R})$:

$$g(\mathbf{x}) = \mathbf{R}\mathbf{x} + \mathbf{a}$$

where $\mathbf{R}$ is an orthogonal matrix and $\mathbf{a}$ is a constant vector. In order to preserve the orientation we require the matrices $\mathbf{R}$ to be rotations, i.e. we only consider transformations in $\text{Isom}^+\mathbb{E}^3 = ISO(3,\mathbb{R})$. The Killing vectors of $\mathbb{E}^3$ are given by the generators of $ISO(3,\mathbb{R})$:

$$
\begin{aligned}
P_i &= \partial_i & \text{(3 generators of translations)} \\
K_i &= \epsilon_{ijk}x_j\partial_k & \text{(3 generators of rotations)}
\end{aligned}
$$

Table 2.1: List of Thurston geometries

| Type | $X$ | $\text{Isom}^+X$ | $ds^2$ |
|------|-----|------------------|--------|
| T1 | $\mathbb{E}^3$ | $ISO(3)$ | $dx^2 + dy^2 + dz^2$ |
| T2 | $S^3$ | $SO(4)$ | $d\alpha^2 + d\beta^2 + d\gamma^2 + 2\cos\beta d\alpha d\gamma$ |
|  |  |  | $(0 \le \alpha < 4\pi,\ 0 \le \beta < 2\pi,\ 0 \le \gamma < \pi)$ |
| T3 | $H^3$ | $PSL(2,\mathbb{C})$ | $\frac{1}{z^2}(dx^2 + dy^2 + dz^2)$ |
| T4 | $S^2 \times \mathbb{R}$ | $SO(3) \times \mathbb{R}$ | $d\Omega^2_{S^2} + dz^2$ |
| T5 | $H^2 \times \mathbb{R}$ | $\text{Isom}^+H^2 \times \mathbb{R}$ | $\frac{1}{y^2}(dx^2 + dy^2) + dz^2$ |
| T6 | $\widetilde{SL}(2,\mathbb{R})$ | $\text{Isom}^+\widetilde{SL}(2,\mathbb{R})$ | $\frac{1}{y^2}(dx^2 + dy^2 + (dx^2 + ydz)^2)$ |
| T7 | Nil | $\text{Isom}^+\text{Nil}$ | $dx^2 + dy^2 + (dz - xdy)^2$ |
| T8 | Sol | $\text{Isom}^+\text{Sol}$ | $e^{2z}dx^2 + e^{-2z}dy^2 + dz^2$ |

### 2.2.3 Bianchi Classification

The so-called Bianchi classification gives a classification of all simply connected three-dimensional Lie groups up to isomorphisms. The relation with the eight Thurston geometries was pointed out in [44, 45]. Shortly, any minimal (in the sense of Def. 2), simply connected three-dimensional geometry is equivalent to $(X, S)$ where $X = \mathbb{R}^3$, $S =$ one of the Bianchi I-VIII groups; $X = S^3$, $S =$ Bianchi IX group; or $X = S^2 \times \mathbb{R}$, $S = SO(3) \times \mathbb{R}$ (KS). Such minimal geometries are called Bianchi-Kantowski-Sachs (BKS) minimal geometries.

**Construction of an Invariant Metric**

Given a symmetry group $S$ we shall generate an invariant metric. We need the following definition:

**Definition 3.** *A diffeomorphism $\phi : \Sigma \to \Sigma$ is an isometry if it preserves the metric, i.e. $\phi_* g_{\phi(p)} = g_p$. An infinitesimal isometry $\xi$ is called a Killing vector field.*

The Killing vector fields satisfy $\mathcal{L}_\xi g = 0$ and generate a Lie algebra in the sense that given $\xi_1$, $\xi_2$ the commutator $[\xi_1, \xi_2]$ is also a Killing field:

$$[\xi_I, \xi_J] = -C^K_{IJ}\xi_K,$$

where the $C_{IJK}$ are called the structure constants of the symmetry group $S$. These constants can be written as

$$C_{IJK} = \epsilon_{JKL}m^L{}_I + \delta_{IK}a_J - \delta_{IJ}a_K$$

and are used to classify the symmetry groups depending on the matrix $\mathbf{m} = (m_{IJ})$ and the vector $a_I$. If $a_I = 0$ we have a class A type and if $a_I \neq 0$ a class B type. Both classes

are then divided into several subgroups called Bianchi types depending on the value of the matrix $\mathbf{m}$. For example a Bianchi type I (class A) satisfies $\mathbf{m} = 0$, i.e. all structure constants vanish. This type describes the manifold $\mathbb{R}^3$ with the translation group $\mathbb{R}^3$ as symmetry group. Further information can be found in [92].

To construct an invariant metric we have to find invariant vector fields $X_I$ satisfying

$$\mathcal{L}_{\xi_I} X_J = [\xi_I, X_J] = 0$$

with structure constants $D_{IJK}$. This equation defines a set of first order differential subsection with solution $D_{IJK} = -C_{IJK}$ such that

$$[X_I, X_J] = C_{IJK} X_K.$$

Let us define the left-invariant 1-form $\omega^I$ on $S$ which is dual to $X_I$ such that $\omega^I(X_J) = \delta^I_J$. The Maurer-Cartan form on $S$ is given by $\theta_{\text{MC}} = \omega^I T_I$ where $T_I$ are the generators of the Lie algebra $\mathcal{L}(S)$ and satisfy the Maurer-Cartan equation

$$d\omega^I = -\frac{1}{2}C^I_{JK}\omega^J \wedge \omega^K.$$

The invariant metric is now given by

$$g_{\mu\nu} = \eta_{IJ}\omega^I_\mu\omega^J_\nu.$$

Specializing once again to the Bianchi type I model the left-invariant 1-forms are given by

$$\omega^1 = dx^1 \equiv dx, \quad \omega^2 = dx^2 \equiv dy, \quad \omega^3 = dx^3 \equiv dz.$$

The left-invariant vector fields $X_I$ dual to $\omega^I$ are given by

$$X_1 = \partial_1, \quad X_2 = \partial_2, \quad X_3 = \partial_3$$

satisfying $\omega^I(X_J) \equiv dx^I(\partial_J) = \delta^I_J$. The invariant metric is then given by

$$ds^2 = \eta_{IJ}dx^I dx^J = dx^2 + dy^2 + dz^2.$$

This is the well known metric of the three-dimensional Euclidean space which is invariant under the translation group $ISO(3)$. The metrics for all Bianchi groups are listed in Table 2.2.


**Relation with Thurston Geometries**

While Thuston's theorem only applies to maximal geometries admitting a compact quotient the Bianchi geometries are minimal and do not require a compact quotient. It is thus not surprising that not every Bianchi geometry admits a compact quotient. Bianchi types IV and VI for $A \neq 0, 1$ do not admit spatially closed cosmologies. On the other hand, since Thurston geometries $(X, S)$ are maximal they can have different minimal subgeometries, e.g. there may exist two groups $S_1, S_2 \subset S$ defining two different Bianchi minimal geometries. For instance the Thurston geometry $T1 = (\mathbb{E}^3, ISO(3))$ admits two Bianchi minimal geometries: BI and BVII for $A = 0$. The reason is that the 3-dimensional groups B1 and BVII(0) are different transitive subgroups of the 6-dimensional group $ISO(3)$. The other correspondences between Thurston and BKS types are listed in Table 2.3.

Table 2.2: List of Kantowski-Sachs and Bianchi metrics

| BKS type | $ds^2$ | class |
|---|---|---|
| BI | $dx^2 + dy^2 + dz^2$ | A |
| BII | $(dx - zdy)^2 + dy^2 + dz^2$ | A |
| BIII | $dx^2 + e^{-2x}dy^2 + dz^2$ | B |
| BIV | $dx^2 + e^{2x}dy^2 + e^{2x}(dz + xdy)^2$ | B |
| BV | $dx^2 + e^{2x}(dy^2 + dz^2)$ | B |
| BVI | $dx^2 + e^{2(A-1)x}dy^2 + e^{(A+1)x}dz^2, \quad 0 \le A \le 1$ | A,B |
| BVII | $dx^2 + e^{2Ax}(dy^2 + dz^2), \quad 0 \le A \le 1$ | A,B |
| BVIII | $\cosh^2 ydx^2 + dy^2 + (dz + \sinh ydx)^2$ | A |
| BIX | $\cos^2 ydx^2 + dy^2 + (dz - \sin ydx)^2$ | A |
| BKS | $dx^2 + dy^2 + \sin^2 ydz^2$ | - |

Table 2.3: Correspondence between Thurston and BKS types

| Thurston type | BKS type |
|---|---|
| T1 | BI, BVIII(0) |
| T2 | BIX |
| T3 | BV, BVII($A > 0$) |
| T4 | KS |
| T5 | BVI(1) |
| T6 | BVIII |
| T7 | BII |
| T8 | BVI(0) |

### 2.2.4   Teichmüller Space

The construction of a compact quotient $M$ from the covering $\tilde{\Sigma}$ is not unique as we are allowed to take a priori any discrete isometry group $\Gamma$. On the other hand we are only interested in transformations of $\Gamma$ which leave the covering $\tilde{\Sigma}$ globally conformally invariant. A diffeomorphism $\phi : \tilde{\Sigma} \to \tilde{\Sigma}$ is a global conformal isometry if $\phi_* \tilde{g} = \text{const} \cdot \tilde{g}$. Let us now define Rep($M$) as the space of all discrete and faithful representations $\rho : \pi(M) \to \text{Isom}^+\tilde{\Sigma}$. This space is too big since it contains transformations which are connected to the identity. We thus define a relation $\sim$ in Rep($M$) such that two representations $\rho, \rho' : \pi_1(M) \to \text{Isom}^+\tilde{\Sigma}$ are equivalent, i.e. $\rho \sim \rho'$, if there exists a global conformal isometry $\phi$ of $\tilde{\Sigma}$ connected to the identity such that $\rho'(a) = \phi \circ \rho(a) \circ \phi^{-1}$, for all $a \in \pi_1(M)$.

**Definition 4.** *The Teichmüller space is defined as Teich(M) =Rep(M)/ $\sim$ and is a manifold. The numbers used to parametrize the Teichmüller space are called the Teichmüller parameters.*

In other words, smooth and nonisometric deformations of the metric $g_{ab}$ are called Teichmüller deformations if they leave the universal cover $(\tilde{\Sigma}, \tilde{g}_{ab})$ gloabally conformally invariant.
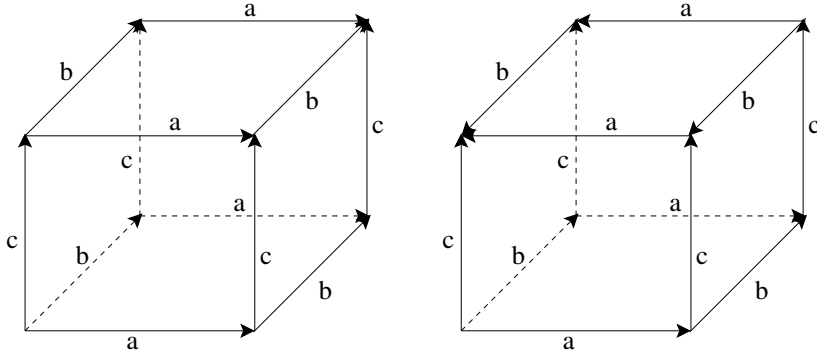
18

Figure 2.1: *Left panel:* 3-dimensional torus $\mathbb{T}^3 = S^1 \times S^1 \times S^1$ where the generators $a$, $b$ and $c$ are translations. *Right panel:* The manifold is $\mathbb{T}^3/\mathbb{Z}^2$. The generators $a$ and $b$ are translations and $c$ is a screw motion with rotation angle $\pi$.

### Teichmüller Space of the Torus

In [60] all compact quotients and their Teichmüller spaces were constructed and discussed. Since we are only interested in spaces with vanishing curvature we will only consider the Euclidean space $\mathbb{E}^3$ as Thurston geometry. There are six compact orientable quotients modeled on $\mathbb{E}^3$ [112]: the torus $\mathbb{T}^3$, $\mathbb{T}^3/\mathbb{Z}_2$, $\mathbb{T}^3/\mathbb{Z}_3$, $\mathbb{T}^3/\mathbb{Z}_4$, $\mathbb{T}^3/\mathbb{Z}_6$ and a space where all generators are screw motions with a rotation angle $\pi/2$. In all six cases the fundamental group $\pi_1(\Sigma)$, where $\Sigma$ is one of the six possible compact quotients, is generated by three elements we shall call $a$, $b$ and $c$. Depending on the case they have different meaning, e.g., they can generate translations or screw motions. We introduce the following notation

$$[a, b] := aba^{-1}b^{-1},$$

where $ab$ denotes a turn of curve $b$ followed by a turn of curve $a$. The meaning of $a$ and $b$ being related by $[a, b]$ is that they 'commute', i.e. they are translations in two different directions.

- $\mathbb{T}^3$: The fundamental group is genenared by three translations $a$, $b$ and $c$ such that

$$\pi_1(\mathbb{T}^3) = \langle a, b, c; [a, b], [a, c], [b, c] \rangle.$$

- $\mathbb{T}^3/\mathbb{Z}_2$: The fundamental group is generated by two translations $a$ and $b$ and a screw motion with a rotation angle $\pi$. The fundamental group is given by

$$\pi_1(\mathbb{T}^3/\mathbb{Z}_2) = \langle a, b, c; [a, b], cac^{-1}a, cbc^{-1}b \rangle.$$

- $\mathbb{T}^3/\mathbb{Z}_3$: The fundamental group is generated by two translations $a$ and $b$ and a screw motion with a rotation angle $2\pi/3$. The fundamental group is given by

$$\pi_1(\mathbb{T}^3/\mathbb{Z}_3) = \langle a, b, c; [a, b], cac^{-1}b^{-1}, cbc^{-1}ba \rangle.$$

- $\mathbb{T}^3/\mathbb{Z}_4$: The fundamental group is generated by two translations $a$ and $b$ and a screw motion with a rotation angle $\pi/2$. The fundamental group is given by

$$\pi_1(\mathbb{T}^3/\mathbb{Z}_4) = \langle a, b, c; [a, b], cac^{-1}b^{-1}, cbc^{-1}a \rangle.$$

19

- $\mathbb{T}^3/\mathbb{Z}_6$: The fundamental group is generated by two translations $a$ and $b$ and a screw motion with a rotation angle $\pi/3$. The fundamental group is given by

$$\pi_1(\mathbb{T}^3/\mathbb{Z}_6) = \langle a, b, c; [a, b], cac^{-1}b^{-1}, cbc^{-1}b^{-1}a \rangle.$$

- All generators are screw motions with a rotation angle $\pi/2$ such that the fundamental group is given by

$$\pi_1(\Sigma) = \langle a, b, c; cab^{-1}, ab^2a^{-1}b^2, ba^2b^{-1}a^2 \rangle.$$

We would like to derive the Teichmüller space of the three-torus $\mathbb{T}^3$. To do so we first note that the Teichmüller space is defined as the space of all smooth deformations which leave the covering globally conformally isometric. Since a rotation is a conformal transformation we can choose to rotate the torus so that the generator $a$ is aligned with the Killing vector $\xi_1$ parallel to the x-axis and the generator $b$ lies in the $xy$-plane generated by the Killing vectors $\xi_1$ and $\xi_2$. We thus have six Teichmüller parameters in the following three generators (see Figure 2.2):

$$a_1 = \begin{pmatrix} a_1{}^1 \\ 0 \\ 0 \end{pmatrix}, \quad a_2 = \begin{pmatrix} a_2{}^1 \\ a_2{}^2 \\ 0 \end{pmatrix}, \quad a_3 = \begin{pmatrix} a_3{}^1 \\ a_3{}^2 \\ a_3{}^3 \end{pmatrix}. \tag{2.3}$$
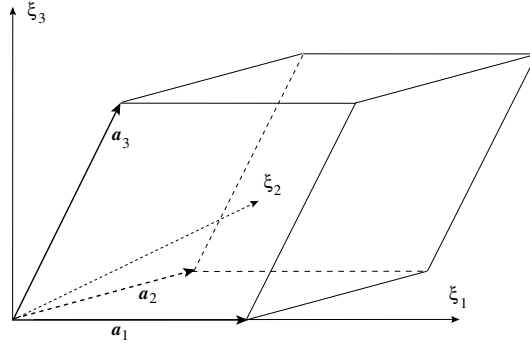


Figure 2.2: The vectors $a_1$, $a_2$ and $a_3$ span the torus with six Teichmüller parameters. The global conformal invariance was used in order to align $a_1$ with $\xi_1$ and $a_2$ with span$\{\xi_1, \xi_2\}$.


### 2.2.5 Metric of the Torus

We define the configuration space $\mathcal{C}$ of the torus as the space spanned by the six Teichmüller parameters, i.e. $\mathcal{C} \subset \mathbb{R}^6$. The metric can be constructed from the three vectors (2.3) as follows:

$$ds^2 = h_{ab}dx^a dx^b, \quad h_{ab} = \sum_{c=1}^{3} a_a{}^c a_b{}^c. \tag{2.4}$$

For example, $h_{21} = a_2{}^1 a_1{}^1 + a_2{}^2 a_1{}^2 + a_2{}^3 a_1{}^3 = a_1{}^1 a_2{}^1$. All components can be cast into the following matrix:

$$(h_{ab}) = \begin{pmatrix} (a_1{}^1)^2 & a_1{}^1 a_2{}^1 & a_1{}^1 a_3{}^1 \\ a_1{}^1 a_2{}^1 & (a_2{}^1)^2 + (a_2{}^2)^2 & a_2{}^1 a_3{}^1 + a_2{}^2 a_3{}^2 \\ a_1{}^1 a_3{}^1 & a_2{}^1 a_3{}^1 + a_2{}^2 a_3{}^2 & (a_3{}^1)^2 + (a_3{}^2)^2 + (a_3{}^3)^2 \end{pmatrix}. \tag{2.5}$$

This metric is flat because the parameters $a_i{}^j$ are independent of the spatial coordinates.

## 2.3 Dynamics of the Torus

In order to derive the dynamics of the torus we first introduce a smooth four-dimensional Lorentzian manifold $(\tilde{M}, \tilde{g})$, where the metric $\tilde{g}$ has the signature $(-, +, +, +)$. Since we want to study only problems with a well-defined inital value problem we choose the topology $\tilde{M} = \mathbb{R} \times \tilde{\Sigma}$ [51]. Furthermore we require $\tilde{\Sigma}$ to admit a compact quotient $\Sigma$ such that $M := \mathbb{R} \times \Sigma$ is a smooth Lorentzian manifold with universal cover $\tilde{M}$. We call such manifolds $M$ *compact homogeneous universes.*

In the previous section we constructed compact spatial manifolds $\Sigma$ by identifying points on the three-dimensional universal cover $\tilde{\Sigma}$ according to the covering group $\Gamma$. Extending this construction to the four-dimensional Lorentzian case is subtle for we have to ensure that the covering group preserves the extrinsic curvature and the spatial metric as well. We thus define

**Definition 5.** *Let $(\tilde{\Sigma}, \tilde{h}_{ab})$ be a spatial section of $(\tilde{M}, \tilde{g}_{\mu\nu})$. An extendible isometry is defined by the restriction of an isometry of $(\tilde{M}, \tilde{g}_{ab})$ on $\tilde{\Sigma}$ which preserves $\tilde{\Sigma}$ and forms a subgroup $\mathrm{Esom}(\tilde{\Sigma})$ of $S$.*

Thus, in order to get a compact homogeneous manifold from $\tilde{M}$ the covering group $\Gamma$ must be a subgroup of $\mathrm{Esom}(\tilde{\Sigma})$, i.e.

$$\Gamma \subset \mathrm{Esom}(\tilde{\Sigma}).$$

As shown in [100], the covering group $\Gamma$ must be implemented in $\mathrm{Esom}(\tilde{\Sigma})$ in order to get a compact homogeneous universe out of a given four-dimensional universal cover.

We saw in Section 2.2.2 that for a fixed topology of $M$ the manifold $\tilde{M}$ is uniquely determined. Consider the case in which the homogeneous spatial section $(\tilde{\Sigma}, \tilde{h}_{ab})$ corresponds to a Bianchi minimal geometry. To construct a metric on $\tilde{M}$ we can follow the prescription given in Section 2.2.3. The most general metric of $\tilde{M}$ with a compact homogeneous section and a nontrivial group $\mathrm{Esom}(\tilde{\Sigma})$ is given by

$$ds^2 = -N^2(t)dt^2 + \tilde{h}_{IJ}\left[N^I(t)dt + \omega^I\right]\left[N^J(t)dt + \omega^J\right],$$

where $\omega^I$ are the invariant one-forms (see Section 2.2.3), $N$ the lapse and $N^I$ the shift vector. The spatial metric $\tilde{h}_{IJ}\omega^I\omega^J$ is homogeneous on each spatial section $t =$const. In the sequel we will study metrics of the form

$$ds^2 = -dt^2 + h_{IJ}\omega^I\omega^J. \tag{2.6}$$

Since we are interested in a torus universe we know that $\tilde{\Sigma}$ has to be flat, i.e. we choose a Bianchi type I spatial section corresponding to the first Thurston geometry according to Table 2.3. At the end of Section 2.2.3 we saw that the metric corresponding to this geometry is given by $ds^2 = dx^2 + dy^2 + dz^2$ such that the metric of $\tilde{M}$ is given by

$$ds^2 = -dt^2 + a_1^2(t)dx^2 + a_2^2(t)dy^2 + a_3^2(t)dz^2,$$

where $a_I(t)$ is the time-dependent scale factor of the direction $I$. If one further requires isotropy, i.e. an isotropy group $SO(3)$, this metric can be reduced to

$$ds^2 = -dt^2 + a^2(t)(dx^2 + dy^2 + dz^2).$$

By the same token the metric of the compact homogeneous universe $M$ can be found by inserting the metric $h_{ab}$ of the compact space $\Sigma$. The spatial metric of a torus is given by Eq. (2.5) such that inserting this metric into Eq. (2.6) leads to the metric of a torus universe.

### 2.3.1 Geometrical Hamiltonian

In the previous section we derived the metric of a toroidal universe which enables us to compute the components of the affine connection $\nabla$, the Riemann tensor, the Ricci scalar and finally the Einstein-Hilbert action given by

$$S_{\text{E-H}}[g] = \frac{1}{2\kappa} \int_{\mathbb{R}\times\mathbb{T}^3} *R[g] = \int_{\mathbb{R}} dt \int_{\mathbb{T}^3} d^3x \mathcal{L}, \quad \kappa = 8\pi G \tag{2.7}$$

where $*$ is the Hodge star operator. Because of the complexity of the metric we used a computer program to compute the expressions for these quantities and it turned out that they are very complicated and long. We thus only write the result of the Lagrange density given by

$$
\begin{aligned}
\mathcal{L} = \quad & \frac{1}{4\kappa} \frac{1}{a_1{}^1 a_2{}^2 a_3{}^3} \times \\
& \Bigg[ \left( (a_3{}^2)^2 + (a_3{}^3)^2 \right) \left( a_2{}^1 \dot{a}_1{}^1 - a_1{}^1 \dot{a}_2{}^1 \right)^2 + (a_1{}^1)^2 (a_3{}^2)^2 (\dot{a}_2{}^2)^2 \\
& + 2a_2{}^2 \Big\{ \dot{a}_1{}^1 a_2{}^1 a_3{}^2 \left( a_1{}^1 \dot{a}_3{}^1 - \dot{a}_1{}^1 a_3{}^1 \right) \\
& \qquad\quad + a_1{}^1 \Big[ \dot{a}_1{}^1 \dot{a}_2{}^1 a_3{}^1 a_3{}^2 - a_1{}^1 a_3{}^2 \dot{a}_2{}^1 \dot{a}_3{}^1 \\
& \qquad\qquad\qquad + \dot{a}_2{}^2 \left( -a_1{}^1 a_3{}^2 \dot{a}_3{}^2 + 2a_3{}^3 \frac{d}{dt}(a_1{}^1 a_3{}^3) \right) \\
& \qquad\qquad\qquad + 2a_1{}^1 (a_3{}^3)^2 \ddot{a}_2{}^2 \Big] \Big\} \\
& + (a_2{}^2)^2 \Big\{ (\dot{a}_1{}^1)^2 (a_3{}^1)^2 - 2a_1{}^1 \dot{a}_1{}^1 a_3{}^1 \dot{a}_3{}^1 \\
& \qquad\quad + a_1{}^1 \Big[ 4a_3{}^3 \frac{d}{dt}(\dot{a}_1{}^1 a_3{}^3) + a_1{}^1 \left( (\dot{a}_3{}^1)^2 + (\dot{a}_3{}^2)^2 + 4a_3{}^3 \ddot{a}_3{}^3 \right) \Big] \Big\} \Bigg]
\end{aligned}
$$

The second order time derivatives $\ddot{a}_i{}^i$ can be eliminated with a partial integration[1] such that

$$
\begin{aligned}
\mathcal{L} = \quad & \frac{1}{4\kappa} \frac{1}{a_1{}^1 a_2{}^2 a_3{}^3} \times \\
& \Bigg[ \left( (a_3{}^2)^2 + (a_3{}^3)^2 \right) \left( a_2{}^1 \dot{a}_1{}^1 - a_1{}^1 \dot{a}_2{}^1 \right)^2 + (a_1{}^1)^2 (a_3{}^2)^2 (\dot{a}_2{}^2)^2 \\
& + (a_2{}^2)^2 \Big\{ (a_3{}^1)^2 (\dot{a}_1{}^1)^2 - 2a_1{}^1 a_3{}^1 \dot{a}_1{}^1 \dot{a}_3{}^1 \\
& \qquad\quad + a_1{}^1 \left( a_1{}^1 \left( (\dot{a}_3{}^1)^2 + (\dot{a}_3{}^2)^2 \right) - 4a_3{}^3 \dot{a}_1{}^1 \dot{a}_3{}^3 \right) \Big\} \\
& - 2a_2{}^2 \Big\{ a_2{}^1 a_3{}^2 \dot{a}_1{}^1 \left( a_3{}^1 \dot{a}_1{}^1 - a_1{}^1 \dot{a}_3{}^1 \right) \\
& \qquad\quad + a_1{}^1 \Big[ a_1{}^1 a_3{}^2 \dot{a}_2{}^1 \dot{a}_3{}^1 - a_3{}^1 a_3{}^2 \dot{a}_1{}^1 \dot{a}_2{}^1 \\
& \qquad\qquad\qquad + \dot{a}_2{}^2 \left( a_1{}^1 a_3{}^2 \dot{a}_3{}^2 + 2a_3{}^3 (a_3{}^3 \dot{a}_1{}^1 + a_1{}^1 \dot{a}_3{}^3) \right) \Big] \Big\} \Bigg]
\end{aligned}
$$

---

[1] The boundary term arising from the partial integration annihilates the boundary term in the Einstein-Hilbert action given by

$$\frac{1}{\kappa} \int_{\mathbb{R}^3} d^3x \sqrt{h} K,$$

where $K$ is the trace of the second fundamental form.

This Lagrangian can also be written as $\mathcal{L} = \frac{1}{2\kappa}G_{AB}\dot{q}^A\dot{q}^B$, where $q = 1\ldots,6$, $\dot{q}^A = (a_1{}^1, a_2{}^1, a_2{}^2, a_3{}^1, a_3{}^2, a_3{}^3)$ and

$$(G_{AB}) =$$

$$\begin{pmatrix}
\frac{(a_2{}^2 a_3{}^1 - a_2{}^1 a_3{}^2)^2 + (a_2{}^1)^2(a_3{}^3)^2}{2a_1{}^1 a_2{}^2 a_3{}^3} & \frac{a_2{}^2 a_3{}^1 a_3{}^2 - a_2{}^1((a_3{}^2)^2+(a_3{}^3)^2)}{2a_2{}^2 a_3{}^3} & -a_3{}^3 & -\frac{a_2{}^2 a_3{}^1 + a_2{}^1 a_3{}^2}{2a_3{}^3} & 0 & -a_2{}^2 \\
\frac{a_2{}^2 a_3{}^1 a_3{}^2 - a_2{}^1((a_3{}^2)^2+(a_3{}^3)^2)}{2a_2{}^2 a_3{}^3} & \frac{a_1{}^1((a_3{}^2)^2+(a_3{}^3)^2)}{2a_2{}^2 a_3{}^3} & 0 & -\frac{a_1{}^1 a_3{}^2}{2a_3{}^3} & 0 & 0 \\
-a_3{}^3 & 0 & \frac{a_1{}^1(a_3{}^2)^2}{2a_2{}^2 a_3{}^3} & 0 & -\frac{a_1{}^1 a_3{}^2}{2a_3{}^3} & -a_1{}^1 \\
-\frac{a_2{}^2 a_3{}^1 + a_2{}^1 a_3{}^2}{2a_3{}^3} & -\frac{a_1{}^1 a_3{}^2}{2a_3{}^3} & 0 & \frac{a_1{}^1 a_2{}^2}{2a_3{}^3} & 0 & 0 \\
0 & 0 & -\frac{a_1{}^1 a_3{}^2}{2a_3{}^3} & 0 & \frac{a_1{}^1 a_2{}^2}{2a_3{}^3} & 0 \\
-a_2{}^2 & 0 & -a_1{}^1 & 0 & 0 & 0
\end{pmatrix}$$

We introduce the momenta

$$p^a{}_b := \frac{\partial\mathcal{L}}{\partial\dot{a}_a{}^b} \tag{2.8}$$

conjugate to the configuration variables $a_a{}^b$ such that the phase space $\mathcal{P} = T^*\mathcal{C} \subset \mathbb{R}^{12}$ is the cotangent bundle over $\mathcal{C}$ with

$$\{a_a{}^b, p^c{}_d\} = \delta_a^c\delta_d^b, \quad \{a_a{}^b, a_c{}^d\} = 0, \quad \{p^a{}_b, p^c{}_d\} = 0. \tag{2.9}$$

Inserting $\dot{a}_a{}^b = \dot{a}_a{}^b(p^c{}_d)$ into the Legendre transform of Eq. (2.7) we get the Hamiltonian

$$\mathcal{H}_g = \frac{\kappa}{4}\frac{1}{a_1{}^1 a_2{}^2 a_3{}^3} \times$$

$$\begin{aligned}
\Big[ & (a_1{}^1 p^1{}_1)^2 + (a_2{}^2 p^2{}_2)^2 + (a_3{}^3 p^3{}_3)^2 + (a_2{}^1 p^2{}_1)^2 + 4(a_2{}^2 p^2{}_1)^2 \\
+ & (a_3{}^1 p^3{}_1)^2 + 4(a_3{}^2 p^3{}_1)^2 + 4(a_3{}^3 p^3{}_1)^2 + (a_3{}^2 p^3{}_2)^2 \\
+ & 4(a_3{}^3 p^3{}_2)^2 - 2a_3{}^2 a_3{}^3 p^3{}_2 p^3{}_3 \\
+ & 2a_1{}^1 p^1{}_1\left(a_2{}^1 p^2{}_1 - a_2{}^2 p^2{}_2 + a_3{}^1 p^3{}_1 - a_3{}^2 p^3{}_2 - a_3{}^3 p^3{}_3\right) \\
- & 2a_3{}^1 p^3{}_1\left(a_3{}^2 p^3{}_2 + a_3{}^3 p^3{}_3\right) \\
- & 2a_2{}^1 p^2{}_1\left(a_2{}^2 p^2{}_2 - a_3{}^1 p^3{}_1 + a_3{}^2 p^3{}_2 + a_3{}^3 p^3{}_3\right) \\
+ & 2a_2{}^2\left\{a_3{}^2\left(4p^2{}_1 p^3{}_1 + p^2{}_2 p^3{}_2\right) - p^2{}_2\left(a_3{}^1 p^3{}_1 + a_3{}^3 p^3{}_3\right)\right\}\Big]
\end{aligned} \tag{2.10}$$

This Hamiltonian can also be written as $\mathcal{H}_g = \frac{1}{2}G^{AB}p_A p_B$, where $G^{AB}$ is the inverse matrix of $G_{AB}$. The equations of motion for the phase space variables can be found with

$$\dot{a}_i{}^j = \{a_i{}^j, \mathcal{H}\}, \quad \dot{p}_i{}^j = \{p_i{}^j, \mathcal{H}\}$$

and are rather complicated functions. The Hamiltonian constraint[2] $\mathcal{H}_g \approx 0$ reduces the dynamical degrees of freedom from dim $\mathcal{P} = 12$ to dim $\mathcal{P} = 10$, which agrees with [15]. To compare this Hamiltonian with the usual Bianchi type I models we set all offdiagonal elements to zero and $a_i{}^i = a_i$, $p^i{}_i = p^i$ (no summation) we get

$$\mathcal{H}_g = \frac{\kappa}{4}\left(\frac{a_1(p^1)^2}{a_2 a_3} + \frac{a_2(p^2)^2}{a_1 a_3} + \frac{a_3(p^3)^2}{a_1 a_2} - 2\frac{p^1 p^2}{a_3} - 2\frac{p^2 p^3}{a_1} - 2\frac{p^1 p^3}{a_2}\right), \tag{2.11}$$

---

[2]We use the convention $C \approx 0$ when the constraint $C$ is required to vanish.

23

which corresponds to the result given in [36] up to a factor 2 in the definition of the action. To get the isotropic case we further set $a_i = a$, $p^i = p/3$ and find that the Hamiltonian constraint (2.10) reduces to the usual first Friedmann equation

$$\mathcal{H}_g = -\frac{\kappa p^2}{12a}$$

and the Hamiltonian equation $\dot{p}^i{}_j = -\partial \mathcal{H}_g / \partial a_i{}^j$ to the usual second Friedmann equation

$$\dot{p} = -\frac{\partial \mathcal{H}_g}{\partial a} = \frac{\kappa p^2}{12a^2}.$$

The second Hamiltonian equation is given by

$$\dot{a} = \partial \mathcal{H}_g / \partial p = -\kappa p/(6a)$$

and allows us to recast the first Friedmann equation into the usual form

$$\mathcal{H}_g = -3a\dot{a}^2/\kappa.$$

Furthermore, notice that all $a_i{}^j$ and $p^i{}_j$, $i \neq j$ have to vanish in order for the torus to remain aligned with the Killing fields $\xi_a$. However we know that the universe is not perfectly homogeneous from e.g. the temperature fluctuations of the CMB. Therefore we are led to the conclusion that the evolution of the universe is also influenced by off-diagonal terms, which means that a torus universe does not simply mean that it has a cubic form.

### 2.3.2 Matter Hamiltonian

Before we compute the evolution of a torus universe we have to add matter for reasons given in Appendix B. The simplest form of matter is a scalar field $\phi$ which is homogeneous in space[3] and has mass $m$ such that the action is given by

$$I_\phi = -\int \left[ \frac{1}{2} d\phi \wedge *d\phi + * \left( \frac{1}{2} m_\phi^2 \phi^2 - V(\phi) \right) \right],$$

where $V(\phi)$ is the potential of the scalar field. A Legendre transform of the action yields the Hamiltonian

$$\mathcal{H}_\phi = \frac{1}{2\sqrt{h}} \pi^2 + \frac{\sqrt{h}}{2} m_\phi^2 \phi^2 + \sqrt{h} V(\phi),$$

where $\pi$ is the momentum field conjugate to the scalar field and $h = (a_1{}^1)^2 (a_2{}^2)^2 (a_3{}^3)^2$ the determinant of the spacial metric (2.5). The total Hamiltonian is then given by

$$\mathcal{H} = \mathcal{H}_g + \mathcal{H}_\phi = \mathcal{H}_g + \frac{1}{2\sqrt{h}} \pi^2 + \frac{\sqrt{h}}{2} m_\phi^2 \phi^2 + \sqrt{h} V(\phi), \qquad (2.12)$$

where $\mathcal{H}_g$ is given by Eq. (2.10). From this equation the Friedmann equations can be computed according to (2.8) and $\mathcal{H} \approx 0$. In the sequel we only consider a scalar field without potential, i.e. $V(\phi) \equiv 0$. We present two numerical solutions: the first one is a massless scalar field (see Figure 2.3) and the second one a massive scalar field (see Figure 2.4).

---

[3]Since scalar fields live by definition in the trivial representation of the rotation group $SO(3)$ it is not possible to construct a scalar field which is homogeneous but not isotropic
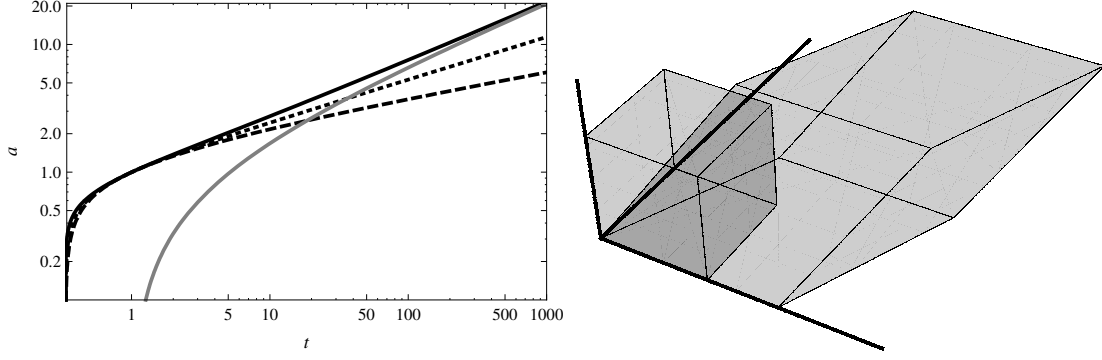
Figure 2.3: *Left panel*: Solutions of (2.12) with the conditions $a_i{}^i(1) = 1$, $p^i{}_i(1) = -1$ (no summation), $a_i{}^j(1) = 0$ $(i \neq j)$, $p^3{}_1(1) = p^3{}_2(1) = 0$, $p^2{}_1(1) = 0.2$, $\phi(1) = 10^{-3}$, $\pi(1) = 1.2$. The diagonal momenta $p^i{}_i$ are chosen to be negative such that all sides of the torus expand. The solid black line is $a_1{}^1$, the dashed one $a_2{}^2$, the dotted one $a_3{}^3$ and the gray one the off-diagonal $a_2{}^1$. The time $t$ parametrizes the coordinate time in natural units $(c = \kappa = \hbar = 1)$. *Right panel*: Solution of (2.12) at two different times. The initial condition is a cubic universe with $a_i{}^i \equiv a_0$, $p^i{}_i \equiv p_0$, $a_i{}^j = 0$ $(i \neq j)$, $p^i{}_j \neq 0$ $(i \neq j)$. In both cases the mass and the potential of the scalar field have been set to zero.
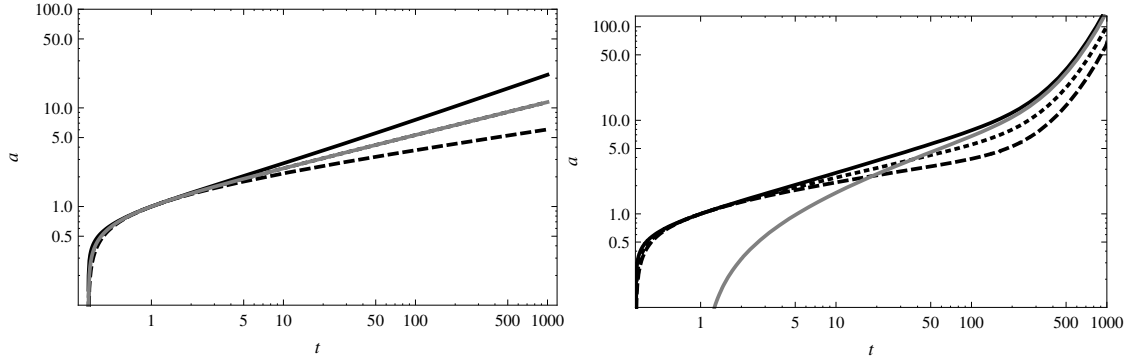


Figure 2.4: *Left panel*: Comparison between the scale factor of the isotropic case (gray line) and the general case with the initial conditions as in Figure 2.3. *Right panel*: As Figure 2.3 but for a scalar field with mass $m_\phi = 0.002$. Starting from $t \sim 100$ the mass of the scalar field induces an inflationary expansion of the universe.

## 2.4   Ashtekar Variables for the Torus Universe

In Section 1.2 we introduced the Ashtekar variables $A_a^i(x)$ and $E_i^a(x)$, where $A_a^i$ is an $su(2)$-valued connection and $E_i^a$ a densitized triad, and described general relativity in terms of these fields. Thanks to spatial homogeneity gravity reduces from an infinite dimensional field theory to a finite dimensional theory. Let $\tilde{S}$ be the spatial isometry group acting transitively on $\tilde{\Sigma}$. A pair of Ashtekar variables $(A_a^i, E_i^a)$ is said to be symmetric if for all $s \in \tilde{S}$ there exists a local gauge transformation $g : \tilde{\Sigma} \to SU(2)$ such that

$$(s^*A, s^*E) = (g^{-1}Ag + g^{-1}dg, g^{-1}Eg), \tag{2.13}$$

25

where $s^*$ is the pullback. In Appendix A we reduce the degrees of freedom of the Ashtekar connection for the general torus (see Figure 2.2). For the sake of simplicity we would like to consider a torus with one degree of freedom less, namely one generated by the vectors $a_1 = (a_1{}^1, 0, 0)^T$, $a_2 = (0, a_2{}^2, a_2{}^3)^T$ and $a_3 = (0, a_3{}^2, a_3{}^3)^T$ (see Figure 2.5) such that the metric is given by

$$h_{ab} = \sum_c a_a{}^c a_b{}^c = \begin{pmatrix} (a_1{}^1)^2 & 0 & 0 \\ 0 & (a_2{}^2)^2 + (a_2{}^3)^2 & a_2{}^2 a_3{}^2 + a_2{}^3 a_3{}^3 \\ 0 & a_2{}^2 a_3{}^2 + a_2{}^3 a_3{}^3 & (a_3{}^2)^2 + (a_3{}^3)^2 \end{pmatrix}. \tag{2.14}$$
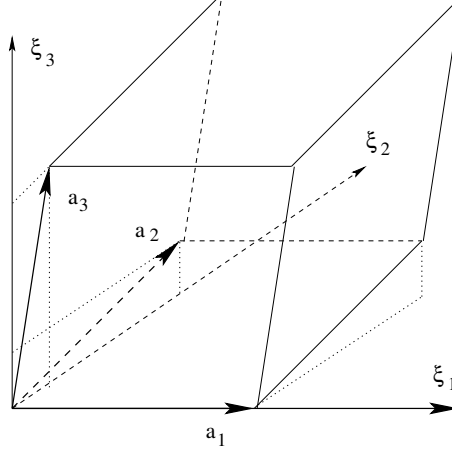


Figure 2.5: The vectors $a_1$, $a_2$ and $a_3$ span the torus with five Teichmüller parameters. The vectors $a_2$ and $a_3$ lie in the $\xi_2\xi_3$-plane while $a_1$ is aligned with $\xi_1$

In terms of cotriads we have

$$h_{ab} = \eta_{IJ}\omega_a^I \omega_b^J$$

with

$$(\omega_a^I) = \begin{pmatrix} a_1{}^1 & 0 & 0 \\ 0 & a_2{}^2 & a_3{}^2 \\ 0 & a_2{}^3 & a_3{}^3 \end{pmatrix}.$$

These one-forms $\omega^I = \omega_a^I dx^a$ are dual to the vector fields $X_I = X_I^a \partial_a$, i.e. $\omega^I(X_J) = \delta_J^I$, where $X_I$ is given by

$$X_1 = \begin{pmatrix} \frac{1}{a_1{}^1} \\ 0 \\ 0 \end{pmatrix}, \quad X_2 = \frac{1}{\mathfrak{h}} \begin{pmatrix} 0 \\ a_3{}^3 \\ -a_2{}^3 \end{pmatrix}, \quad X_3 = \frac{1}{\mathfrak{h}} \begin{pmatrix} 0 \\ -a_3{}^2 \\ a_2{}^2 \end{pmatrix},$$

where we defined $\mathfrak{h} = a_2{}^2 a_3{}^3 - a_2{}^3 a_3{}^2$. The Ashtekar connection is given by $A_a^i = \bar{\phi}_I{}^i \omega_a^I$ (see Appendix A) with

$$(\bar{\phi}_I{}^i) = \begin{pmatrix} \bar{\phi}_1{}^1 & 0 & 0 \\ 0 & \bar{\phi}_2{}^2 & \bar{\phi}_3{}^2 \\ 0 & \bar{\phi}_2{}^3 & \bar{\phi}_3{}^3 \end{pmatrix} \tag{2.15}$$

such that

$$(A_a^i) = \begin{pmatrix} a_1{}^1 \bar{\phi}_1{}^1 & 0 & 0 \\ 0 & a_2{}^2 \bar{\phi}_2{}^2 + a_2{}^3 \bar{\phi}_3{}^2 & a_3{}^2 \bar{\phi}_2{}^2 + a_3{}^3 \bar{\phi}_3{}^2 \\ 0 & a_2{}^2 \bar{\phi}_2{}^3 + a_2{}^3 \bar{\phi}_3{}^3 & a_3{}^2 \bar{\phi}_2{}^3 + a_3{}^3 \bar{\phi}_3{}^3 \end{pmatrix}.$$

26

We saw in Section 1.2 that the variable dual to the Ashtekar connection $A_a^i$ is the densitized triad $E_i^a$. A symmetry reduction of this triad leads to

$$(E_i^a) = \sqrt{h}\,\bar{p}^I{}_i X_I^a = \sqrt{h} \begin{pmatrix} \frac{\bar{p}^1{}_1}{a_1{}^1} & 0 & 0 \\ 0 & \frac{a_3{}^3\bar{p}^2{}_2 - a_3{}^2\bar{p}^3{}_2}{\hbar} & \frac{a_3{}^3\bar{p}^2{}_3 - a_3{}^2\bar{p}^3{}_3}{\hbar} \\ 0 & \frac{a_2{}^2\bar{p}^3{}_2 - a_2{}^3\bar{p}^2{}_2}{\hbar} & \frac{a_2{}^2\bar{p}^3{}_3 - a_2{}^3\bar{p}^2{}_3}{\hbar} \end{pmatrix}, \tag{2.16}$$

where we inserted Eq. (2.4) and defined

$$(\bar{p}^I{}_i) = \begin{pmatrix} \bar{p}^1{}_1 & 0 & 0 \\ 0 & \bar{p}^2{}_2 & \bar{p}^2{}_3 \\ 0 & \bar{p}^3{}_2 & \bar{p}^3{}_3 \end{pmatrix},$$

where $h = (a_1{}^1)^2(a_2{}^3 a_3{}^2 - a_2{}^2 a_3{}^3)^2$ is the determinant of the spatial metric (2.14). The symplectic structure in terms of the reduced variables can be derived from

$$\frac{1}{\kappa\gamma}\int_{\mathbb{T}^3} \dot{A}_a^i E_i^a d^3x = \frac{1}{\kappa\gamma}\int_{\mathbb{T}^3} \sqrt{h}\,\dot{\bar{\phi}}_I{}^i \bar{p}^J{}_i \omega_a^I X_J^a d^3x = \frac{V_0}{\kappa\gamma}\dot{\bar{\phi}}_I{}^i \bar{p}_I{}^i,$$

where we defined the volume $V_0 = \int_{\mathbb{T}^3} d^3x\sqrt{h}$ of $\mathbb{T}^3$ as measured by the metric $h$, to obtain

$$\{\bar{\phi}_I{}^i, \bar{p}^J{}_j\} = \frac{\kappa\gamma}{V_0}\delta_I^J\delta_j^i. \tag{2.17}$$

We would like to get rid of the dependence of these brackets on the volume. We thus define new variables

$$\phi_I{}^i = L_I\bar{\phi}_I{}^i, \quad p^I{}_i = \frac{V_0}{L_I}\bar{p}^I{}_i, \tag{2.18}$$

such that

$$\{\phi_I{}^i, p^J{}_j\} = \kappa\gamma\delta_I^J\delta_j^i, \tag{2.19}$$

where $L_1 = a_1{}^1$, $L_2 = \sqrt{(a_2{}^2)^2 + (a_2{}^3)^2}$ and $L_3 = \sqrt{(a_3{}^2)^2 + (a_3{}^3)^2}$. Therefore we conclude that

**Proposition 1.** *The classical configuration space $\mathcal{A}_S = \mathbb{R}^5$ is spanned by the five configuration variables $\phi_I{}^i$. The phase space $\mathcal{P} = \mathbb{R}^{10}$ is spanned by $\phi_I{}^i$ and the five momenta $p^J{}_j$ satisfying the Poisson bracket (2.19).*

Furthermore, note that the determinant of the densitized triad is given by

$$\det E_i^a = \mathfrak{k}\,p^1{}_1(p^2{}_3 p^3{}_2 - p^2{}_2 p^3{}_3), \quad \mathfrak{k} := \frac{L_1 L_2 L_3}{V_0}. \tag{2.20}$$

The relation between the new variables $(\phi_I{}^i, p^J{}_j)$ and the 'scale factors' $a_a{}^b$ and their respective momenta $p^a{}_b$ can be found by using Eq. (1.3) and the Poisson brackets (2.9) and (2.19). A closed form could only be found for $p^1{}_1$ and is given by

$$|p^1{}_1| = |a_2{}^2 a_3{}^3 - a_2{}^3 a_3{}^2|.$$

27

## 2.5 Constraints in Ashtekar Variables for the Torus

We saw in Section 1.2 that the Hamiltonian formulation of GR is a fully constrained system. Thanks to homogeneity the complicated expressions of these constraints simplify dramatically. For example homogeneity requires that $N \neq N(x)$. Since we consider topologies with flat spatial curvature the Hamiltonian is given by Eq. (1.13). Inserting Eqs. (2.15) and (2.16) into Eq. (1.13) we get

$$
C_{\text{grav}} := \frac{1}{2\kappa} N \mathcal{H} = \quad -\frac{1}{\kappa\gamma^2} \frac{1}{\sqrt{|p^1{}_1(p^2{}_2 p^3{}_3 - p^2{}_3 p^3{}_2)|}} \times
$$
$$
\left[ \quad \phi_1{}^1 p^1{}_1 \left\{ (\phi_2{}^2 - \phi_2{}^3)(p^2{}_2 - p^2{}_3) + (\phi_3{}^2 - \phi_3{}^3)(p^3{}_2 - p^3{}_3) \right\} \right.
$$
$$
\left. + (\phi_2{}^3 \phi_3{}^2 - \phi_2{}^2 \phi_3{}^3)(p^2{}_3 p^3{}_2 - p^2{}_2 p^3{}_3) \right], \tag{2.21}
$$

where we defined $N = \sqrt{L_1 L_2 L_3 / V_0}$ =const in order to simplify the Hamiltonian. Using this expression we can compute the time evolution of the basic variables $\phi_i{}^j$ and $p^i{}_j$ (see Figure 2.6). Setting all off-diagonal terms to zero we see that Eq. (2.21) matches with Eq. (3.20) in [36]. If we further set $\phi_{(i)}{}^i = c$ and $p^{(i)}{}_i = p$ we get

$$
C_{\text{grav}} = -\frac{3}{\kappa\gamma^2} c^2 \sqrt{|p|}, \tag{2.22}
$$

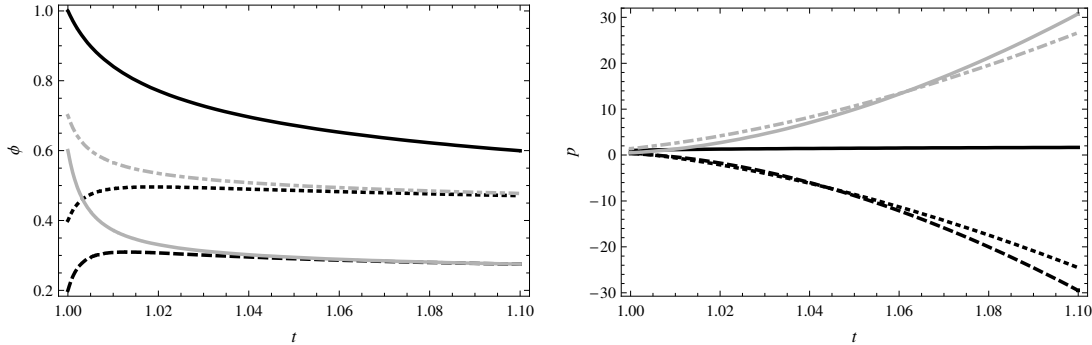which is exactly the same result as the homogeneous and isotropic case [29].



Figure 2.6: Solutions corresponding to the Hamiltonian (2.21) coupled to a massless scalar field with vanishing potential. *Left panel*: the black thick solid line shows the evolution of $\phi_1{}^1$, $\phi_2{}^2$ corresponds to the black dashed line, $\phi_3{}^3$ the dotted line, $\phi_2{}^3$ the gray dashdotted one and $\phi_3{}^2$ the solid gray one. *Right panel*: the black thick solid shows the evolution of $p^1{}_1$, $p^2{}_2$ is the black dashed line, $p^3{}_3$ the dotted line, $p^2{}_3$ the gray dashdotted one and $p^3{}_2$ the solid gray one. In both cases the initial conditions are $\phi_1{}^1 = 1.0$, $\phi_2{}^2 = 0.2$, $\phi_3{}^3 = 0.4$, $\phi_2{}^3 = 0.6$, $\phi_3{}^2 = 0.7$, $p^1{}_1 = 1.0$, $p^2{}_2 = 0.3$, $p^3{}_3 = 0.5$, $p^2{}_3 0.5$, $p^3{}_2 = 1.4$, $\phi = 0.01$ and $p_\phi = 8.1$. The time $t$ parametrizes the coordinate time in natural units ($c = \kappa = \hbar = 1$).

The Gauss constraint for a homogeneous model is given by

$$
G_i = \epsilon_{ijk} \phi_I{}^i p^I{}_k. \tag{2.23}
$$

With our choice of variables two Gauss constraints are automatically satisfied, namely $G_2 = G_3 \equiv 0$. However, we can still perform a global $SU(2)$ transformation along $\tau_1$ which

is implemented by the nonvanishing Gauss constraint

$$G_1 = \phi_2{}^2 p^2{}_3 + \phi_3{}^2 p^3{}_3 - \phi_2{}^3 p^2{}_2 - \phi_3{}^3 p^3{}_2 \approx 0 \tag{2.24}$$

generating simultaneous rotations of the pairs $(\phi_2{}^2, \phi_2{}^3)$, $(p^2{}_2, p^2{}_3)$ resp. $(\phi_3{}^2, \phi_3{}^3)$, $(p^3{}_2, p^3{}_3)$. Thus the norms of these vectors and the scalar products between them are gauge invariant. The Gauss constraint allows us to get rid of e.g. the pair $(\phi_3{}^2, p^3{}_2)$ by fixing the gauge in the following way: we rotate the connection components such that $\phi_3{}^2 = 0$. Because the length $\|\phi_3\| = \sqrt{(\phi_3{}^2)^2 + (\phi_3{}^3)^2}$ is preserved we know that $\phi_3{}^3 \neq 0$. The Gauss constraint then implies that $p^3{}_2 = (\phi_2{}^2 p^2{}_3 - \phi_2{}^3 p^2{}_2)/\phi_3{}^3$. This gauge fixing reduces the degrees of freedom by two.

The diffeomorphism constraint is given by Eq. (1.10) and since $F^i_{ab} = \epsilon^i{}_{jk} A^j_a A^k_b$ ($\partial_a A^i_b = 0$ thanks to homogeneity) we find that

$$H_a = \epsilon^i{}_{jk} A^j_a A^k_b E^b_i \propto A^i_a G_i. \tag{2.25}$$

The gauge fixing we just performed ensures that the diffeomorphism constraint also vanishes.

## 2.6 Canonical Transformation

In this subsection we introduce a set of new variables which will greatly simplify the analysis of the kinematical Hilbert space. We first perform a canonical transformation on the unreduced phase space:

$$Q_1 = \phi_1{}^1, \qquad\qquad P^1 = p^1{}_1,$$

$$Q_2 = \sqrt{(\phi_2{}^2)^2 + (\phi_2{}^3)^2}, \qquad P^2 = \frac{p^2{}_2 \phi_2{}^2 + p^2{}_3 \phi_2{}^3}{\sqrt{(\phi_2{}^2)^2 + (\phi_2{}^3)^2}}$$

$$Q_3 = \sqrt{(\phi_3{}^2)^2 + (\phi_3{}^3)^2}, \qquad P^3 = \frac{p^3{}_2 \phi_3{}^2 + p^3{}_3 \phi_3{}^3}{\sqrt{(\phi_3{}^2)^2 + (\phi_3{}^3)^2}} \tag{2.26}$$

$$\theta_1 = \mathrm{arc}_k\cos\left(\frac{\phi_2{}^2}{\sqrt{(\phi_2{}^2)^2 + (\phi_2{}^3)^2}}\right), \qquad P_{\theta_1} = p^2{}_3 \phi_2{}^2 - p^2{}_2 \phi_2{}^3$$

$$\theta_2 = \mathrm{arc}_k\cos\left(\frac{\phi_3{}^3}{\sqrt{(\phi_3{}^2)^2 + (\phi_3{}^3)^2}}\right), \qquad P_{\theta_2} = -p^3{}_3 \phi_3{}^2 + p^3{}_2 \phi_3{}^3,$$

where $k \in \mathbb{Z}$ ($k = 0$ denotes the principal value), such that the variables are mutually conjugate:

$$\{Q_I, P^J\} = \kappa\gamma\delta^J_I, \quad \{\theta_\alpha, P_{\theta_\beta}\} = \kappa\gamma\delta_{\alpha,\beta}. \tag{2.27}$$

We choose the convention that the diagonal limit can be recovered by setting $\theta_1 = \theta_2 = 0$. The inverse of this canonical transformation will be important in the sequel and is given by:

$$\phi_2{}^2 = Q_2 \cos(\theta_1), \qquad\qquad \phi_2{}^3 = Q_2 \sin(\theta_1),$$

$$p^2{}_2 = P^2 \cos(\theta_1) - \frac{P_{\theta_1} \sin(\theta_1)}{Q_2}, \qquad p^2{}_3 = \frac{P_{\theta_1} \cos(\theta_1)}{Q_2} + P^2 \sin(\theta_1), \tag{2.28}$$

$$\phi_3{}^2 = Q_3 \sin(\theta_2), \qquad\qquad \phi_3{}^3 = Q_3 \cos(\theta_2),$$

$$p^3{}_2 = P^3 \sin(\theta_2) + \frac{P_{\theta_2} \cos(\theta_2)}{Q_3}, \qquad p^3{}_3 = -\frac{P_{\theta_2} \sin(\theta_2)}{Q_3} + P^3 \cos(\theta_2).$$

29

It is important to note that $Q_2, Q_3 \in \mathbb{R}_+$ and $\theta_1, \theta_2 \in [k\pi, (k+1)\pi]$ where we restrict the values of $k$ to be either $k = 0$ if $\mathrm{sgn}(\phi_2{}^3) > 0$ or $k = 1$ if $\mathrm{sgn}(\phi_2{}^3) < 0$. If $\mathrm{sgn}(\phi_2{}^3) = 0$ then we have the case $k = 0$ if $\mathrm{sgn}(\phi_2{}^2) > 0$ or $k = 1$ if $\mathrm{sgn}(\phi_2{}^2) < 0$. The function $\mathrm{arc}_1\cos(x)$ is related to the principal value via $\mathrm{arc}_1\cos(x) = 2\pi - \arccos(x)$. With this convention we can recover Eq. (2.26) unambiguously from Eq. (2.28).

The Hamiltonian constraint (2.21) is given in terms of the new variables by

$$
C_{\text{grav}} = \frac{(2\kappa\gamma^2)^{-1}}{\sqrt{\left| \dfrac{P^1\left[\cos(\theta_1+\theta_2)(P_{\theta_1}P_{\theta_2} - P^2 P^3 Q_2 Q_3) + (P^2 P_{\theta_2} Q_2 + P^3 P_{\theta_1} Q_3)\sin(\theta_1+\theta_2)\right]}{Q_2 Q_3} \right|}} \times
$$

$$
\times \left\{ 2P^1 Q_1 \left[\cos(2\theta_2)P_{\theta_2} + P^2 Q_2(\sin(2\theta_1) - 1) + P^3 Q_3(\sin(2\theta_2) - 1)\right] \right.
$$

$$
+ P^2 Q_2 \left[P_{\theta_2}\sin(2(\theta_1 + \theta_2)) - 2\cos^2(\theta_1 + \theta_2)P^3 Q_3\right] \tag{2.29}
$$

$$
\left. + P_{\theta_1}\left[2\cos^2(\theta_1 + \theta_2)P_{\theta_2} + 2\cos(2\theta_1)P^1 Q_1 + P^3 P_{\theta_3}\sin(2(\theta_1 + \theta_2))\right] \right\}
$$

Using this Hamiltonian we can compute the time evolution of the basic variables $Q_i$, $\theta_\alpha$, $P^i$ and $P_{\theta_\alpha}$ (see Figure 2.7). We choose the initial conditions so that they correspond to the values of the old variables (see caption of Figure 2.6). Comparing the solutions to Eq. (2.21) with the solutions to Eq. (2.29) allowed us to ensure that the canonical transformation (2.26) was performed correctly as both solutions matched up to numerical accuracy.
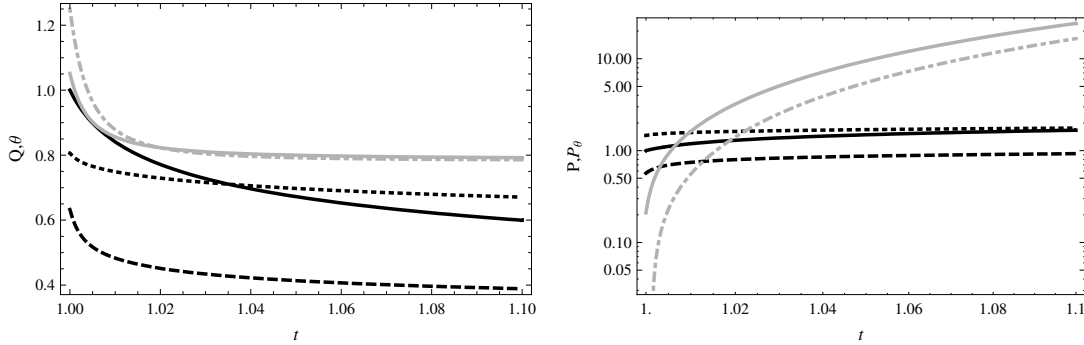


Figure 2.7: Solutions corresponding to the Hamiltonian (2.29) coupled to a massless scalar field with vanishing potential. *Left panel*: the black thick solid shows the evolution of $Q_1$, $Q_2$ is the black dashed line, $Q_3$ the dotted line, $\theta_1$ the gray dashdotted one and $\theta_2$ the solid gray one. *Right panel*: the black thick solid shows the evolution of $P^1$, $P^2$ is the black dashed line, $P^3$ the dotted line, $P_{\theta_1}$ the gray dashdotted one and $P_{\theta_2}$ the solid gray one. In both cases the initial conditions are $Q_1 = 1$, $Q_2 = 0.63$, $Q_3 = 0.81$, $\theta_1 = 1.25$, $\theta_2 = 1.05$, $P^1 = 1$, $P^2 = 0.57$, $P^3 = 1.46$, $P_{\theta_1} = -0.08$, $P_{\theta_2} = 0.21$, $\phi = 0.01$ and $p_\phi = 8.1$.

The only nontrivial Gauss constraint (2.24) is then given by

$$
G_1 = P_{\theta_1} - P_{\theta_2}, \tag{2.30}
$$

which vanishes only when $P_{\theta_2} = P_{\theta_1}$. We are free to fix the gauge by setting $\theta_2 = 0$. The same result can be obtained from the gauge fixing performed in Section 2.5 so that

$$
Q_3 = \phi_3{}^3, \quad P^3 = p^3{}_3, \quad \theta_2 = 0 \quad \text{and} \quad P_{\theta_2} = P_{\theta_1}.
$$

The symplectic structure of the reduced 8-dimensional phase space is given by

$$\mathbf{\Omega} = \frac{V_0}{\kappa\gamma}(dQ_1 \wedge dP^1 + dQ_2 \wedge dP^2 + dQ_3 \wedge dP^3 + d\theta_1 \wedge dP_{\theta_1}).$$

# Chapter 3

# Toroidal Loop Quantum Cosmology

In this chapter we shall quantize the torus universe derived in the former chapter. Since we have to deal with a constrained system we first give an example of a quantization of constrained systems. We shall then give the guidelines of the canonical quantization with constraints and apply them to our torus universe.

## 3.1 Electromagnetism as an Example of a Quantization with Constraints

Let us briefly explain the quantization of systems with constraints with the theory of electromagnetism, further details can be found in [98, 114]. In Section 2.1 we introduced the Maxwell action and its resulting equations of motion for the 4-potential $A_\mu$. Since a quantization usually requires a Hamiltonian we have to perform a Legendre transform of the Maxwell action (2.1). This action can explicitly written in terms of electric and magnetic fields:

$$S_M[\vec{E}, \vec{B}; \vec{A}, \phi] = \int dt \int d^3x \left[ -\frac{1}{2} \left( \vec{E}^2 - \vec{B}^2 \right) + \vec{A} \cdot \left( \frac{\partial \vec{E}}{\partial t} - \vec{\nabla} \wedge \vec{B} \right) + \phi \vec{\nabla} \cdot \vec{E} \right].$$

The stationarity of the action leads to the four Maxwell equations

$$\frac{\delta S_M}{\delta \vec{A}} = \frac{\partial \vec{E}}{\partial t} - \vec{\nabla} \wedge \vec{B} = 0, \qquad \frac{\delta S_M}{\delta \phi} = -\vec{\nabla} \cdot \vec{E} = 0, \qquad (3.1)$$

$$\frac{\delta S_M}{\delta \vec{E}} = -\vec{E} - \frac{\partial \vec{A}}{\partial t} - \vec{\nabla} \phi = 0, \qquad \frac{\delta S_M}{\delta \vec{B}} = \vec{B} - \vec{\nabla} \wedge \vec{A} = 0. \qquad (3.2)$$

The canonical momenta $\pi^0$, $\pi^a$ of the configuration variables $\phi$, $\vec{A}$ are tensor densities of weight $+1$ and are defined by

$$\pi_\phi \quad := \quad \frac{\delta S}{\delta \dot{\phi}} = 0, \qquad (3.3)$$

$$\vec{\pi} \quad := \quad \frac{\delta S}{\delta \dot{\vec{A}}} = \dot{\vec{A}} - \vec{\nabla} \phi = \vec{E}. \qquad (3.4)$$

The first equation is a primary constraint because the momentum conjugated to $\phi$ vanishes. The Hamiltonian density is

$$\mathcal{H} = \frac{1}{2}(\vec{E}^2 + \vec{B}^2) + \phi \vec{\nabla} \cdot \vec{E} + \pi_\phi \frac{\partial \phi}{\partial t}. \qquad (3.5)$$

The equations of motion are then given by taking the Poisson brackets with the Hamiltonian. For example the time evolution of $\pi^0$ is given by

$$\dot{\pi}^0 = -\frac{\delta \mathcal{H}}{\delta A_0} = \partial_a E^a = 0$$

which guarantees that the primary constraint $\pi^0 = 0$ is preserved in time. This equation defines the Gauss constraint which is automatically conserved. The last term in Eq. (3.5) can be taken to vanish if we impose the constraint (3.3), that is, we can get rid of this term by fixing a gauge (e.g. $\phi = 0$). However we would like to include the pair $(\phi, \pi_\phi)$ in the phase space such that

$$\{A_i(\vec{x}, t), E_j(\vec{y}, t)\} = -\delta_{ij}\delta^3(\vec{x} - \vec{y}), \quad \{\phi(\vec{x}, t), \pi_\phi(\vec{y}, t)\} = \delta^3(\vec{x} - \vec{y}).$$

The reason is that in a relativistic notation $A_\mu = (\phi, \vec{A})$, $\pi^\mu = (\pi_\phi, \vec{E})$ we have

$$\{A_\mu(\vec{x}, t), \pi^\nu(\vec{y}, t)\} = \delta^\nu_\mu \delta^3(\vec{x} - \vec{y}).$$

The Maxwell equations can be recovered with $\dot{\Phi} = \{\Phi, H\}$ for any $\Phi \in (\vec{A}, \vec{E}, \phi, \pi_\phi)$.

The Maxwell equations are invariant under a gauge transformation

$$A' = A + d\Lambda$$

provided the gauge parameter $\Lambda$ vanishes sufficiently fast at spatial infinity. The generator of the gauge transformation is given by

$$G[\Lambda] = -\int d^3x \, \pi^\mu \partial_\mu \Lambda$$

such that

$$\delta\Phi = \{\Phi, G[\Lambda]\}.$$

In order for $\delta\vec{E}$ and $\delta\pi_\phi$ to vanish the two constraints

$$\vec{\nabla} \cdot \vec{E} = 0, \quad \pi_\phi = 0$$

have to be fulfilled. This in turn implies that $G[\Lambda] = 0$.

On the other hand, we can use the gauge invariance to fix e.g. $\phi = 0$. The implication is that the term $\phi \vec{\nabla} \cdot \vec{E}$ vanishes from the action such that the reduced phase space is spanned by $\{A_i(\vec{x}, t), E_j(\vec{y}, t)\} = -\delta_{ij}\delta^3(\vec{x} - \vec{y})$. The degrees of freedom of the phase space have thus been reduced by one component (at every point). The Hamiltonian is then given by

$$\mathcal{H}_{\text{red}} = \frac{1}{2}\left(\vec{E}^2 + \vec{B}^2\right).$$

Since the constraint $\vec{\nabla} \cdot \vec{E} = 0$ has disappeared from the Hamiltonian it has to be imposed separately. This constraint requires the longitudinal electric field to vanish, implying that the dimensionality of the physical phase space is again reduced by one unit at every point. Physically it means that both the longitudinal and the scalar polarizations have disappeared from the physical phase space, leaving only two transversal components.

Given a momentum $\vec{k}$ choose three vectors

$$\vec{e}_3 = \frac{\vec{p}}{|\vec{p}|}, \quad \vec{e}_1, \quad \vec{e}_2$$

which form a right-handed orthonormal system. Consider the classical plane wave in a box of volume $V$:

$$A_\mu(\vec{x}, t) = \frac{1}{\sqrt{V}} \sum_{\mathbf{k}} \sum_{s=0}^{3} \left( a_{\mathbf{k},s}^- e^{i(\mathbf{k}\cdot\mathbf{x}-\omega t)} + a_{\mathbf{k},s}^+ e^{-i(\mathbf{k}\cdot\mathbf{x}-\omega t)} \right) e_s^\mu(\mathbf{k})$$

where the component $e_0^\mu$ is the scalar polarization. The Fourier transform of the constraint $\vec{\nabla} \cdot \vec{A} = 0$ implies the relation

$$\vec{k} \cdot \vec{e}_k = 0,$$

i.e. the longitudinal component of the photon vanishes. Because of the gauge fixing $\phi = 0$ the photon has only two transversal components $\vec{e}_1$ and $\vec{e}_2$.

### 3.1.1  Quantization of the Electromagnetic Field

The gauge condition $\partial_\mu A^\mu = 0$ implies

$$a_{\vec{k},0}^- = a_{\vec{k},3}^-.$$

The quantization of the field $A_\mu$ is obtained by using creation operators $\hat{a}_{\vec{k},s}^+$ and annihilation operators $\hat{a}_{\vec{k},s}^-$ defined on a Fock space $\mathcal{F}(\mathcal{H})$. Let $|\vec{k}, e_\mu\rangle$ be a basis of the one photon vector space[1] $X$. If we equip this space with a sesquilinear form

$$\langle \vec{k}, e_\mu | \vec{k}', e_\nu \rangle = \eta_{\mu\nu} \frac{1}{2|\vec{k}|} \delta(\vec{k} - \vec{k}')$$

we see that the norm is negative for scalar polarizations and zero for longitudinal polarizations. On the other hand we know that these polarizations are unphysical. However, imposing the gauge condition at the operator level contradicts the relations for the creation and annihilation operators since $[\hat{a}_{\vec{k},3}^-, \hat{a}_{\vec{k},3}^+] = Id$ but $[\hat{a}_{\vec{k},0}^-, \hat{a}_{\vec{k},0}^+] = -Id$, thus requiring us to weaken this condition. Following Gupta and Bleuler we construct the physical Hilbert space $\mathcal{H}_{\text{phys}}$ which consists of all states $\Psi \in X$ with the property

$$\hat{a}_{\vec{k},0}^- \Psi = 0, \quad \hat{a}_{\vec{k},3}^- \Psi = 0$$

with the property $\langle \Psi | \Psi \rangle > 0$ ($\Psi \neq 0$). For further details see e.g. [98, 114].

The construction sketched above is typical when a system with constraints has to be quantized. In LQG the $SU(2)$-Gauss constraint is solved by taking only gauge invariant variables. The diffeomorphism constraint is more difficult to solve because it fails to be weakly continuous, thus requiring to find a (distributional) space through group averaging. We shall see that in the case of loop quantum cosmology on a torus the Gauss constraint is not trivially solved.

## 3.2  Canonical Quantization with Constraints

The example just given of the quantization of electromagnetism can be generalized to Yang-Mills fields. The underlying principle of every known interaction is a gauge theory, i.e. a field theory with constraints. In this section we give the relevant points of a canonical

---

[1]Since the 4-momentum is null $k_\mu$ is uniquely determined by $\vec{k}$.

quantization with constraints. The general case as well as further details can be found in [104].

Let $(\mathcal{M}, \Omega)$ be a constrained symplectic manifold with a symplectic structure $\Omega$ and constraints $C_I(N^I)$ satisfying $\{C_I, C_J\} = f_{IJ}^K C_K$ for some smooth functions $f_{IJ}^K$. The index $I$ takes values in some finite index set and $N^I$ is a Lagrange multiplier corresponding to the constraint $C_I$.

1. *Polarization*: Since there are many ways to coordinatize the phase space a judicious choice can be found by requiring that either the equations of motion or the constraints be as simple as possible. The variables on this phase space have to be split by a polarization of the symplectic manifold into configuration variables and momentum variables. In the previous chapter we already introduced two sets of canonical variables given in Eqs. (2.19) and (2.27).

2. *Quantum Configuration Space*: In general the classical configuration space $\mathcal{C}$ has to be extended to a more general quantum configuration space $\bar{\mathcal{C}}$. In a field theory, while the classical configuration space is typically some space of smooth fields the quantum configuration space is a distributional space. For instance the classical configuration space of a free scalar field is given by e.g. the space of smooth functions with compact support $C_0^\infty(\mathbb{R}^3)$. When passing to quantum theory this space has to be enlarged to the space of distributions, e.g. $\mathcal{S}'$.

3. *Kinematical Hilbert Space*: The quantum configuration space $\bar{\mathcal{C}}$ has to be equipped with a structure of a Hilbert space $\mathcal{H}_{\text{kin}} := L^2(\bar{\mathcal{C}}, d\mu)$ which must carry an irreducible representation of the canonical commutation relations, i.e. we impose the relations $[\hat{Q}, \hat{P}] = i\hbar\widehat{\{Q, P\}}$. Furthermore the Hilbert must implement the classical complex conjugation relations among the elementary variables as adjointness relations on the corresponding operators.

4. *Constraint Operators*: Represent the constraints $C_I$ as self-adjoint operators $\hat{C}_I$ on $\mathcal{H}_{\text{kin}}$. These operators have to be densely defined in $\mathcal{H}_{\text{kin}}$, i.e. their domain of definition $\mathcal{D}(\hat{C}^I)$ is dense in the Hilbert space.

5. *Imposing the Constraints*: Solve the constraints in the quantum theory by imposing[2] $\hat{C}_I\psi = 0$ for $\psi \in \mathcal{H}_{\text{phys}}$.

## 3.3 Holonomies

In this chapter we would like to introduce the concept of holonomies as they play a central role in both LQG and LQC. We shall first give a geometrical definition along the lines of [21, 74].

Let $P(M, SU(2))$ be a principal fiber bundle over the base manifold $M$ with projection $\pi : P \to M$. For simplicity we assume the fiber bundle is trivial such that $P \cong M \times SU(2)$. Let $A = A_a^i \tau_i dx^a \in \Lambda^1(M) \otimes su(2)$ be a connection. We would like to define a parallel transport along a smooth path $\gamma : [0, 1] \to M$ with $\gamma(0) = p$ and $\gamma(1) = q$, that is, given a group element $u(t)$ in the fiber $P_{\gamma(t)}$ over $\gamma$ we define the parallel transport of $u(t)$ along $\gamma$

---

[2]Normally one has to choose a triplet $\mathcal{D} \subset \mathcal{H} \subset \mathcal{D}^*$ and a $\Psi \in \mathcal{D}^*$ such that $\Psi(\hat{C}_I\psi) = 0$, $\forall\psi \in \mathcal{D}$. But since we will only solve the Gauss constraint we can restrict the analysis to $\hat{C}_I\psi = 0$.

as[3]

$$D_{\dot\gamma(t)}u(t) = \frac{d}{dt}u(t) - u(t)A(\dot\gamma(t)) = \frac{d}{dt}u(t) - u(t)A_\mu\dot\gamma^\mu = 0, \tag{3.6}$$

where $D_{\dot\gamma}$ is the covariant derivative along $\gamma$ and $\dot\gamma(t) \equiv \frac{d}{dt}\gamma(t)$ defines a vector tangential to $\gamma$ at time $t$. The second equality was obtained by expanding $\dot\gamma(t)$ in the basis $\partial_\nu$ of the tangential space $TM$ and noting that $dx^\mu$ is an element of the cotangent space $T^*M$ such that

$$A(\dot\gamma(t)) = A_\mu dx^\mu(\dot\gamma(t)) = A_\mu dx^\mu(\dot\gamma^\nu\partial_\nu) = A_\mu\dot\gamma^\nu dx^\mu(\partial_\nu) = A_\mu\dot\gamma^\mu.$$

The solution to Eq. (3.6) is given by

$$u(t) = u(0)\mathcal{P}\exp\left(\int_0^t A(\dot\gamma(s))ds\right),$$

where $u(0) = \pi^{-1}(p)$ and $\mathcal{P}$ is the path ordering operator.

**Definition 6.** *Let us denote $u(0)h_\gamma[A]$ the result of parallel transporting $u(0) \in P_p$ to $u(1) \in P_q$ along $\gamma$, where $P_{p,q}$ is the fiber over the point $p, q \in M$. The map*

$$h_\gamma[A] : P_p \to P_q$$

*is called the holonomy along the path $\gamma$.*

To obtain the transformation rule of holonomies consider a gauge transformation $g$ of $u(t)$ such that

$$w(t) = u(t)g(\gamma(t)).$$

The time derivative of $w(t)$ is given by

$$\begin{aligned}\frac{d}{dt}w(t) &= u(t)A_\mu g\dot\gamma^\mu(t) + u(t)(\partial_\mu g)\dot\gamma^\mu \\ &= w(t)g^{-1}A_\mu g\dot\gamma^\mu + w(t)g^{-1}(\partial_\mu g)\dot\gamma^\mu,\end{aligned}$$

where we inserted Eq. (3.6). Furthermore we have

$$\frac{d}{dt}w(t) = w(t)A'_\mu\dot\gamma^\mu,$$

where the transformation rule (1.6) has been used. Thus $w(t)$ also satisfies the parallel transport equation

$$D'_{\dot\gamma(t)}w(t) = 0.$$

Recall from Definition 6 that the holonomy $h_\gamma[A]$ is a map from $u(0)$ to $u(1)$. Similarly $h_\gamma[A']$ sends $w(0) = u(0)g(\gamma(0))$ to $w(1) = w(1)g(\gamma(1))$ such that

$$h_\gamma[A'] = g^{-1}(\gamma(0))h_\gamma[A]g(\gamma(1)).$$

Suppose $\gamma : [0,1] \to M$ is a loop, i.e. $\gamma(0) = \gamma(1)$. A consequence of the above transformation rule is that the so-called Wilson loop

$$W(\gamma, A) = \text{tr}(h_\gamma[A]) = \text{tr}\left(\mathcal{P}\exp\oint_\gamma A\right)$$

is gauge invariant.

---

[3]Most books define the covariant derivative as $D_{\dot\gamma(t)}u(t) = \frac{d}{dt}u(t) + A(\dot\gamma(t))u(t) = 0$ with solution

$$u(t) = \mathcal{P}\exp\left(-\int_0^t A(\dot\gamma(s))ds\right)u(0).$$

Nevertheless we will follow the convention in LQG and LQC.

## 3.4 Foundation of Loop Quantum Cosmology on $\mathbb{R}^3$

In Sec. 1.2 we saw that GR can be written in terms of Ashtekar variables $A_a^i$ such that it becomes a constrained Yang-Mills theory. According to the second step in Section 3.2 we have to find the quantum configuration space. One of the fundamental assumptions of LQG is that holonomies of the $su(2)$-valued connection of general relativity in the Ashtekar formulation become densely defined operators. As shown in Appendix C there exists no operator analog corresponding to the connection $A$. Thus, if we want to quantize cosmology along the lines of LQG we are only allowed to use holonomies as our basic variables.

Let us consider the case of isotropic cosmology where the isotropy group is the Euclidean group. Using Eq. (2.13) the pair $(A, E)$ can be written as [11] $A = \tilde{c}\,^0\omega^i\tau_i$, $\quad E = \tilde{p}\sqrt{^0q}\,^0e_i\tau^i$, where the constants $\tilde{c}$ and $\tilde{p}$ carry the only non-trivial information of $(A, E)$, $^0q$ is the determinant of the fiducial flat metric $^0q_{ab} = \,^0\omega_a^i\,^0\omega_b^i$ and $\tau_i$ are the traceless generators of $SU(2)$ proportional to the Pauli matrices (see footnote on page 6). Since $\mathbb{R}^3$ is noncompact and the fields are spatially homogeneous the integrals in Eq. (1.8) diverge. We thus restrict a cell $\mathcal{V}$ adapted to $^0q_{ab}$ with volume $V_0$. Defining the variables

$$c = V_0^{\frac{1}{3}}\tilde{c} \quad \text{and} \quad p = V_0^{\frac{2}{3}}\tilde{p}$$

the symplectic structure is given by

$$\Omega = \frac{3}{\gamma\kappa}dc \wedge dp. \tag{3.7}$$

Thanks to homogeneity we only need holonomies along straight lines to recover the connection $A$. The reason is that the holonomy along the straight edges $\gamma_k(t) = \gamma_k(0) + (\mu V_0^{1/3}\,^0e_k)t$, $t \in [0, 1]$, with length $\mu V_0^{1/3}$ is given by

$$h_k^{(\mu)} = \mathcal{P}\exp\int_{\gamma_k} A = \exp\int_{\gamma_k}\frac{c}{V_0^{1/3}}\,^0\omega^i\tau_i = \exp\int_0^1\frac{c}{V_0^{1/3}}\mu V_0^{1/3}\,^0\omega_a^i(\,^0e_k^a)\tau_i dt$$

$$= \exp(\mu c\tau_k) = \cos\frac{\mu c}{2}\mathbb{1} + 2\sin\frac{\mu c}{2}\tau_k \tag{3.8}$$

where $\mathbb{1}$ is the identity $2 \times 2$ matrix such that

$$-2\lim_{\mu\to 0}\text{tr}\left(\frac{h_k^{(\mu)}\tau_k}{\mu}\right) = -2\lim_{\mu\to 0}\text{tr}\left(\frac{2\sin\frac{\mu c}{2}(\tau_k)^2}{\mu}\right) = 2\lim_{\mu\to 0}\frac{\sin\frac{\mu c}{2}}{\mu} = c.$$

Thus the elementary variables can be chosen to be $\exp(i\mu c/2) =: \mathcal{N}_\mu(c)$. These functions span the algebra of almost periodic functions as explained in Appendix D and form an orthonormal basis in the Hilbert space $\mathcal{H}_B = L^2(\bar{\mathbb{R}}_B, d\mu_B)$ with scalar product

$$\langle\mathcal{N}_\mu(c), \mathcal{N}_{\mu'}(c)\rangle := \mu_B(\overline{\mathcal{N}_\mu(c)}\mathcal{N}_{\mu'}(c)) = \lim_{T\to\infty}\frac{1}{2T}\int_{-T}^T\overline{\mathcal{N}_\mu(c)}\mathcal{N}_{\mu'}(c)dc = \delta_{\mu,\mu'}.$$

Note that the basis spanned by $\mathcal{N}_\mu(c)$ is uncountable such that the Hilbert space $L^2(\bar{\mathbb{R}}_B, d\mu_B)$ is non-separable. Let $\pi : \bar{\mathcal{C}} \to L(\mathcal{H}_B)$ be a representation of the $C^*$-algebra of almost periodic functions defined by (see Appendix C)

$$(\pi(\exp(i\lambda c/2))\mathcal{N}_\mu)(c) = \mathcal{N}_{\mu+\lambda}(c).$$

This representation fails to be weakly continuous since

$$\lim_{\delta \to 0} \langle \mathcal{N}_\mu(c), (\pi(\exp(i\delta c/2))\mathcal{N}_{\mu'})(c) \rangle = \lim_{\delta \to 0} \langle \mathcal{N}_\mu(c), \mathcal{N}_{\mu'+\delta}(c) \rangle = 0$$

such that we have a representation inequivalent to the Schrödinger representation of quantum cosmology. Furthermore, according to Theorem 7 there is no well defined operator $\hat{c}$ on $\mathcal{H}_B$.

In isotropic LQC the momentum conjugated to the Ashtekar connection component $c$ is the densitized triad component $p$ (see Eq. (3.7)). The operator $\hat{p}$ acts by derivation with eigenfunctions

$$\hat{p}|\mu\rangle = \frac{8\pi\gamma l_{\mathrm{Pl}}^2}{6}\mu|\mu\rangle \equiv p_\mu|\mu\rangle, \tag{3.9}$$

where $\mathcal{N}_\mu(c) = \langle c|\mu\rangle$ and $l_{\mathrm{Pl}} = \sqrt{G\hbar}$ is the Planck length. Moreover we have

$$\hat{p}\,\mathrm{tr}(h_k^{(\mu)}) = 2\hat{p}\cos\frac{\mu c}{2} = i\frac{8\pi\gamma l_{\mathrm{Pl}}^2}{3}\mu\sin\frac{\mu c}{2}. \tag{3.10}$$

The commutator between these two operators is

$$[\exp(i\mu c/2), \hat{p}] = i\frac{\gamma l_{\mathrm{Pl}}^2}{2}.$$

Moreover the operator $\hat{V}$ representing the volume of the cell $\mathcal{V}$ is given by $\hat{V} = |\hat{p}|^{3/2}$ such that

$$\hat{V}|\mu\rangle = \left(\frac{8\pi\gamma}{6}|\mu|\right)^{\frac{3}{2}} l_{\mathrm{Pl}}^3|\mu\rangle.$$

To fulfill points 4 and 5 of the quantization program we first note that both the diffeomorphism and Gauss constraints are satisfied by the choice of variables. The gravitational quantum Hamiltonian constraint coupled to a scalar field has been rigorously solved in [13, 14].

## 3.5 Foundation of LQC for a Toroidal Topology

In this section we shall follow the guidelines given in Section 3.2 for a toroidal topology. The situation will be more complicated because of additional degrees of freedom. Moreover the Gauss constraint (2.24) does not vanish and has also to be solved at the quantum level.

Let us compute the holonomies along the path

$$\gamma_I : [0,1] \to \mathbb{T}^3, \quad t \mapsto \gamma_I(t) \tag{3.11}$$

with length $\lambda_I$ such that the velocity vector $\dot{\gamma}_I(t)$ is parallel to $X_I$ defined in Eq. (2.4). The holonomy is then given by

$$h_I^{(\lambda_I)}[A] = \mathcal{P}\exp\left(\int_{\gamma_I} A\right) = \exp\left(\int_0^1 A_a^i \tau_i |\dot{\gamma}_I^a| dt\right)$$
$$= \exp\left(\lambda_{(I)}\phi_J{}^i \tau_i \omega_a^J(X_I^a)\right) = \exp(\lambda_{(I)}\phi_I{}^i \tau_i). \tag{3.12}$$

This expression can be written as

$$h_I^{(\lambda_I)} = \cos\left(\lambda_{(I)}\|\vec{\phi}_I\|/2\right) + 2\frac{\phi_I{}^i \tau_i}{\|\vec{\phi}_I\|}\sin\left(\lambda_{(I)}\|\vec{\phi}_I\|/2\right) \quad \text{(no summation over } I\text{)},$$

where

$$\|\vec{\phi}_\alpha\| := \sqrt{\sum_i (\phi_\alpha{}^i)^2}.$$

As we shall see the problem is that this expression cannot be used in this form. Using the canonical transformation (2.26) we can re-express the holonomies such that

$$
\begin{aligned}
h_1^{(\lambda_1)} &= \cos(\lambda_1 Q_1/2)\mathbb{1} + 2\tau_1 \sin(\lambda_1 Q_1/2),\\
h_2^{(\lambda_2)} &= \cos(\lambda_2 Q_2/2)\mathbb{1} + 2(\tau_2 \cos\theta_1 + \tau_3 \sin\theta_1)\sin(\lambda_2 Q_2/2),\\
h_3^{(\lambda_3)} &= \cos(\lambda_3 Q_3/2)\mathbb{1} + 2(\tau_2 \sin\theta_2 + \tau_3 \cos\theta_2)\sin(\lambda_3 Q_3/2).
\end{aligned}
\tag{3.13}
$$

Thus, matrix elements of the exponentials of $Q_1$, $Q_2$ and $Q_3$ are trigonometric functions. The situation is similar to Eq. (3.8) such that we can choose the elementary variables to be $\exp(i\lambda_I Q_I/2)$, $I = 1, 2, 3$. These variables are periodic functions with period $2\pi/\lambda_I$, $\lambda_I \in \mathbb{R}$, and form a $C^*$-algebra of almost periodic functions (see Appendix D). On the other hand the variables $\theta_{1,2}$ are periodic angles such that only strictly periodic functions $\exp(ik_\alpha\theta_\alpha) \in U(1)$ with $k_\alpha \in \mathbb{Z}$ are allowed. Thus, any function generated by this set can be written as

$$
g(Q_1, Q_2, Q_3, \theta_1, \theta_2) = \sum_{\lambda_1, \lambda_2, \lambda_3, k_1, k_2} \xi_{\lambda_1, \lambda_2, \lambda_3, k_1, k_2} \times
$$

$$
\times \exp\left(\frac{1}{2}i\lambda_1 Q_1 + \frac{1}{2}i\lambda_2 Q_2 + \frac{1}{2}i\lambda_3 Q_3 + ik_1\theta_1 + ik_2\theta_2\right)
\tag{3.14}
$$

where $\xi_{\lambda_1, \lambda_2, \lambda_3, k_1, k_2} \in \mathbb{C}$, generating a $C^*$-algebra called $\mathcal{A}_S$. Note that this function is almost periodic in $Q_1, Q_2$ and $Q_3$ and strictly periodic in $\theta_1$ and $\theta_2$. As explained in Appendix D the spectrum of the algebra of the almost periodic functions is the Bohr compactification $\bar{\mathbb{R}}_B := \Delta(\mathrm{Cyl}_S)$ of the real line and can be seen as the space of generalized connections [11, 107]. Thus the functions (3.14) provide us a complete set of continuous functions on $\bar{\mathbb{R}}_B \times \bar{\mathbb{R}}_B \times \bar{\mathbb{R}}_B \times S^1 \times S^1$.

A Cauchy completion leads to a Hilbert space $\mathcal{H}^S$ defined by the tensor product $\mathcal{H}^S = \mathcal{H}_B^{\otimes 3} \otimes \mathcal{H}_{S^1}^{\otimes 2}$ with the Hilbert spaces $\mathcal{H}_B = L^2(\bar{\mathbb{R}}_B, d\mu(c))$ and $\mathcal{H}_{S^1} = L^2(S^1, d\phi)$ of square integrable functions on $\bar{\mathbb{R}}_B$ and the circle respectively, where $d\phi$ is the Haar measure for $S^1$. The scalar product on e.g. $\mathcal{H}_B^{\otimes 3} \otimes \mathcal{H}_{S^1}^{\otimes 2}$ is given by (see Appendix D):

$$
\langle f_\lambda, f_{\lambda'}\rangle = \lim_{T\to\infty} \frac{1}{2T}\int_{-T}^{T} d\xi \int_0^{2\pi} \frac{d\theta}{2\pi} \bar{f}_\lambda f_{\lambda'}.
\tag{3.15}
$$

An orthonormal basis for $\mathcal{H}_B$ is given by the almost periodic functions $\langle Q_I|\mu_I\rangle = \exp(i\mu_I Q_I/2)$ (no summation) with $\mu_I \in \mathbb{R}$ with $\langle \mu_I|\mu_I'\rangle = \delta_{\mu_I, \mu_I'}$. Analogously a basis for $\mathcal{H}_{S^1}$ is given by the strictly periodic functions $\langle \theta_\alpha|k_\alpha\rangle = \exp(ik_\alpha\theta_\alpha)$ with $\langle k_\alpha|k_\alpha'\rangle = \delta_{k_\alpha, k_\alpha'}$.

We choose a representation where the configuration variables, now promoted to operators, act by multiplication via:

$$(\hat{g}f)(\vec{Q}, \vec{\theta}) = g(\vec{Q}, \vec{\theta})f(\vec{Q}, \vec{\theta}).$$

The momentum operators act by derivation in the following way:

$$\hat{P}^I = -i\gamma l_{\mathrm{Pl}}^2 \frac{\partial}{\partial Q_I}, \quad \hat{P}_{\theta_\alpha} = -i\gamma l_{\mathrm{Pl}}^2 \frac{\partial}{\partial \theta_\alpha},
\tag{3.16}$$

where the Planck length is defined by $l_{\text{Pl}}^2 = G\hbar$. The eigenstates of all momentum operators are given by

$$|\vec{\lambda}, \vec{k}\rangle \; := \; |\lambda_1, \lambda_2, \lambda_3, k_1, k_2\rangle$$
$$\qquad\; := \; |\lambda_1\rangle \otimes |\lambda_2\rangle \otimes |\lambda_3\rangle \otimes |k_1\rangle \otimes |k_2\rangle$$

with

$$\hat{P}^I |\vec{\lambda}, \vec{k}\rangle = \gamma l_{\text{Pl}}^2 \lambda_I |\vec{\lambda}, \vec{k}\rangle, \quad \hat{P}_{\theta_\alpha} |\vec{\lambda}, \vec{k}\rangle = \frac{\gamma l_{\text{Pl}}^2}{2} k_\alpha |\vec{\lambda}, \vec{k}\rangle. \tag{3.17}$$

The simple form of the momentum operators (3.16) may suggest that the Hilbert space of LQC on a torus is simply expanded from $L^2(\mathbb{R}_B^3)$ to $L^2(\mathbb{R}_B^3) \times L^2(U(1)^2)$. However the situation is far more complicated because the important variables for the Gauss and Hamiltonian constraints are not the new momenta $P^I$ and $P_{\theta_\alpha}$ but the components $p^I{}_i$ of the triad. In terms of the new canonical variables they are complicated functions of both the configuration and momentum variables, as can be seen from Eq. (2.28). These expressions cannot be quantized directly because the Weyl operators corresponding to the variables $Q_{2,3}$ fail to be weakly continuous so that, by Theorem 7, no well defined operators $\hat{Q}_{2,3}$ exist. The solution is to consider the momentum operators of the full theory given by a sum of left and right invariant vector fields (see [104] for further details). In [26] the same strategy was used to show that the triad components $p^I{}_i$ act by derivation. In our case the situation is more complicated since the triad components contain both configuration and momentum variables. The triad operators act on functions in $\mathcal{H}^S$ and are given by

$$\hat{p}^I{}_i = -i \frac{8\pi\gamma l_{\text{Pl}}^2}{2} \left( X_i^{(R)}(h_I) + X_i^{(L)}(h_I) \right), \tag{3.18}$$

where $X_i^{(R)}(h_I)$ and $X_i^{(L)}(h_I)$ are the right and left invariant vector fields acting on the copy of $SU(2)$ associated with the edge $e_I$ of length 1 and are given by

$$X_i^{(R)}(h_I) = \text{tr}\left[ (\tau_i h_I)^T \frac{\partial}{\partial h_I} \right], \quad X_i^{(L)}(h_I) = \text{tr}\left[ (h_I \tau_i)^T \frac{\partial}{\partial h_I} \right].$$

So for example we have

$$X_2^{(R)}(h_2)\text{tr}(h_2) = (\tau_2 h_2)_B^A \frac{\partial}{\partial (h)_B^A}((h_2)_1^1 + (h_2)_2^2)$$

$$= (\tau_2 h_2)_1^1 + (\tau_2 h_2)_2^2 = -\cos\theta_1 \sin\frac{\lambda_2 Q_2}{2}.$$

Similarly, applying the operators $\hat{p}^2{}_2$ and $\hat{p}^2{}_3$ on the function $\text{tr}(h_2)$ we get

$$\hat{p}^2{}_2\text{tr}(h_2) = 2\hat{p}^2{}_2 \cos(\lambda_2 Q_2/2) = 8\pi i\gamma l_{\text{Pl}}^2 \lambda_2 \sin(\lambda_2 Q_2/2) \cos(\theta_1),$$
$$\hat{p}^2{}_3\text{tr}(h_2) = 2\hat{p}^2{}_3 \cos(\lambda_2 Q_2/2) = 8\pi i\gamma l_{\text{Pl}}^2 \lambda_2 \sin(\lambda_2 Q_2/2) \sin(\theta_1). \tag{3.19}$$

On page 23 we showed how to reduce the symplectic structure for a homogeneous and isotropic universe. In order to show that Eq. (3.19) reduces to Eq. (3.10) all diagonal components must be equal and all offdiagonal components must be set to zero. Analogously, $\theta_{1,2} = 0$, $Q_1 = Q_2 = Q_3 \equiv c$ and $\lambda_1 = \lambda_2 = \lambda_3 \equiv \mu$. The second equation in Eq. (3.19) reduces to $\hat{p}^2{}_3\text{tr}(h_2) = 0$ as expected. The first equation in Eq. (3.19) reduces to

$$\hat{p}^2{}_2\text{tr}(h_2) = 8\pi i\gamma l_{\text{Pl}}^2 \sin\frac{\mu c}{2},$$

which differs from Eq. (3.10) by a factor of 3 caused by the factor $1/3$ in the definition of $\hat{p}$ (see Eq. (3.9)). Applying these operators once again we get the expressions:

$$(\hat{p}^2{}_2)^2 \text{tr}(h_2) = \frac{1}{2}(8\pi\gamma)^2 l_{\text{Pl}}^4 \lambda_2^2 \cos(\lambda_2 Q_2/2) = (\hat{p}^2{}_3)^2 \text{tr}(h_2),$$

which means that $\cos(\lambda_2 Q_2/2)$ is an eigenfunction of both $(\hat{p}^2{}_2)^2$ and $(\hat{p}^2{}_3)^2$ with eigenvalue $(8\pi\gamma)^2 l_{\text{Pl}}^4/2\lambda_2^2$. On the other hand we have

$$\hat{p}^2{}_2 \hat{p}^2{}_3 \text{tr}(h_2) = \hat{p}^2{}_3 \hat{p}^2{}_2 \text{tr}(h_2) = 0.$$

## 3.6   Quantization of the Triad Components

This section is devoted to the quantization of the components $p^I{}_i$ of the densitized triad $E_i^a$. As previously mentioned we cannot directly quantize the expressions (2.28) because $\hat{Q}_I$ does not exist as multiplication operator on $\mathcal{H}^S$. In a loop quantization only holonomies of the connections are represented as well-defined operators on $\mathcal{H}^S$. We shall see that there are two ways of quantizing the components (2.28).

### 3.6.1   Quantization: 1$^{\text{st}}$ Possibility

In this subsection we follow the usual way in LQC by replacing every configuration variable $Q_I$ in Eq. (2.28) by $\sin(\delta_I Q_I/2)/\delta_I$ [31], where $\delta_I \in \mathbb{R}\backslash\{0\}$ plays the role of a regulator, and compare it with the results just obtained in terms of left and right invariant vector fields. For later purpose we order the operators in a symmetrical way to get the following operators acting on functions of $\mathcal{H}^S$:

$$\hat{\phi}_2{}^2 = \frac{\sin(\delta_2 Q_2)}{\delta_2}\cos\theta_1, \qquad \hat{p}^2{}_2 = \cos\theta_1 \hat{P}^2 - \frac{\delta_2\sqrt{\sin\theta_1}}{\sin(\delta_2 Q_2)}\hat{P}_{\theta_1}\sqrt{\sin\theta_1},$$

$$\hat{\phi}_2{}^3 = \frac{\sin(\delta_2 Q_2)}{\delta_2}\sin\theta_1, \qquad \hat{p}^2{}_3 = \sin\theta_1 \hat{P}^2 + \frac{\delta_2\sqrt{\cos\theta_1}}{\sin(\delta_2 Q_2)}\hat{P}_{\theta_1}\sqrt{\cos\theta_1},$$

$$\hat{\phi}_3{}^2 = \frac{\sin(\delta_3 Q_3)}{\delta_3}\sin\theta_2, \qquad \hat{p}^3{}_2 = \sin\theta_2 \hat{P}^3 + \frac{\delta_3\sqrt{\cos\theta_2}}{\sin(\delta_3 Q_3)}\hat{P}_{\theta_2}\sqrt{\cos\theta_2}, \qquad (3.20)$$

$$\hat{\phi}_3{}^3 = \frac{\sin(\delta_3 Q_3)}{\delta_3}\cos\theta_2, \qquad \hat{p}^3{}_3 = \cos\theta_2 \hat{P}^3 - \frac{\delta_3\sqrt{\sin\theta_2}}{\sin(\delta_3 Q_3)}\hat{P}_{\theta_2}\sqrt{\sin\theta_2}.$$

Applying e.g. the operator $\hat{p}^2{}_2$ on $\cos(\lambda_2 Q_2/2)$ with the definitions (3.17) we see that we obtain the same result as Eq. (3.19) for $\delta = 1$. This is not surprising in view of the fact that we defined the operator $\hat{p}^I{}_i$ in Eq. (3.18) with holonomies along edges $e_I$ of length 1.

This substitution is problematic since the configuration variables $Q_{2,3}$ are by definition positive (see Eq. (2.26)). Therefore, for $Q_{2,3} \rightarrow \sin(\delta_{2,3}Q_{2,3})/\delta_{2,3}$ to be valid we restrict the analysis to the domain $0 < Q_{2,3} < \pi$. In the diagonal case the situation is less problematic because the configuration variable $c$ is arbitrary such that $\sin(\delta c)$ is also allowed to be negative.

Classically, since the change of variables (2.28) is a canonical transformation the symplectic structure is conserved, i.e. the Poisson bracket between $p^2{}_2$ and $p^2{}_3$ vanishes:

$$\{p^2{}_2, p^2{}_3\}_{Q,P} = 0$$

A quantization of the above expression is obtained with the substitution $\{,\} \to -i[,]\hbar$ such that the commutator between $\hat{p}^2{}_2$ and $\hat{p}^2{}_3$ should also vanish. However, the consequence of the substitution of $1/Q_I$ by $\delta_I/\sin(\delta_I Q_I)$ is that the commutator between these two variables doesn't vanish anymore:

$$\left[\hat{p}^2{}_2, \hat{p}^2{}_3\right] f(Q_2, \theta_1) = -\gamma^2 l_{\text{Pl}}^4 \frac{(\delta_2)^2}{1 + \cos(\delta_2 Q_2)} \frac{\partial f}{\partial \theta_1} \tag{3.21}$$

Formally we can recover the classical limit by taking the limit

$$\lim_{\delta_2 \to 0} [\hat{p}^2{}_2, \hat{p}^2{}_3] f(Q_2, \theta_1) = 0,$$

which however fails to exist on $\mathcal{H}^S$.

The operators $\hat{p}^I{}_i$ are partial differential operators with periodic coefficients in both $\theta$ and $Q$. In spherically symmetric quantum geometry a similar situation arises when considering the quantization of a nondiagonal triad component [31, 70, 71, 72]. However the expression of this component reduces to a Hamiltonian whose eigenvalues are discrete, resulting in an avoidance of the Schwarzschild singularity $r \to 0$ inside of black holes. As shown in the next section the situation is more complicated for a torus universe.

**Quantization of $p^2{}_2$**

In order to find eigenfunctions of the triad operators let us consider an operator of the form

$$\hat{A}_\delta := -i \cos\theta \frac{\partial}{\partial Q} + i \frac{\delta \sin\theta}{\sin(\delta Q)} \frac{\partial}{\partial\theta} + \frac{i\delta}{2} \frac{\cos\theta}{\sin Q}, \quad \theta \in (0, 2\pi).$$

A substitution $\xi = \delta Q$ shows that $\hat{A}_\delta = \delta \hat{A}_1 \equiv \delta \hat{A}$ so that it is sufficient to determine the spectrum for $\delta = 1$, i.e.

$$\hat{A} := -i \cos\theta \frac{\partial}{\partial\xi} + i \frac{\sin\theta}{\sin\xi} \frac{\partial}{\partial\theta} + \frac{i}{2} \frac{\cos\theta}{\sin\xi}$$

This operator is symmetric on $\mathcal{H}_A := L^2(\bar{\mathbb{R}}_B, d\mu_B) \otimes L^2(U(1))$:

$$\langle f, \hat{A}g \rangle = \langle \hat{A}f, g \rangle, \quad \forall f, g \in \mathcal{D}(\hat{A}),$$

where $\mathcal{D}(\hat{A}) \subset \mathcal{H}_A$ is the domain of $\hat{A}$. The eigenfunctions of $\hat{A}$ are obtained by solving $\hat{A}f_\lambda(\xi, \theta) = \lambda f_\lambda(\xi, \theta)$, i.e.

$$-i \cos\theta \frac{\partial f_\lambda(\xi, \theta)}{\partial\xi} + i \frac{\sin\theta}{\sin\xi} \frac{\partial f_\lambda(\xi, \theta)}{\partial\theta} + \frac{i}{2} \frac{\cos\theta}{\sin\xi} f_\lambda(\xi, \theta) = \lambda f_\lambda(\xi, \theta). \tag{3.22}$$

We look for a solution of the form $w = w(\xi, \theta)$ [58] satisfying

$$-i \cos\theta \frac{\partial w}{\partial\xi} + i \frac{\sin\theta}{\sin\xi} \frac{\partial w}{\partial\theta} = \left(\lambda - \frac{i}{2} \frac{\cos\theta}{\sin\xi}\right) f_\lambda \frac{\partial w}{\partial f_\lambda} \tag{3.23}$$

such that the characteristic functions are given by

$$\dot{\xi} = -i \cos\theta(t), \quad \dot{\theta} = i \frac{\sin\theta(t)}{\sin\xi(t)} \quad \text{and} \quad \dot{f}_\lambda = \left(\lambda - \frac{i}{2} \frac{\cos\theta(t)}{\sin\xi(t)}\right) f_\lambda(t), \tag{3.24}$$

43

where the dot is the time derivative. Combining the first two equations gives after integration

$$\sin\theta\tan\frac{\xi}{2} = C_1, \tag{3.25}$$

i.e. every $C^1$-function $\Omega_1 \equiv \Omega_1(\sin\theta\tan(\xi/2))$ solves the left-hand side of Eq. (3.23). In order to solve Eq. (3.22) we first note that

$$\cos\theta(t) = \pm\sqrt{1 - C_1^2\cot^2(\xi/2)} \equiv i\dot{\xi}, \tag{3.26}$$

where the upper sign is for $\theta \in [-\pi/2, \pi/2]$ and the lower one for $\theta \in (\pi/2, 3\pi/2)$. An integration of this equation gives the result

$$t = \mp i\frac{\sqrt{2}b\log(\sqrt{2}a\cos(\xi/2) + b)}{a\sqrt{1 - C_1^2\cot^2(\xi/2)}|\sin(\xi/2)|}, \tag{3.27}$$

where

$$a = \sqrt{1 + C_1^2} \quad \text{and} \quad b = \sqrt{-1 + C_1^2 + \cos\xi(1 + C_1^2)}.$$

The last characteristic equation in (3.24) can be written as

$$\dot{f}_\lambda = \frac{\partial f_\lambda}{\partial\xi}\dot{\xi} = \left(\lambda - \frac{i\cos\theta}{2\sin\xi}\right)f_\lambda$$

such that

$$\frac{\partial f_\lambda}{\partial\xi} = \left(i\frac{\lambda}{\cos\theta} + \frac{1}{2\sin\xi}\right)f_\lambda.$$

Eq. (3.26) can be inserted into the last equation such that after an integration we get the result

$$\log f_\lambda = \lambda t + \log\left(\sqrt{\tan(\xi/2)}\right) + C,$$

where $t$ is given by Eq. (3.27) and $C$ is an integration constant. The final solution to the PDE (3.22) is thus given by

$$f_\lambda(\xi, \theta) = \mathcal{N}_1\left[\sqrt{\tan(\xi/2)}\left(\sqrt{2}\cos(\xi/2)\alpha_1 + \sqrt{2}i\cos\theta\sin(\xi/2)\right)^{\frac{2\lambda}{\alpha_1}}\right]\Omega_1(\sin\theta\tan(\xi/2)), \tag{3.28}$$

where

$$\alpha_1(\xi, \theta) = \sqrt{1 + \sin^2\theta\tan^2(\xi/2)}.$$

The $\pm$ disappeared when we inserted Eq. (3.25) into $b$. In summary, the function (3.28) is a product of two independent parts: the term in the square brackets solves Eq. (3.22) and the $C^1$-function $\Omega_1(\sin\theta\tan(\xi/2))$ is annihilated by the left hand side of Eq. (3.23) (see Appendix E). Though an arbitrary choice for $\Omega_1$ still solves Eq. (3.22), boundary conditions determine this function unambiguously.

In the next two subsections we will study the spectrum of the operator $\hat{A}$ on the two Hilbert spaces $\mathcal{H}_A = L^2(\bar{\mathbb{R}}_B, d\mu_B) \otimes L^2(U(1), d\theta)$ and $L^2(S^2, d\mu_H)$. This will be a neat example to show the importance of the quantization procedure and the resulting Hilbert space.

44

## Spectrum of $\hat{A}$ on $\mathcal{H}_A$

In the previous section we constructed a symmetric operator $\hat{A}$ with respect to the scalar product (3.15) on $\mathcal{H}_A$, i.e. $\hat{A} = \hat{A}^+$ with domain $\mathcal{D}(\hat{A}) \subset \mathcal{D}(\hat{A}^+)$. However, whether the functions $f_\lambda$ are normalizable on $\mathcal{H}_A$ depends on the initial value problem, i.e. on the function $\Omega_1(\sin\theta\tan(\xi/2))$. The simplest case $\Omega_1(\sin\theta\tan(\xi/2)) \equiv 1$ results in a non-normalizable function $f_\lambda$ as the integral of $\tan(\xi/2)$ over one period is not finite. The conclusion is that the the spectrum of $\hat{A}$ does not have a discrete part. On the other hand if we choose $\Omega_1 = \exp(\gamma\sin^2\theta\tan^2(\xi/2))$, $\gamma > 0$, the eigenfunctions $f_\lambda$ become normalizable. In this subsection we study the more difficult case $\Omega_1 \equiv 1$ and give a possible domain for $\hat{A}$ to check if there exists a self-adjoint extension of $\hat{A}$. However, we do not intend to give a rigorous proof but just a sketch of a possible construction.

Since every almost periodic function $f(x)$ is bounded a necessary condition for the inverse $(f(x))^{-1}$ to be almost periodic is that $\min_x |f(x)| \neq 0$. It follows that $(\sin\xi)^{-1}$ is not an almost periodic function. We thus define the domain

$$\mathcal{D}(\hat{A}) := \{\varphi \in L^2(\bar{\mathbb{R}}_B) \otimes L^2(U(1)) | \hat{A}\varphi \in L^2(\bar{\mathbb{R}}_B) \otimes L^2(U(1))\} \subset H^1(\bar{\mathbb{R}}_B) \otimes H^1(U(1)). \tag{3.29}$$

The reason why $\mathcal{D}(\hat{A})$ is a subset of $H^1(\bar{\mathbb{R}}_B) \otimes H^1(U(1))$ is that any $\varphi \in \mathcal{D}(\hat{A})$ has to remove the pole caused by $(\sin\xi)^{-1}$. On the other hand, thanks to $\sin\theta$ in front of the differential operator $i\partial/\partial\theta$, the boundary term of an integration by part is automatically annihilated so that no boundary conditions on $\theta$ have to be imposed.

A criterion to check for possible self-adjoint extentions of an operator is to check

$$\langle g, \hat{A}f + if\rangle = 0 \implies g = 0, \ \forall f \in \mathcal{D}(\hat{A}). \tag{3.30}$$

If we assume that the weak derivative of $g$ exists we have

$$\langle g, \hat{A}f\rangle = \lim_{T\to\infty} \frac{1}{2T} \int_{-T}^{T} d\xi \int_0^{2\pi} d\theta f\left(\bar{g} + \cos\theta(\partial_\xi\bar{g}) - \frac{\cos\theta}{2\sin\xi}\bar{g} - \frac{\sin\theta}{\sin\xi}(\partial_\theta\bar{g})\right),$$

i.e.

$$\bar{g} + \cos\theta(\partial_\xi\bar{g}) - \frac{\cos\theta}{2\sin\xi}\bar{g} - \frac{\sin\theta}{\sin\xi}(\partial_\theta\bar{g}) = 0.$$

The solution to this nonlinear partial differential equation also contains the function $\sqrt{\tan(\xi/2)}$ such that $g \notin L^2(\bar{\mathbb{R}}_B) \otimes L^2(U(1))$. Thus, the only solution to the criterium (3.30) is $g = 0$. However, we would like to point out that we had to assume that the weak derivative of $g$ exists. If this assumption is correct then the operator $\hat{A}$ should be self-adjoint with real continuous spectrum.

## Spectrum of $\hat{A}$ on $L^2(S^2)$

Although the LQC-operator $\hat{A}$ acts on functions in $\mathcal{H}_A$ this subsection is devoted to interpreting this operator on $L^2(S^2, d\mu_H)$ which are the square integrable functions on the two-dimensional sphere $S^2$ with Haar measure $d\mu_H = \sin\xi d\xi d\theta$ for $\xi \in [0,\pi]$ and $\theta \in [0,2\pi]$. Thus, this Hilbert space has the following scalar product:

$$\langle f, g\rangle_{S^2} = \int_0^{2\pi}\int_0^\pi \sin\xi \bar{f}(\xi,\theta)g(\xi,\theta)d\xi d\theta.$$

Surprisingly the functions $f_\lambda$ are normalizable such that the spectrum of $\hat{A}$ is discrete. This is in stark contrast with the Bohr compactification where they were not normalizable, thus showing beautifully the fact that LQC chooses a unitarily inequivalent representation.

**Quantization of $p^2{}_3$**

The eigenfunctions of $\hat{p}^2{}_3$ can be obtained by applying the same procedure on the symmetrized operator

$$\hat{B} := -i\sin\theta\frac{\partial}{\partial\xi} - i\frac{\cos\theta}{\sin\xi}\frac{\partial}{\partial\theta} + \frac{i}{2}\frac{\sin\theta}{\sin\xi}$$

The eigenfunctions $g_\lambda(\xi,\theta)$ are given by

$$g_\lambda(\xi,\theta) = \frac{\sqrt{2}\mathcal{N}_2}{\sqrt{\tan(\xi/2)}}\left(\cos(\xi/2)\alpha_2 + i\cos(\xi/2)\tan\theta\right)^{\frac{2\lambda}{\sqrt{\cos^2\theta\tan^2(\xi/2)-1}}}\Omega_2(\cos\theta\tan(\xi/2)),$$

(3.31)

where

$$\alpha_2 = \sqrt{1 - \frac{\cot^2(\xi/2)}{\cos^2\theta}}$$

and $\Omega_2$ is any $C^1$-function that can be determined by boundary conditions. Both the exponent and the base can be complex such that $g_\lambda$ is not uniquely determined. We can write $g_\lambda$ as

$$g_\lambda(\xi,\theta) = \frac{k_2}{\sqrt{\tan(\xi/2)}}e^{F_1(\xi,\theta)\ln F_2(\xi,\theta)}$$

with the logarithm defined by $\ln F_2 = \mathrm{Ln}F_2 + 2\pi i n$, where $n \in \mathbb{Z}$ and $\mathrm{Ln}$ is the principal value of the logarithm. Inserting this solution into the eigenvalue problem $\hat{B}g_\lambda = \lambda g_\lambda$ it can be shown that there is only a solution for $n = 0$. For the case $\Omega_2 \equiv 1$ the eigenfunctions $g_\lambda$ are not normalizable since the integral of $1/|\tan(\xi/2)|$ over one period is not finite. In such a case we are led to the conclusion that the spectrum of $\hat{B}$ does not contain a discrete part. We can construct a dense subspace $\mathcal{D}(\hat{B})$ along the lines described in Section 3.6.1, the only difference being that $g_\lambda$ has poles at $\xi = 2k\pi$ and $\theta = (2k+1)\pi/2$ whereas $f_\lambda$ has poles at $\xi = (2k+1)\pi$, $k \in \mathbb{Z}$.



Figure 3.1: Absolute value of the eigenfunctions $f_\lambda(\xi,\theta)$ (left panel) and $g_\lambda(\xi,\theta)$ (right panel). The black thick line is the eigenfunction for $\lambda = 1$, $\theta = 1$ and the black dashed line for $\lambda = 2$, $\theta = 1$.

### 3.6.2   Quantization: $2^{\mathrm{nd}}$ Possibility

In the last section we replaced the configuration variables $Q_I$ with $\sin(\delta_I Q_I)/\delta_I$, where $\delta_I$ played the role of a regulator. The question we may ask is to what extend this substitution
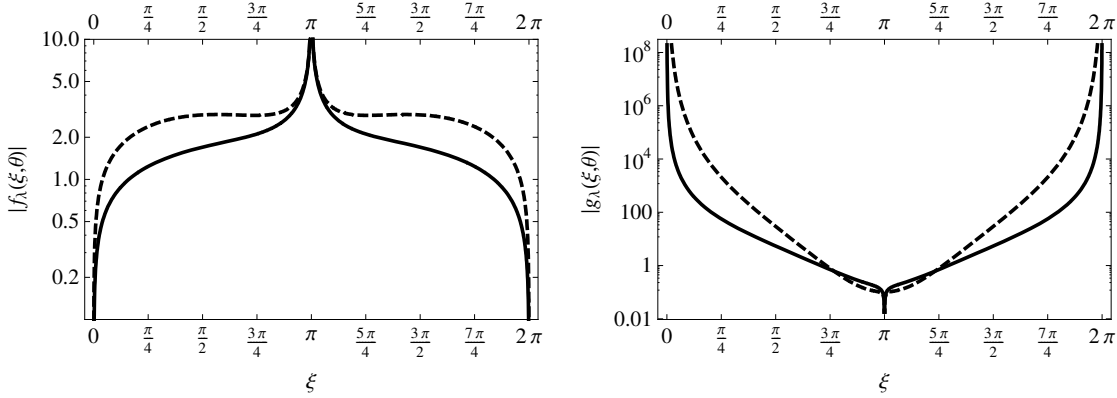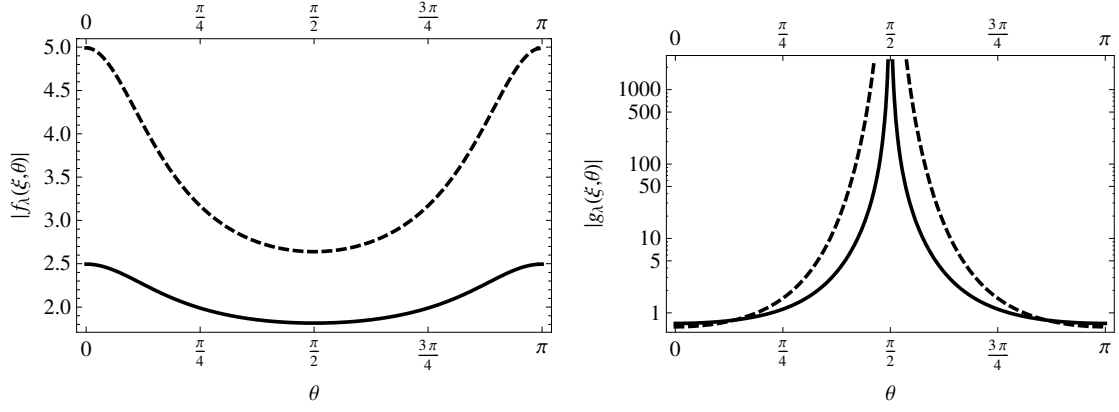
Figure 3.2: Absolute value of the eigenfunctions $f_\lambda(\xi, \theta)$ (left panel) and $g_\lambda(\xi, \theta)$ (right panel). The black thick line is the eigenfunction for $\lambda = 1$, $\xi = 2$ and the black dashed line for $\lambda = 2$, $\xi = 2$.

changes the eigenfunctions. Let us define the symmetrized operator $\hat{A}_2$ quantized without the substition of $Q_I$ as

$$\hat{A}_2 = -i\cos\theta \frac{\partial}{\partial \xi} + i\frac{\sin\theta}{\xi}\frac{\partial}{\partial \theta} + \frac{i}{2}\frac{\cos\theta}{\xi}.$$

The solution to the eigenvalue problem $\hat{A}_2 f_\lambda(\xi, \theta) = \lambda f_\lambda(\xi, \theta)$ is given by

$$f_\lambda(\xi, \theta) = \exp\left(i\lambda\xi\cos\theta\right)\sqrt{\xi}\Gamma(\log(\xi\sin\theta)),$$

These eigenfunctions are not almost periodic in $\xi$ because of the term $\sqrt{\xi}$. However we can choose the function $\Gamma$ such that $\sqrt{\xi}$ disappears, i.e. we set

$$\Gamma = \mathcal{N}_1 \exp\left(-\frac{1}{2}\log(\xi\sin\theta)\right),$$

where $\mathcal{N}_1$ is a constant, such that the eigenfunctions to $\hat{A}_2$ are given by

$$f_\lambda(\xi, \theta) = \mathcal{N}_1 \frac{\exp(i\lambda\xi\cos\theta)}{\sqrt{\sin\theta}}. \tag{3.32}$$

The above eigenfunction is almost periodic in $\xi$ but fails to be normalizable on $L^2(\bar{\mathbb{R}}_B) \otimes L^2(U(1))$. As in the preceding section the spectrum of $\hat{A}_2$ is thus continuous. Note that the eigenfunction is constant in the non-diagonal limit $\theta \to \pi/2$.

Similarly the eigenfunctions of the symmetrized operator

$$\hat{B}_2 = -i\sin\theta\frac{\partial}{\partial \xi} - i\frac{\cos\theta}{\xi}\frac{\partial}{\partial \theta} + \frac{i}{2}\frac{\sin\theta}{\xi}$$

are given by

$$g_\lambda(\xi, \theta) = \mathcal{N}_2\frac{\exp\left(-i\lambda\xi\sin\theta\right)}{\sqrt{\cos\theta}}. \tag{3.33}$$

The diagonal limit $\theta \to 0$ of $g_\lambda$ is just a constant function such that $\hat{p}^2{}_3$, i.e. the expectation value $\langle \hat{p}^2{}_2 \rangle$ measures the 'diagonality' of the torus and $\langle \hat{p}^2{}_3 \rangle$ its departure. Once again,

47

the eigenfunctions $g_\lambda$ fail to be normalizable on the Hilbert space such that the spectrum of $\hat{B}_2$ is continuous. Also note that contrary to the first method the commutator between both operators vanishes

$$[\hat{A}_2, \hat{B}_2] = 0. \tag{3.34}$$

such that both $\hat{A}_2$ and $\hat{B}_2$ can be diagonalized simultaneously which will be important in Section 3.6.3.

### 3.6.3  Volume Operator

The classical expression for the volume of $V$ is given by

$$\mathcal{V}(V) = \int_V \sqrt{\left| \frac{1}{6} \epsilon_{abc} \epsilon_{ijk} E^{ai} E^{bj} E^{ck} \right|} d^3 x.$$

Inserting the definition of the homogeneous densitized triad (2.16) we get:

$$\mathcal{V}(V) = \sqrt{\mathfrak{k} \, |p^1{}_1 (p^2{}_2 p^3{}_3 - p^2{}_3 p^3{}_2)|} \tag{3.35}$$

The factor $\mathfrak{k}$ depends on the specific form of the torus. If the torus is cubic we have $\mathfrak{k} = 1$ such that Eq. (3.6.3) reduces to Eq. (4.5) in [36]. Using the classical solution of the Gauss constraint we get the following expression for the physical volume of the torus:

$$\mathcal{V}(V) = \sqrt{\mathfrak{k} \left| p^1{}_1 \left[ p^2{}_2 p^3{}_3 - p^2{}_3 \frac{\phi_2{}^2 p^2{}_3 - \phi_2{}^3 p^2{}_2}{\phi_3{}^3} \right] \right|}$$

or in terms of the new variables

$$\mathcal{V}(V) = \sqrt{\mathfrak{k} \left| \frac{P^1}{Q_2 Q_3} \right| \times \left| \left( (P_\Theta)^2 - P^2 P^3 Q_2 Q_3 \right) \cos \Theta + \right.}$$

$$\left. + P_\Theta (P^2 Q_2 + P^3 Q_3) \sin \Theta \right|^{1/2}. \tag{3.36}$$

**Quantization of the Volume Operator according to 1ˢᵗ Method**

To perform a quantization of the volume operator we insert the definitions (3.20) into $\hat{\mathcal{V}}(V)$. Despite the fact that we know the eigenfunctions of the operators $\hat{p}^I{}_i$ it is not straightforward to give the eigenfunctions of the volume operator $\hat{\mathcal{V}}$ because, as explained in Section 3.6, the $\hat{p}^I{}_i$ do not necessarily commute. Thus the difficult task is to determine the spectrum of the operator

$$\hat{\mathfrak{V}} := \hat{p}^2{}_2 \hat{p}^3{}_3 - \hat{p}^3{}_2 \hat{p}^2{}_3 = \frac{\cos \Theta}{\sin Q_2 \sin Q_3} \frac{\partial^2}{\partial \Theta^2} - \cos \Theta \frac{\partial^2}{\partial Q_2 \partial Q_3}$$

$$+ \frac{\sin \Theta}{\sin Q_3} \frac{\partial^2}{\partial \Theta \partial Q_2} + \frac{\sin \Theta}{\sin Q_2} \frac{\partial^2}{\partial \Theta \partial Q_3}. \tag{3.37}$$

However, this operator is not symmetric on $\mathcal{H}^S$. Let us define the symmetric operator

$$\hat{\mathfrak{V}}^S := \frac{1}{2} \left( \hat{\mathfrak{V}}^+ + \hat{\mathfrak{V}} \right).$$

A calculation shows that $\hat{\mathfrak{V}}^S$ is given by

$$\hat{\mathfrak{V}}^S = \hat{\mathfrak{V}} + \frac{1}{2}\left(-\frac{\cos\Theta}{\sin Q_2 \sin Q_3} - 2\frac{\sin\Theta}{\sin Q_2 \sin Q_3}\frac{\partial}{\partial\Theta} + \frac{\cos\Theta}{\sin Q_3}\frac{\partial}{\partial Q_2} + \frac{\cos\Theta}{\sin Q_2}\frac{\partial}{\partial Q_3}\right)$$

This operator is rather complicated and no analytic solutions to the eigenvalue problem could be found.

### Quantization of the Volume Operator according to 2$^{\text{nd}}$ Method

In this subsection we consider the quantization of $\mathcal{V}$ as described in Section 3.6.2 where the commutator between $\hat{p}^I{}_i$ and $\hat{p}^J{}_j$ vanishes. This fact simplifies dramatically the analysis because the (generalized) eigenvalue problem can now be written in terms of products and sums of the eigenfunctions of the $\hat{p}^I{}_i$. Let us define

$$T_{\lambda_1,\lambda_{22},\lambda_{23},\gamma_{33},\gamma_{32}} := \mathcal{N}_{\lambda_1} \otimes (f_{\lambda_{22}}g_{\lambda_{23}}) \otimes (f'_{\gamma_{33}}g'_{\gamma_{32}}),$$

where $f_\gamma(Q_2,\theta_1)$, $g_\gamma(Q_2,\theta_1)$, $f'_\gamma(Q_3,\theta_2)$ and $g'_\gamma(Q_3,\theta_2)$ are the (generalized) eigenfunctions of $\hat{p}^2{}_2$, $\hat{p}^2{}_3$, $\hat{p}^3{}_3$ and $\hat{p}^3{}_2$, respectively, given in Section 3.6.2. Furthermore we denoted the eigenfunctions of $\hat{p}^1{}_1$ by $\mathcal{N}_{\lambda_1} := \langle Q_1|\lambda_1\rangle$. Since we have

$$(f_{\lambda_{22}}g_{\lambda_{23}})(f'_{\gamma_{33}}g'_{\gamma_{32}}) \propto \frac{\exp\left(iQ_2(\lambda_{22}\cos\theta_1 - \lambda_{23}\sin\theta_1)\right)}{\sqrt{\sin\theta_1\cos\theta_1}}\frac{\exp\left(iQ_3(\gamma_{33}\cos\theta_2 - \gamma_{32}\sin\theta_2)\right)}{\sqrt{\sin\theta_2\cos\theta_2}}$$

we see that $T_{\lambda_1,\lambda_{22},\lambda_{23},\gamma_{33},\gamma_{32}}$ is not normalizable in $\mathcal{H}^S$. The generalized eigenvalue problem is thus given by

$$\hat{\mathcal{V}}T_{\lambda_1,\lambda_{22},\lambda_{23},\gamma_{33},\gamma_{32}}[\varphi] = T_{\lambda_1,\lambda_{22},\lambda_{23},\gamma_{33},\gamma_{32}}[\hat{\mathcal{V}}\varphi]$$
$$= \gamma^{3/2}l_{\text{Pl}}^3\sqrt{k|\lambda_1(\lambda_{22}\gamma_{33} - \lambda_{23}\gamma_{32})|}T_{\lambda_1,\lambda_{22},\lambda_{23},\gamma_{33},\gamma_{32}}[\varphi] \qquad (3.38)$$

for $\varphi \in \mathcal{D}(\hat{\mathcal{V}})$.

### 3.6.4  Quantum Gauss Constraint

In Section 2.4 we computed the classical Gauss constraint for a Bianchi type I model. In the open case, i.e. the topology is $\mathbb{R}^3$, the elementary variables can always be diagonalized such that both the diffeomorphism and Gauss constraints are automatically satisfied. In the closed model or in models with a rotational symmetry [10, 70, 71, 72] this is not the case anymore so that a quantization of the constraints is mandatory. Since in Bianchi type I models the diffeomorphism constraint is proportional to the Gauss constraint we only need to quantize and solve the latter. However, contrary to the diffeomorphism constraint the Gauss constraint can be quantized infinitesimally. The construction is analogous to electromagnetism (see Section 3.1): starting with a kinematic Hilbert space a new Hilbert space is constructed which does not incorporate the unphysical degrees of freedom (in the case of photons we saw that the longitudinal and scalar polarization were unphysical).

A gauge transformation of an $su(2)$-connection is given by

$$A \mapsto A' = \lambda^{-1}A\lambda + \lambda^{-1}d\lambda$$

where $\lambda : \Sigma \mapsto SU(2)$. Infinitesimally we can write this equation as

$$A_a^i \mapsto A_a'^i = A_a^i + \partial_a\epsilon^i + \epsilon^i{}_{jk}\epsilon^j A_a^k + \mathcal{O}(\epsilon^2).$$

The classical Gauss constraint ensuring $SU(2)$-invariance is given by

$$G(\Lambda) = -\int_{\mathbb{T}^3} d^3x\, E_j^a D_a \Lambda^j$$

where $D_a\Lambda^j = \partial_a\Lambda^j + \epsilon^j{}_{kl}A_a^k\Lambda^l$ is the covariant derivative of the smearing field $\Lambda^j$. The infinitesimal quantization of this expression yields an operator containing a sum of right and left invariant vector fields over the edges of the torus. This operator is essentially self-adjoint and can, by Stone's theorem, be exponentiated to a unitary operator $U_\phi$ defining a strongly continuous one-parameter group in $\phi$. Usually, in order to find the kernel of the Gauss constraint operator one restricts the scalar product on $\mathcal{H}_{\mathrm{kin}}$ to the gauge-invariant scalar product on $\mathcal{H}_{\mathrm{inv}}^G$. This Hilbert space is a true subspace of $\mathcal{H}_{\mathrm{kin}}$ since zero is in the discrete part of the spectrum of the Gauss constraint operator.

We saw in Section 2.6 that thanks to the symmetry reduction two of the Gauss constraints are automatically satisfied. While the nonvanishing Gauss constraint (2.24) is still a complicated function in $\phi_I{}^i$ and $p^J{}_j$ it simplifies to Eq. (2.30) after the canonical transformation. A quantization of this expression is then given by

$$\hat{G}_1 = \hat{P}_{\theta_1} - \hat{P}_{\theta_2}.$$

Since the eigenstates of the momentum operators $\hat{P}_{\theta_\alpha}$ are the strict periodic functions satisfying Eq. (3.17) the action of the Gauss constraint on $|\vec{\mu}, \vec{k}\rangle$ is given by

$$\hat{G}_1|\vec{\mu}, \vec{k}\rangle = \frac{\gamma l_{\mathrm{Pl}}^2}{2}(k_1 - k_2)|\vec{\mu}, \vec{k}\rangle$$

which vanishes if

$$k_1 = k_2.$$

We can thus introduce a new variable $\Theta := \theta_1 + \theta_2$ such that the algebra $\mathcal{A}_S$ given by Eq. (3.14) reduces to the invariant algebra $\mathcal{A}_S^{\mathrm{inv}}$ generated by the functions

$$\begin{aligned}
g(Q_1, Q_2, Q_3, \Theta) &= \sum_{\lambda_1,\lambda_2,\lambda_3,k} \xi_{\lambda_1,\lambda_2,\lambda_3,k} \times \\
&\times \exp\left(\frac{1}{2}i\lambda_1 Q_1 + \frac{1}{2}i\lambda_2 Q_2 + \frac{1}{2}i\lambda_3 Q_3 + ik\Theta\right).
\end{aligned} \tag{3.39}$$

A Cauchy completion leads to the invariant Hilbert space $\mathcal{H}_{\mathrm{inv}}^S = \mathcal{H}_B^{\otimes 3} \times \mathcal{H}_{S^1}$. A comparison with $\mathcal{H}^S$ shows that we 'lost' one Hilbert space $\mathcal{H}_{S^1}$ by solving the quantum Gauss constraint. Furthermore, instead of two momentum operators conjugated to $\theta_1$ and $\theta_2$ we have just one momentum operator conjugated to $\Theta$ defined by

$$\hat{P}_\Theta = -i\gamma l_{\mathrm{Pl}}^2 \frac{\partial}{\partial\Theta}.$$

The eigenstates of all momentum operators are given by

$$|\vec{\mu}, k\rangle := |\mu_1, \mu_2, \mu_3, k\rangle,$$

where $k \in \mathbb{Z}$ defines the representation of $U(1)$.

## 3.7 Quantum Dynamics

In this section we are interested in the quantum dynamics of loop quantum cosmology. We shall first introduce the novel way of quantizing the Hamilton constraint and apply it to isotropic LQC. As a next step we shall derive this constraint in the case of toroidal topology.

### 3.7.1 The Hamiltonian Constraint in Isotropic LQC

Thanks to spatial flatness the Hamiltonian constraint (1.12) simplifies to Eq. (1.13). Inserting the homogeneous and isotropic variables we get the Hamiltonian (2.22). However, we saw in Sec. 3.4 that there is no well defined operator $\hat{c}$ on the Hilbert space $L^2(\bar{\mathbb{R}}_B, d\mu_B)$. The solution was to write all expressions in terms of holonomies. The same strategy has to be followed for the quantization of the Hamiltonian constraint. But the situation is far more complicated since Eq. (1.13) incorporates the components of the curvature two-form and a non-polynomial dependence on the densitized triad. We will only give a short review of the quantization of the Hamiltonian constraint, further details can be found in [11, 101, 103, 102, 104].

In order to quantize the curvature two-form we use well known results from lattice quantum field theory and compute holomomies around a square $\Box_{ij}$ in the $i - j$ plane spanned by two of the triad vectors ${}^0e_i^a$ with length $\mu_0 V_0^{1/3}$ w.r.t. ${}^0q_{ab}$ (see Sec. 3.4). The curvature is then given by

$$F_{ab}^i \tau_i = {}^0\omega_a^i {}^0\omega_b^j \left( \frac{h_{\Box_{ij}}^{(\mu_0)}}{\mu_0^2 V_0^{2/3}} + \mathcal{O}(c^3 \mu_0) \right),$$

where the holomony $h_{\Box_{ij}}^{(\mu_0)}$ is given by

$$h_{\Box_{ij}}^{(\mu_0)} = h_i^{(\mu_0)} h_j^{(\mu_0)} (h_i^{(\mu_0)})^{-1} (h_j^{(\mu_0)})^{-1}$$

and $h_i^{(\mu_0)}$ by Eq. (3.8).

Turning our attention to the quantization of the inverse of the triad we see that in the isotropic case $e$ only vanishes when the triad itself vanishes, implying that the expression $\epsilon_{ijk} e^{-1} E^{aj} E^{bk}$ is not singular. However, such a procedure is not available in the full theory and one has to use Thiemann's trick [101] to reexpress this singular term in terms of Poisson brackets (no summation over $k$):

$$\epsilon_{ijk} \tau^i e^{-1} E^{aj} E^{bk} = -\frac{(\mathrm{sgn}p)}{2\pi G \gamma \mu_0 V_0^{1/3}} \epsilon^{abc} {}^0\omega_c^k h_k^{(\mu_0)} \{h_k^{(\mu_0)-1}, V\}.$$

Inserting the last three equations into the Hamiltonian constraint Eq. (1.13) yields

$$
\begin{aligned}
C_{\mathrm{grav}} &\equiv \frac{1}{2\kappa} N\mathcal{H} \\
&= -\frac{4(\mathrm{sgn}p)}{8\pi G \gamma^3 \mu_0^3} \sum_{ijk} \epsilon^{ijk} \mathrm{tr}\left( h_i^{(\mu_0)} h_j^{(\mu_0)} (h_i^{(\mu_0)})^{-1} (h_j^{(\mu_0)})^{-1} h_k^{(\mu_0)} \{h_k^{(\mu_0)-1}, V\} \right) + \mathcal{O}(c^3\mu_0).
\end{aligned}
$$

The leading term is finite and, following the canonical quantization program (see Sec. 3.2), can be faithfully promoted to an operator by replacing the Poisson bracket by a commutator

and promoting the holonomies and the volume to operators. The resulting constraint is then given by [11]

$$
\begin{aligned}
\hat{C}_{\mathrm{grav}}^{(\mu_0)} &= \frac{4i(\mathrm{sgn}p)}{8\pi\gamma^3\mu_0^3 l_{\mathrm{Pl}}^2} \sum_{ijk} \epsilon^{ijk} \mathrm{tr}\left(\hat{h}_i^{(\mu_0)}\hat{h}_j^{(\mu_0)}(\hat{h}_i^{(\mu_0)})^{-1}(\hat{h}_j^{(\mu_0)})^{-1}\hat{h}_k^{(\mu_0)}[\hat{h}_k^{(\mu_0)-1},\hat{V}]\right) \\
&= \frac{24i(\mathrm{sgn}p)}{8\pi\gamma^3\mu_0^3 l_{\mathrm{Pl}}^2} \sin^2\frac{\mu_0 c}{2}\cos^2\frac{\mu_0 c}{2} \\
&\quad \times \left(\sin\frac{\mu_0 c}{2}\hat{V}\cos\frac{\mu_0 c}{2} - \cos\frac{\mu_0 c}{2}\hat{V}\sin\frac{\mu_0 c}{2}\right).
\end{aligned}
\tag{3.40}
$$

Its action on eigenstates of $\hat{p}$ is given by

$$
C_{\mathrm{grav}}^{(\mu_0)}|\mu\rangle = \frac{3}{8\pi\gamma^3\mu_0^3 l_{\mathrm{Pl}}^2}(V_{\mu+\mu_0} - V_{\mu-\mu_0})(|\mu + 4\mu_0\rangle - 2|\mu\rangle + |\mu - 4\mu_0\rangle).
\tag{3.41}
$$

When coupled to a scalar field the quantum constraint has the form

$$
\hat{C}_{\mathrm{grav}}^{(\mu_0)} + \hat{C}_\phi = 0,
\tag{3.42}
$$

where $\hat{C}_\phi = \kappa(\widehat{1/p^{3/2}})(\hat{p}_\phi^2)$. In such a case the program described in Sec. 3.2 could be carried out for the first time [13, 14], that is, compute physical observables, the physical Hilbert space and a physical Hamiltonian. The main result is that the big bang is replaced by a big bounce and the quantum evolution is deterministic across the Planck regime. For further details we refer the reader to these beautiful works.

### 3.7.2 The Hamiltonian Constraint in Toroidal LQC

Here we are interested in deriving the gravitational Hamiltonian for the case of toroidal topology. Inserting Eq. (3.13) into the first line of (3.40) we get

$$\hat{C}_{\text{grav}} = \frac{4i(\text{sgn}p)}{\gamma^3 \mu_0^3 l_{\text{Pl}}^2} \times$$

$$\left[ 4 \cos\left(\theta_1 + \theta_2 - \frac{{}^0\mu_1 Q_1}{2}\right) \sin\frac{{}^0\mu_1 Q_1}{2} \sin({}^0\mu_3 Q_3) \sin\frac{{}^0\mu_2 Q_2}{2} \hat{V} \cos\frac{{}^0\mu_2 Q_2}{2} \right.$$

$$- 4 \cos^2\theta_2 \sin\theta_1 \sin({}^0\mu_1 Q_1) \sin^2\frac{{}^0\mu_3 Q_3}{2} \sin\frac{{}^0\mu_2 Q_2}{2} \hat{V} \cos\frac{{}^0\mu_2 Q_2}{2}$$

$$- 2 \cos\theta_2 \sin({}^0\mu_1 Q_1) \sin({}^0\mu_3 Q_3) \cos\frac{{}^0\mu_2 Q_2}{2} \hat{V} \sin\frac{{}^0\mu_2 Q_2}{2}$$

$$- 4 \sin\theta_1 \sin^2\theta_2 \sin({}^0\mu_1 Q_1) \sin^2\frac{{}^0\mu_3 Q_3}{2} \sin\frac{{}^0\mu_2 Q_2}{2} \hat{V} \sin\frac{{}^0\mu_2 Q_2}{2}$$

$$- 4 \sin\theta_2 \sin^2\frac{{}^0\mu_1 Q_1}{2} \sin({}^0\mu_3 Q_3) \cos\frac{{}^0\mu_2 Q_2}{2} \hat{V} \sin\frac{{}^0\mu_2 Q_2}{2} \qquad (3.43)$$

$$+ 4 \cos\left(\theta_1 + \theta_2 + \frac{{}^0\mu_1 Q_1}{2}\right) \sin\frac{{}^0\mu_1 Q_1}{2} \sin({}^0\mu_2 Q_2) \sin\frac{{}^0\mu_3 Q_3}{2} \hat{V} \cos\frac{{}^0\mu_3 Q_3}{2}$$

$$- 4 \cos\left(\theta_1 + \frac{{}^0\mu_1 Q_1}{2}\right) \sin\frac{{}^0\mu_1 Q_1}{2} \sin({}^0\mu_2 Q_2) \cos\frac{{}^0\mu_3 Q_3}{2} \hat{V} \sin\frac{{}^0\mu_3 Q_3}{2}$$

$$- 4 \sin\theta_2 \sin({}^0\mu_1 Q_1) \sin^2\frac{{}^0\mu_2 Q_2}{2} \sin\frac{{}^0\mu_3 Q_3}{2} \hat{V} \sin\frac{{}^0\mu_3 Q_3}{2}$$

$$+ 8 \cos(\theta_1 + \theta_2) \sin\frac{{}^0\mu_2 Q_2}{2} \sin\frac{{}^0\mu_3 Q_3}{2}$$

$$\times \left( \sin(\theta_1 + \theta_2) \sin\frac{{}^0\mu_2 Q_2}{2} \sin\frac{{}^0\mu_3 Q_3}{2} - \cos\frac{{}^0\mu_2 Q_2}{2} \cos\frac{{}^0\mu_3 Q_3}{2} \right)$$

$$\left. \times \left( \cos\frac{{}^0\mu_1 Q_1}{2} \hat{V} \sin\frac{{}^0\mu_1 Q_1}{2} - \sin\frac{{}^0\mu_1 Q_1}{2} \hat{V} \cos\frac{{}^0\mu_1 Q_1}{2} \right) \right]$$

As a cross-check, setting $\theta_1 = \theta_2 = 0$, ${}^0\mu_1 = {}^0\mu_2 = {}^0\mu_3 \equiv {}^0\mu$ and $Q_1 = Q_2 = Q_3 \equiv Q$ we see that Eq. (3.43) reduces to Eq. (3.40). However, with this complicated an expression it seems hopeless to even write a difference equation such as Eq. (3.41) since even the (generalized) eigenfunctions of $\hat{V}$ are either unknown as in the 1$^{\text{st}}$ quantization method or very complicated as in the 2$^{\text{nd}}$ method (see Sec. 3.6.3). Moreover this Hamiltonian constraint must be symmetrized which can be done by defining

$$\hat{C}_{\text{grav}}^S = \frac{1}{2}\left( \hat{C}_{\text{grav}} + \hat{C}_{\text{grav}}^\dagger \right),$$

where $\hat{C}_{\text{grav}}$ is the adjoint of $\hat{C}_{\text{grav}}$ on $L^2(\bar{\mathbb{R}}_B^3) \otimes L^2(U(1)^2)$. In principle numerical solutions could be found by e.g. coupling $\hat{C}_{\text{grav}}^S$ with a massless scalar field to obtain an equation similar to Eq. (3.42). In spite of the fact that it would be very interesting to know the behavior of such an LQC torus, the numerical endeavor is well beyond the scope of this thesis.

# Chapter 4

# Conclusion

In this part we studied how a torus universe affects the results of LQC. To do so we followed known mathematical results by first introducing the most general tori using Thurston's theorem. Six Teichmüller parameters are needed to parametrize such general tori. We construted a metric describing a flat space but respecting the periodicity of the covering group used to construct the torus and used it to derive a gravitational Hamiltonian. We studied the dynamics of a torus universe driven by a homogeneous scalar field by numerically solving the full Hamiltonian and saw that its form only remains cubic if all off-diagonal terms vanish. The Ashtekar connection and the densitized triad for a torus were then derived for both the most general and a slighty simplified torus. The reason for this simplification was that a simple solution to the Gauss constraint could be given. We also derived the Hamiltonian constraint in these new variables and showed that it reduces to the standard constraint of isotropic LQC in case of a cubical torus.

The passage to the quantum theory required a canonical transformation so as to be able to write the holonomies as a product of strictly and almost periodic functions. A Cauchy completion then led to a Hilbert space given by square integrable functions over both $\bar{\mathbb{R}}_B$ and $U(1)$. However the drawback of the canonical transformation is a much more complicated expression for the components of the densitized triad containing both the momentum and the configuration variables. Following the standard procedure of LQC we substituted these configuration variables with the sine thereof and were able to solve the eigenvalue problem analytically. Surprisingly it turned out that the spectrum of the triad operators can be either discrete or continuous, depending on the initial value problem. On the other hand we were also able to find almost periodic solutions to the eigenvalue problem of the triad operators without performing the substitution just described, but once again the spectrum depends can be either continuous or discrete. The reason why both ways can lead to a continuous spectrum is the non-cubical form of the torus, for if we set the angles $\theta_{1,2} = 0$ in Eq. (2.26) the triads correspond to the ones obtained in isotropic models. Furthermore we were able to find the spectrum of the volume operator for the second case because, contrary to the first case, it is a product of commuting triad operators.

We then considered the quantization of the Hamiltonian constraint. We first reviewed the isotropic case where quantum dynamics is governed by a difference equation which resolves the big bang singularity. For a torus universe it was not possible to find a difference equation because the (generalized) eigenfunctions of the volume are not known (1st method) or very complicated (2nd method). It is thus not possible to address the question whether LQC with toroidal topology resolves the big bang singularity. As a first step it would be useful to know the property of the spectrum of the Hamiltonian constraint, e.g. if it is continuous or discrete. But even this task seems to be very difficult to solve as a short

glance at Eq. (3.43).

# Part II

# Gamma-ray Bursts and Lorentz Violation

# Chapter 5

# Lorentz violation

## 5.1 Introduction

The chapter deals with something we could call phenomenological quantum gravity and its experimental implications. Since there is not yet a full quantum theory of gravity we are reduced to studying possible experimental signatures of e.g. a minimal length on the propagation of photons without a rigorous proof. In what follows we shall study the effect of such a minimal length on high energy photons emanating from so-called gamma-ray bursts. First we introduce deformed special relativity in Sec. 5.3 before explaining the important characteristics of gamma-ray bursts in Sec. 5.4 and studying the light propagation in an expanding universe in Sec. 5.5. The first main part of this chapter, based on the work [65], is devoted to giving a bound on a possible Lorentz invariance violating term using gamma-ray bursts detected by the satellite INTEGRAL. The second main part is based on [64] and made predictions whether the Fermi Gamma-ray Space Telescope (formally GLAST) could measure a Lorentz violation by means of Monte Carlo simulations of bursts.

## 5.2 Recent Developments

On May 10 2009 at 00:22:59.97 the Fermi Gamma-ray Space Telescope detected a very short gamma-ray burst (GRB 090510) lasting for less than two seconds [1] (see Figure 5.1). Subsequent ground-based observations measured the distance of this burst to be around a redshift of $z = 0.903 \pm 0.003$. A single 31-GeV photon was detected at 0.829 s after the trigger time, where the directional and temporal coincidence of this photon with GRB 090510 is considered to be with a significance of $> 5\sigma$. No evidence for the violation of Lorentz invariance could be found and, assuming a linear correction to the speed of light, only a lower limit for the quantum gravity scale of $1.2m_{\mathrm{Pl}}$ could be given [1]. Under less conservative assumptions this lower limit shifts to even $100m_{\mathrm{Pl}}$. On the other hand quadratic corrections could not be constrained.

## 5.3 Deformed Special Relativity

Every theory of Quantum Gravity (QG) contains a combination of gravity ($8\pi G$), the quantum ($\hbar$) and relativity $c$, which can for example define the so-called Planck energy $E_P = \sqrt{\hbar c^5/G} \approx 1.2 \times 10^{19}$ GeV. It is assumed that this energy marks the threshold beyond which the classical description of spacetime breaks down, resulting in new phenomena. It is well known that Special Relativity (SR) is the flat spacetime limit of General Relativity
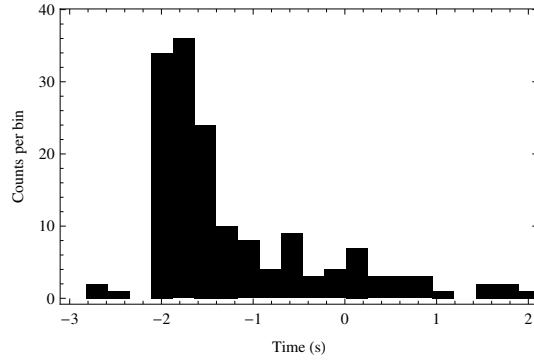
Figure 5.1: GRB 090510 as provided by the Fermi Science Support Center [49]. For the full light curve see [1].

(GR). On the other hand, the question of the flat space, semiclassical limit of QG is still open, as there does not exist a full theory of QG yet. But the Planck energy gives rise to a paradox: despite the fact that it is known from SR that the energies are observer dependent, the Planck energy does not seem to depend on the reference frame. How can this discrepency be solved without having a full QG theory at our disposal? There are at least two proposals, called Doubly or Deformed Special Relativity 1 (DSR1) [4, 5, 63, 62] and DSR2 [68, 67], which try to resolve this paradox. In this section we shall present the first possible construction of DSR.

### 5.3.1   Postulates of DSR

DSR is based on the following postulates:

- The relativity of inertial frames: when gravitational effects can be neglected all observers in free, inertial motion are equivalent. In other words, the describtion of a phenomenon can only depend on the relative motion between the observers.

- There exist two observer-independent scales: the speed of light $c$ and the Planck energy $E_P$.

- The correspondence principle: at energies much lower than $E_P$, SR and GR are valid.

### 5.3.2   Modification of the Poincaré group

**Representations of the Lorentz and Poincaré groups**

The group of isometries of the Minkowski spacetime which leave the origin fixed is called *Lorentz group*. The mathematical definition of the proper Lorentz group is given by the Lie group

$$SO(3,1) = \{M \in GL(4,\mathbb{R})|M^T\eta M = \eta, \ \det(M) = 1\},$$

where $\eta = \text{diag}(-1,1,1,1)$. This group is generated by its Lie algebra $so(3,1)$ containing the elements $L_{IJ}$, $I, J = 0, \ldots, 3$. These elements can be separated into three generators of rotations $M_l = \epsilon^{jk}{}_l L_{jk}$ and three generators of boosts $N_j = L_{j0}$, where $j, k, l = 1, 2, 3$ run over the three spatial coordinates. The commutation relations are then defined by

$$[M_j, M_k] = i\epsilon^l_{jk}M_l, \quad [M_j, N_k] = i\epsilon^l_{jk}N_l, \quad [N_j, N_k] = -i\epsilon_{jkl}M_l. \tag{5.1}$$

The *Poincaré group* is defined by the group of *all* isometries of the Minkowski spacetime, thus also allowing for translations. The Lorentz group is a subgroup of the Poincaré group, whose Lie algebra has therefore the same commutation relations (5.1) for the boosts and rotations, extended by the generators of translations $P_I$ with commutation relations

$$[M_j, P_k] = i\epsilon_{jk}^l P_l, \quad [M_j, P_0] = 0, \quad [N_j, P_k] = -i\delta_{jk} P_0, \quad [N_j, P_0] = iP_j, \quad [P_j, P_k] = 0. \tag{5.2}$$

### 5.3.3 Bicrossproduct

As its name suggests DSR is a deformation of SR with a mass scale $\kappa$, usually identified with the Planck mass. In the so-called bicrossproduct basis the Lorentz subalgebra of the Poincaré algebra is not deformed and follows the commutation relations (5.1). The deformation is only present in the way the boosts $N_j$ act on the momenta $P_k$

$$[N_j, P_k] = i\delta_{jk}\left(\frac{1}{2}(1 - e^{-2P_0/\kappa}) + \frac{\mathbf{P}^2}{2\kappa}\right) - \frac{i}{\kappa}P_j P_k$$

such that the standard commutation relations (5.2) can be recovered in the limit $\kappa \to \infty$. This algebra leads to a non-linear Casimir operator

$$\mathcal{C} = \kappa^2 \cosh\frac{P_0}{\kappa} - \frac{\mathbf{P}^2}{2}e^{P_0/\kappa} - M^2.$$

An expansion of this equation to the leading order in $1/\kappa$ yields the standard dispersion relation with an additional term

$$E^2 = p^2 + m^2 + \frac{E^3}{\kappa}. \tag{5.3}$$

Henceforth we shall define $E_{\mathrm{QG}} := \kappa$ in order to eliminate possible confusions with the gravitation constant $\kappa$.

## 5.4 Gamma-ray Bursts

Gamma-ray bursts (GRBs) are the most luminous electromagnetic events occurring in the universe since the Big Bang, with a duration from a few milliseconds to several minutes (see Fig. 5.2). They are flashes of gamma rays emanating from random places in deep space and the initial burst is followed by an afterglow emitting at longer wavelengths.
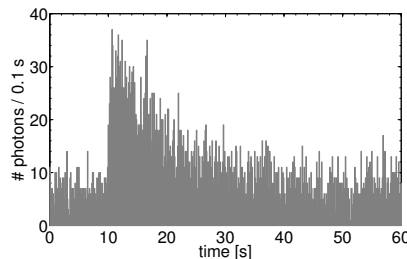


Figure 5.2: Example of a GRB detected by INTEGRAL on December 3, 2003.

The GRBs can be classified in two groups, namely the long and short bursts. The long bursts have a duration time that typically ranges from 1 s to 100s, while the short bursts last for much less than a second. This classification is possible due to the different physical origin of the bursts. The long GRBs are caused by the collapse of the core of a rapidly rotating, high-mass star into a black hole. On the other hand, the collision of two neutron stars seem to be at the origin of the short bursts.

It was pointed out that one way to probe Eq. (5.3) may be provided by GRBs [3, 6, 85]. Several studies have been conducted using measurements of GRBs [40, 41, 42, 43]. Since GRBs are located at cosmological distances, we must know how light propagates in the expanding universe, which is the topic of the next section.

## 5.5 Light Propagation in an Expanding Universe

### 5.5.1 Cosmological Model

Let the isometry group $\mathcal{S}$ be the Euclidean group so that the 3-dimensional group $T$ of translations acts simply and transitively on the 3-manifold $M$, which implies that $M$ is flat. We will assume that $M$ is topologically $\mathbb{R}^3$ with a flat 3-metric ${}^0q_{ab} := \eta_{ij}\,{}^0\omega_a^i\,{}^0\omega_b^j$ constructed from the left invariant co-triads ${}^0\omega_a^i$ satisfying ${}^0\omega_a^i({}^0e_j^a) = \delta_j^i$. The line element of the four-dimensional manifold $\mathcal{M}$ may then be given by

$$
\begin{aligned}
ds^2 &= g_{\mu\nu}\,dx^\mu \otimes dx^\nu = -dt \otimes dt + a(t)^2\,({}^0q_{ab}\,dx^a \otimes dx^b)\\
&= -dt \otimes dt + a(t)^2\,(dx \otimes dx + dy \otimes dy + dz \otimes dz)\,,
\end{aligned}
$$

where $a(t)$ is an arbitrary scale factor which can only depend on time. Solving the Hilbert-Einstein action (2.7) with a matter term given by an ideal fluid, we get a differential relation between time and redshift ($c = 1$)

$$
dt = -H_0^{-1}\frac{dz}{(1+z)h(z)},
$$

where $H_0 = 71$ km s$^{-1}$ Mpc$^{-1}$ is the Hubble parameter and

$$
h(z) = \sqrt{\Omega_\Lambda + \Omega_M(1+z)^3}
$$

with a cosmological constant $\Omega_\Lambda = 0.73$ and matter energy density $\Omega_M = 0.27$ [113].

### 5.5.2 Photon Propagation with Lorentz Invariance Violation Corrections

We consider a model in which there is a breakdown of Lorentz symmetry at an energy scale $E_{\mathrm{QG}} := E_P/\alpha$ where $\alpha \in \mathbb{R}$ and $E_P \approx 1.2 \times 10^{19}$ GeV is the Planck energy. Assuming a Lorentz Invariance Violation (LIV) correction of order $n$ we can approximate the dispersion relation for a photon with

$$
E^2 - p^2 c^2 \approx p^2 c^2 \left(\frac{E}{E_{\mathrm{QG}}}\right)^n, \tag{5.4}
$$

where $c$ is the speed of light of low-energy photons, $E$ the photon energy and $p$ its momentum. Most of the time we will only consider the linear corrections $n = 1$. For such a case, the non-standard dispersion relation (5.4) leads to an energy-dependent velocity of light, $v = v(E)$ defined by the group velocity

$$
v(E) := \frac{dE}{dp} = c\left(1 + \frac{E}{E_{\mathrm{QG}}}\right).
$$

Two photons emitted simultaneously with different propagation speed will arrive at different times. Due to the fact that GRBs are at a cosmological distance the expansion of the universe has to be taken into account, as the physical distances traveled by the particles will differ. The difference in the arrival times of two photons with energies differing by $\Delta E$ is given by [55]

$$\Delta t = \pm H_0^{-1} \frac{\Delta E}{E_{\mathrm{QG}}} \int_0^z \frac{1 + z'}{\sqrt{\Omega_\Lambda + \Omega_M(1 + z')^3}} dz'.$$

(5.5)

# Chapter 6

# Study of Lorentz Violation in INTEGRAL gamma-ray Bursts

## 6.1 INTEGRAL Satellite

INTEGRAL [111] is a mission of the European Space Agency (ESA) devoted to gamma ray astronomy. It features a coded mask instrument ISGRI [66]. This instrument enables us to measure for each photon in the energy range 15 keV to 1 MeV the arrival time with a precision of $6 \cdot 10^{-5}$ s as well as the energy with a precision of 10 %.

The detector has a dead time of about 25 %. This dead time is a function of the incoming rate and can vary during a GRB. The dead time is measured internally by the instrument and is given as a mean dead time over 8 seconds independently for 6 parts of the detector. It can be corrected statistically in weighing each incoming photon by $1/(1 - \text{dead time})$ with the corresponding time slice and detector part dead time. If the rate exceeds telemetry capabilities a data gap is created in wich the dead time is 100 %. In this case it cannot be statistically corrected and we have a hole in the data versus time. This unfortunately happens frequently during very intense GRBs.

The instrument also registers an important rate from the background due to diffuse photons from the sky, internal radioactivity of the instrument and flux from sources present in the field of view. This background rate varies with time but not perceptibly during the typical time scale of a GRB. We have two ways of predicting this background. Before and after the GRB the background can be measured as the full rate registered by the instrument. During the GRB, the pixels that are in the shadow of the mask for the direction of the GRB register only the background photons of the GRB. The illuminated pixels register this background as well as the flux from the GRBs. Statistically the rate from the GRB can be computed by properly weighed subtraction. As, most of the time, the GRBs are in the partially coded field of view, the number of pixels available for background measurement is bigger than the number of pixels seeing the source.

The fraction of a pixel that is illuminated by the GRB (so called PIF value) can be calculated with the knowledge of the coordinate of the GRB and the knowledge of the attitude of the instrument. We are not able to determine individually if a photon comes from the GRB or the background, but the PIF can be used to properly weigh its probability to come from the GRB. For example, a light curve can be built by using only pixels that are fully illuminated by the source and removing the constant rate measured by the completely opaque pixels.

## 6.2 Description of the Analysis Method

The majority of the GRBs seems to follow a pattern called Fast Raise and Exponential Decay (FRED). In order to model a GRB light curve, we parameterize it with five parameters and call the resulting probability distribution $f = f(t_i, E_i; P, B, R, D, \kappa, h)$ (see Fig. 6.1 for the meaning of these parameters). We suppose that a set of measured parameters $t_i$ and $E_i$ came from the probability density function $f$. We use the method of maximum likelihood, which consists of finding the set of values $\hat{P}$, $\hat{B}$, $\hat{R}$, $\hat{D}$, $\hat{\kappa}$ and $\hat{h}$, which maximizes the joint probability distribution for all data, given by

$$\mathcal{F}(P, B, R, D, \kappa, h) = \prod_i f(t_i, E_i; P, B, R, D, \kappa, h) \tag{6.1}$$

together with the constraint

$$\int_{t_0}^{t_1} dt' \, f(t', E_i; P, B, R, D, \kappa, h) = 1, \tag{6.2}$$

where $\mathcal{F}$ is the likelihood function and the integral runs between $t_0$ and $t_1$ as shown in Fig. 6.1. In fact, the condition (6.2) that the integral over time be equal to one reduces the degrees of freedom for $f$ and $\mathcal{F}$ by one. For example, $B$ can be chosen to be fixed by this condition, so we can think of $f$ and $\mathcal{F}$ as not depending on $B$. However, for clarity we write the $B$-term dependence for both functions.

It is easier to search for the parameters that maximize $\ln \mathcal{F}$, as the products on the right hand side of Eq. (6.1) is now a sum. To find these parameters, we use a multidimensional unconstrained nonlinear minimization where we minimize the function $-\ln \mathcal{F}$.
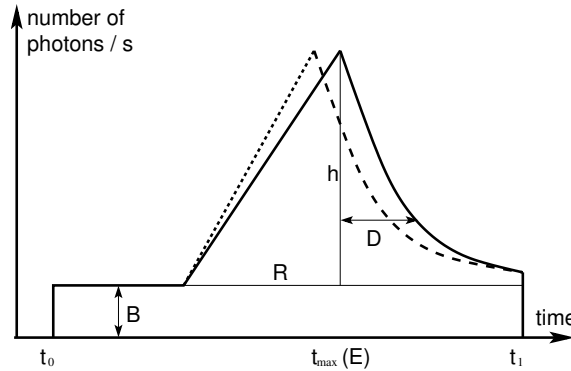


Figure 6.1: Sketch of a typical light curve of a GRB for a given energy interval. The curve is parameterized by five parameters: $B$ is the background level, $R$ the duration of the rise, $h$ the height above the background, $D$ the decay time for $\exp(-t/D)$ and $\kappa$ describes the magnitude of the dependence on the energy of the distribution $f$, $t_{\max} = P + \kappa \cdot E$, where $P$ is the time when the intensity reaches a maximum and $E$ is the photon energy. The area under the curve must be one, so that one parameter, e.g. $B$, is fixed by this condition. The dashed line shows a distribution for another energy interval that is shifted by an amount of $\Delta t = \kappa \cdot \Delta E$ sketching the shift in time due to quantum gravitational effects. This shift is usually much smaller than the other parameters.

Fig. 6.1 shows a typical light curve of a GRB. We always choose time intervals so that such a sketch can be found. However, in order to avoid wrong results, we also take account for other possibilities when for example $R > t_{\max}(E) - t_0$ or $t_1 < t_{\max}(E)$.

## 6.3 Monte Carlo Simulations

The maximum shift in time due to quantum gravity is expected to be of the order of $2 \cdot 10^{-5}$ s, which is smaller by a factor of three than the time resolution of INTEGRAL. Therefore, it is at first highly questionable whether such time differences can be measured, not to speak of the results gotten from unbinned data. In order to get a better feeling of the behavior of the likelihood, we performed Monte Carlo simulations with a total number of photons ranging from 500 to unrealistic 300000. First, we created $N$ events $i$ with energy $E_i$ distributed according to a typical GRB event. That is, a typical energy distribution for the photons of GRBs follows the pattern of the so-called Band function [22] given by the following equation:

$$
\begin{aligned}
N_E(E) \;=\; & A\left(\frac{E}{100 \text{ keV}}\right)^\alpha \exp\left(-\frac{E}{E_0}\right), \\
& \hspace{4cm} (\alpha - \beta)E_0 \geq E, \\
\;=\; & A\left[\frac{(\alpha - \beta)E_0}{100 \text{ keV}}\right]^{\alpha - \beta}\left(\frac{E}{100 \text{ keV}}\right)^\beta \exp(\beta - \alpha), \\
& \hspace{4cm} (\alpha - \beta)E_0 \leq E, \hspace{1cm} (6.3)
\end{aligned}
$$

where we choose typical values for the parameters, i.e. $\alpha = -1$, $\beta = -2.5$ and $E_0 = 200$ keV (see left panel of Fig. 6.2).
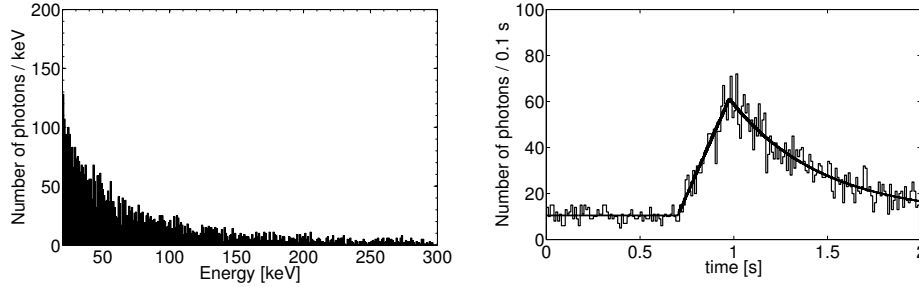


Figure 6.2: Left panel: example of a photon distribution as a function of the energy. The energy ranges from 20 keV to 300 keV according to the Band function (6.3), the total photon number is 5000. Right panel: Example of a simulated GRB for $\kappa = -10^{-5}$ s/keV, $P = 1$ s, $R = 0.3$ s, $h = 50$ s$^{-1}$ and $D = 0.5$ s with a total photon number of 5000. In order to be able to compare the fit with the GRB, we require that the areas under both curves be equal, so that the parameter $B$ is recovered. The overlaid curve is the FRED function with fitted parameters for a photon of energy 0. As the parameter $\kappa$ is very close to 0 this curve represents well the family of FRED curves of the problem.

With this energy distribution, we created arrival times for each photon according to the FRED distribution $f$. In addition, because the time resolution of INTEGRAL is $6.1 \cdot 10^{-5}$ s, we perturbed the arrival time of each photon with a Gaussian distribution with a deviation of $6.1 \cdot 10^{-5}$ s. The Monte Carlo simulations were done with $\kappa = -10^{-5}$ s/keV, $P = 1$ s, $R = 0.3$ s, $h = 50$ s$^{-1}$ and $D = 0.5$ s. Remember that $\Delta t = \kappa \cdot \Delta E$, so that a value for $\kappa$ of $10^{-5}$ s/keV represents a maximum time delay of $\sim 3 \cdot 10^{-3}$ s, which is well longer than the expected time delay due to quantum gravitational effects.

Fig. 6.2 (right panel) gives an example of a simulated GRB for parameters as described above. The histogram shows a typical simulation of a GRB using a FRED distribution,

while the black line shows the solution of the minimization of Eq. (6.1). This curve is defined by $\hat{P} = 0.983$, $\hat{\kappa} = -4.95 \cdot 10^{-5}$ s/keV, $\hat{R} = 0.276$ s, $\hat{h} = 48$ s$^{-1}$ and $\hat{D} = 0.485$ s. Except the value $\kappa$ which is five times too big, the other values are easily recovered by the minimization of Eq. (6.1). However, the Monte Carlo simulations have a tendency to underestimate the parameters. As can be seen in Table 6.1, except the mean value of $D$ for $N = 500$, all values are too low for small $N$. Note that, apart from $\kappa$, $R$ is not well estimated and has therefore a big deviation.

| $N$ | | $P$ [s] | $\kappa$ [s/keV] | $R$ [s] | $h$ [s$^{-1}$] | $D$ [s] |
|---|---|---|---|---|---|---|
| 500 | $\bar{\mu}$ | 0.95 | $-4.7 \cdot 10^{-5}$ | 0.17 | 4.57 | 0.65 |
| | $\sigma$ | 0.10 | $4.0 \cdot 10^{-4}$ | 0.21 | 1.4 | 0.31 |
| 1000 | $\bar{\mu}$ | 0.97 | $-6.5 \cdot 10^{-7}$ | 0.19 | 4.8 | 0.59 |
| | $\sigma$ | 0.08 | $2.7 \cdot 10^{-4}$ | 0.21 | 1.11 | 0.24 |
| 2000 | $\bar{\mu}$ | 0.99 | $-2.3 \cdot 10^{-5}$ | 0.19 | 5.1 | 0.51 |
| | $\sigma$ | 0.03 | $1.6 \cdot 10^{-4}$ | 0.23 | 0.52 | 0.09 |
| 5000 | $\bar{\mu}$ | 0.99 | $-3.3 \cdot 10^{-6}$ | 0.17 | 5.0 | 0.50 |
| | $\sigma$ | 0.02 | $8.6 \cdot 10^{-5}$ | 0.25 | 0.28 | 0.03 |
| 10000 | $\bar{\mu}$ | 1.0 | $-2.0 \cdot 10^{-5}$ | 0.17 | 5.0 | 0.50 |
| | $\sigma$ | 0.01 | $6.8 \cdot 10^{-5}$ | 0.25 | 0.2 | 0.02 |
| $3 \cdot 10^5$ | $\bar{\mu}$ | 1.00 | $-1.0 \cdot 10^{-5}$ | 0.30 | 5.00 | 0.50 |
| | $\sigma$ | 0.002 | $1.2 \cdot 10^{-5}$ | 0.002 | 0.04 | 0.004 |

Table 6.1: Results of 200 Monte Carlo simulations for each value of $N$

From Table 6.1 it should be clear that even with $3 \cdot 10^5$ photons it is not possible to get a trustful result for that small a value $\kappa$. Recall that $\kappa = 10^{-5}$ s/keV is about a factor 100 larger than the expected time lags caused by quantum gravitational effects. A crude way of evaluating the statistics necessary for a convincing measurement is to make the assumption that the FRED distribution may be approximated by a Gaussian distribution. This distribution is obtained by minimizing the error of $N$ independent measurements, where the single parameters are $\bar{\mu}$ and $\sigma$. The error of a single measurement is given by $\sigma/\sqrt{N}$, so that if we want to reach a precision of $\Delta t = 10^{-5}$ s with a burst lasting one second, we need $10^{10}$ photons.

A more careful analysis shows that the standard deviation for a FRED distribution does not behave like const$/\sqrt{N}$. Fig. 6.3 shows the standard deviation $\sigma_\kappa$ as a function of the photon number $N$ as given in Table 6.1. A fit to the data points between $N = 500$ and $N = 10000$ shows that the standard deviation of a FRED distribution is given by

$$\sigma_\kappa = 0.0182 \cdot N^{-0.617}, \tag{6.4}$$

where the exponent is smaller than the usual $1/\sqrt{N}$ for a Gaussian. With this equation we are also able to assess the error for $\kappa$ when using data from GRBs measured by INTEGRAL.
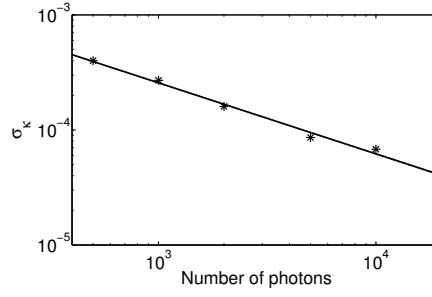
Figure 6.3: Standard deviation $\sigma_\kappa$ for $\kappa$ as a function of the number of photons $N$ . The data points are shown in Table 6.1 in the column $\kappa$. The solid line shows the fit and is given by Eq. (6.4).

## 6.4 Results from GRBs Detected by INTEGRAL

### 6.4.1 Determination of the Parameter $\kappa$

The data provided by INTEGRAL contains for each single registered photon four pieces of information: the arrival time, the energy, the dead time and the PIF value (see Sec. 6.1). In our analysis we take only photons that have a PIF value larger than 0.9, i.e. we exclude pixels that are not completely open to the GRB flux. After correcting the arrival time by weighing it with $1/(1-\text{dead time})$, we determine from the light curve which time intervals have the shape of a FRED distribution. Recall from Eq. (6.4) that the more photons we take the more we are able to constrain $\kappa$.

In [32] the average energy difference $\Delta\langle E\rangle = \Delta\langle E\rangle_3 - \Delta\langle E\rangle_1$ was computed for each GRB using the energy bands of SWIFT, where $\Delta\langle E\rangle_3$ is the average energy of the photons with energies between 110 and 300 keV and $\Delta\langle E\rangle_1$ between 20 and 55 keV (see Table 6.2). In our variables the time difference would then be approximately given by $\Delta t = \kappa \cdot \Delta\langle E\rangle$.

However, from our analysis we obtain the parameter $\kappa$ directly so we do not average over energies in order to get a time difference. Considering only a linear approximation to quantum gravitational effects as proposed by Ellis *et al.* [41, 42], we have the relation

$$\kappa = aI(z) + b(1+z), \tag{6.5}$$

where $a$ and $b$ are coefficients to be fitted. The constant $b$ parameterizes time lags in the rest frame of the source caused by unknown internal processes of the GRBs. Comparing Eq. (6.5) with Eq. (5.5) we find that $I(z)$ is given by

$$I(z) = \int_0^z \frac{dz'}{\sqrt{\Omega_\Lambda + \Omega_m(1+z')^3}} \tag{6.6}$$

and the QG parameter $a$ by

$$a = \pm\frac{H_0^{-1}}{Mc^2}, \tag{6.7}$$

where $E_{QG} = Mc^2$. Fitting all GRBs with known redshift detected by INTEGRAL, we find (units s/keV are used)

$$\kappa = (9.5 \pm 3.0) \cdot 10^{-4} \cdot I(z) - (2.8 \pm 1.1) \cdot 10^{-4} \cdot (1+z) \tag{6.8}$$

69

| GRB | $z$ | $I(z)$ | $K(z)$ | $\kappa$ [s/keV] | $\sigma_\kappa$ [s/keV] |
|---|---|---|---|---|---|
| 030227 | 1.39 [109] | 1.0 | 0.42 | $7.8 \cdot 10^{-4}$ | $4.0 \cdot 10^{-5}$ |
| 031203 | 0.11 [110] | 0.10 | 0.09 | $-1.7 \cdot 10^{-4}$ | $0.1 \cdot 10^{-4}$ |
| 040106 | 0.9 [73] | 0.73 | 0.38 | $2.7 \cdot 10^{-4}$ | $3.7 \cdot 10^{-4}$ |
|  |  |  |  | $4.2 \cdot 10^{-4}$ | $1.5 \cdot 10^{-4}$ |
| 040223 | 0.1 [69] | 0.1 | 0.09 | $2.5 \cdot 10^{-3}$ | $0.4 \cdot 10^{-3}$ |
| 040812 | 0.5 [38] | 0.45 | 0.3 | $-1.4 \cdot 10^{-3}$ | $0.1 \cdot 10^{-3}$ |
|  |  |  |  | $2.6 \cdot 10^{-4}$ | $0.8 \cdot 10^{-4}$ |
| 040827 | 0.9 [39] | 0.73 | 0.38 | $-1.9 \cdot 10^{-4}$ | $5.9 \cdot 10^{-4}$ |
| 041218 | 0.8 [47] | 0.66 | 0.37 | $-1.2 \cdot 10^{-3}$ | $0.1 \cdot 10^{-3}$ |
|  |  |  |  | $1.7 \cdot 10^{-3}$ | $0.2 \cdot 10^{-3}$ |
| 050502 | 3.8 [86] | 1.69 | 0.35 | $-2.2 \cdot 10^{-3}$ | $0.4 \cdot 10^{-3}$ |
|  |  |  |  | $8.2 \cdot 10^{-4}$ | $1.9 \cdot 10^{-4}$ |
| 050714 | 0.26 [87] | 0.25 | 0.19 | $-8.9 \cdot 10^{-4}$ | $3.2 \cdot 10^{-4}$ |
| 050922 | 2.17 [57] | 1.3 | 0.41 | $-1.4 \cdot 10^{-3}$ | $0.2 \cdot 10^{-3}$ |
|  |  |  |  | $7.3 \cdot 10^{-4}$ | $0.2 \cdot 10^{-4}$ |
| 060204 | 3.1 [81] | 1.55 | 0.38 | $2.6 \cdot 10^{-4}$ | $6.3 \cdot 10^{-4}$ |
|  |  |  |  | $2.3 \cdot 10^{-4}$ | $0.1 \cdot 10^{-4}$ |

Table 6.2: Results for the GRBs with known redshifts. Note that in spite of the fact that a couple of redshifts have error bars, we choose to take the mean value of the redshifts without errors. The reason is that then we don't have to introduce arbitrary error bars in order for exact redshifts not to be weighed infinitely strongly. $I(z)$ is given by Eq. (6.6), $K(z)$ by Eq. (6.9), $\kappa$ is the time lag per energy given by the maximization of Eq. (6.1) with $\sigma_\kappa$ its error.

as shown in the left panel of Fig. 6.4. Because redshifts are measured without using a specific cosmological model, this fit was obtained using data that are model-independent. Moreover, a rather questionable energy binning as explained above is not needed due to the fact that our analysis method yields directly values for $\kappa$.

As can be seen from Fig. 6.4 (left panel), a single GRB with two bursts can lead to very different time lags. For example, GRB040812 with average redshift $z = 0.5$ has two peaks that even differ in the sign: the first one has a negative value $\kappa = -1.4 \cdot 10^{-3}$ and the second one a positive value $\kappa = 2.6 \cdot 10^{-4}$. This could be explained by the fact that different internal processes are at the origin of the two bursts, which implies that it may not be sufficient to describe internal time lags with a constant $b$ as in Eq. (6.5). However, the physics involved in GRB is still not well understood, thus limiting the possibility to model intrinsic effects in other ways than through Eq. (6.5).
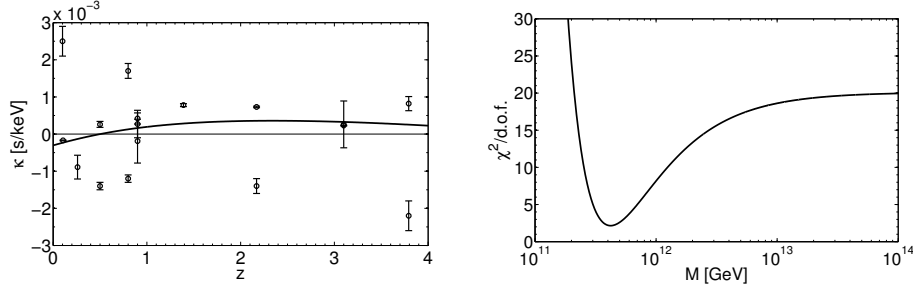


Figure 6.4: Left panel: plot of $\kappa$ as a function of the redshift $z$ for several GRBs detected by INTEGRAL. The nonlinear fit is given by Eq. (6.8), the maximum lies at $z_{\mathrm{max}} \simeq 2.34$ with value $\kappa_{\mathrm{max}} \simeq 3.6 \cdot 10^{-4}$ s/keV. Right panel: evolution of the $\chi^2$ function as a function of $M$. Note that $\chi^2$ has a strong minimum around $4 \cdot 10^{11}$ GeV.

In [42] and [32] a linear fit was obtained by using not $z$ as the independent variable but instead a function $K(z)$. Dividing Eq. (6.5) by $(1 + z)$, $K(z)$ is given by the non-linear function

$$K(z) \equiv \frac{1}{1+z} I(z). \tag{6.9}$$

However, we think that considering $\kappa/(1+z)$ as a linear function of $K$ is delusive because the new function $K(z)$ is not injective. This function maps certain different redshifts $z$ to the same value and has a maximum of $K_{\mathrm{max}} \simeq 0.42$ at $z = 1.64$. For example, a redshift of $z = 4$ has the same value $K$ as a redshift of $z = 0.7$. Thus the two points for GRB050502 at $z = 3.793$ are mapped to $K = 0.353$, which is between GRB040812 and GRB040106. Our opinion is that this method is misleading and does not give reliable results and should therefore not be used.

### 6.4.2 Likelihood test

Following [42], we introduce a likelihood function

$$L_{\mathrm{LH}}(M) = \mathcal{N} \exp\left(-\frac{\chi^2(M)}{2}\right), \tag{6.10}$$

where $M$ is the mass scale, $\mathcal{N}$ the normalization and $\chi^2(M)$ is given by

$$\chi^2(M) = \sum_{\mathrm{all\ GRBs}} \frac{(\kappa_i - b(1 + z_i) - a(M)I_i)^2}{(\sigma_i)^2 + \sigma_b^2}. \tag{6.11}$$

71

The parameter $b$ reflects the instrinsic time lags and $a$ quantum gravitational effects. Thus, $b$ was removed from the linear fit, as can be seen from Eq. (6.11). Note that we used the raw model that doesn't need an energy binning.

The value at the minimum of $\chi^2$/d.o.f. is 303/15, which is well above unity. In such a case, we may expect a high degree of uncertainty for any fitted parameters. If the error bars are underestimated it will lead to underestimated statistical errors for the fitted parameters. In such cases, the Particle Data Group [113] suggests to rescale the error bars so that $\chi^2 \approx$ d.o.f. by a factor $S = [\chi^2/\text{d.o.f.}]^{1/2}$. Such a rescaling has also been proposed in [32, 41, 42].

Fig. 6.4 (right panel) presents the dependence of the rescaled $\chi^2$/d.o.f as a function of $M$. The minimum of this function is found at $M \simeq 3.8 \times 10^{11}$ GeV. This value also minimizes the likelihood function given by Eq. (6.1).

Following Ellis *et al.* [41] we establish a 95 % confidence-level lower limit on the scale $M$ of quantum gravity by solving the equation

$$\frac{\int_M^{M_P} L_{\text{LH}}(\xi)d\xi}{\int_0^{M_P} L_{\text{LH}}(\xi)d\xi} = 0.95, \tag{6.12}$$

where the Planck mass $M_P = 10^{19}$ GeV is the reference point fixing the normalization. The function $L_{\text{LH}}$ is given by Eq. (6.10). Solving this equation for $M$ gives the lower limit of quantum gravity at a 95 % level of confidence at

$$M \geqslant 3.2 \cdot 10^{11} \, \text{GeV}. \tag{6.13}$$

# Chapter 7

# Fermi Gamma-ray Space Telescope

The Gamma Ray Large Area Space Telescope (Fermi) is a space-based gamma-ray telescope designed to explore the high-energy universe. It includes two instruments: the Large Array Telescope (LAT), which is an imaging gamma-ray detector which detects photons with energy from about 30 MeV to 300 GeV, and the Gamma-ray Burst Monitor (GBM) that consists of 14 scintillation detectors which detect photons with an energy between 8 keV and 30 MeV. The LAT has a very large field of view that allows it to see about 20 % of the sky at any time. Despite the fact that it will cover the entire sky every three hours we shall assume that the instrument response changes on timescales longer than a typical burst duration. On the other hand, Fermi can be pointed as needed when a bright GRB is detected by either LAT or GBM so that it will detect around 200 GRBs each year. The energy resolution ranges from 20% at 30 MeV to about 7% at 1 GeV, as can be seen in Fig. 7.1 [52]. The time resolution of an event should be around 10 $\mu$s with a dead time shorter than 100 $\mu$s. In summary, LAT will have superior area, angular resolution, field of view, time resolution and deadtime. This will at least provide an advance of a factor 30 in sensitivity compared to previous missions.

The Fermi Science Support Center (GSSC) provides analysis tools freely available to the scientific community on their homepage [53]. As we are interested in simulating the detection of GRBs by Fermi we mainly used the tool called *gtobssim* which is a software that generates photon events from astrophysical sources with the instrument response functions of Fermi. Because we will only study the measurement of possible Lorentz violation we assumed that LAT pointed in the same direction as the burst. Further information on the effects of QG on LAT GRBs can be found in e.g. [23, 76].

## 7.1 Creation of a photon list

### 7.1.1 Analysis method

We shall use the same method we used to study INTEGRAL GRBs by modeling bursts with a Fast Raise and Exponential Decay (FRED) distribution [65]. We parameterize this distribution with four parameters: $f = f(t_i, E_i; P, R, D, \kappa, h)$ as shown in Fig. 7.2. We suppose that a photon $i$ came from the probability density function $f$ at time $t_i$ with energy $E_i$. We use the method of maximum likelihood which consists in finding the set of values $\hat{P}$, $\hat{R}$, $\hat{D}$, $\hat{\kappa}$ and $\hat{h}$ that maximizes the joint probability distribution of all data, given by

$$\mathcal{F}(P, R, D, \kappa, h) = \prod_i f(t_i, E_i; P, R, D, \kappa, h) \tag{7.1}$$
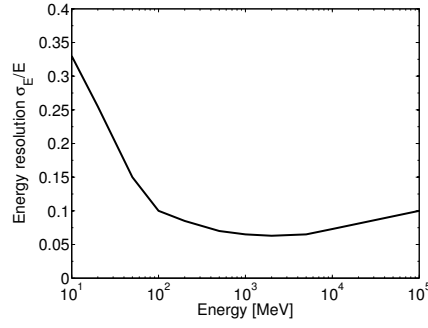
Figure 7.1: Energy resolution as a function of the energy for the LAT [52]. The energy uncertainty at 30 MeV is about 17% before going down to a couple of percent in the GeV range. Most of the photons LAT detects have an energy around $\sim 100$ MeV with an uncertainty of about 10%.

together with the constraint

$$\int_{t_0}^{t_1} dt'\, f(t', E_i; P, R, D, \kappa, h) = 1, \tag{7.2}$$

where $\mathcal{F}$ is the likelihood function and the integral runs between $t_0$ and $t_1$ as shown in Fig. 7.2. The specifics of this distribution does not play a significant role in our study as we are only interested in seeking possible violations of the Lorentz symmetry. In order to further improve our model we also simulated an isotropic background with a spectrum following an exponential decay with exponent 2.1. However, this background does not play a significant role because of the following two reasons. The first one is that LAT shall only be able to detect photons with energies above $\sim 30$ MeV, where such events are rare. The second one is the fact that we are only interested in GRBs, e.g. events of short duration.
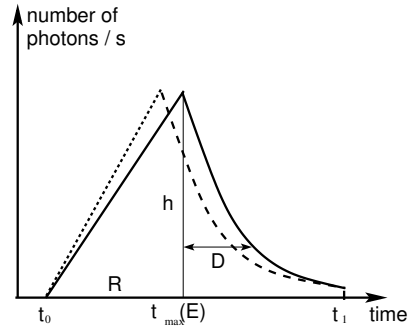


Figure 7.2: Sketch of a typical light curve of a GRB for a given energy interval. The curve is parameterized by four parameters: $R$ the duration of the rise, $h$ the height above the background, $D$ the decay time for $\exp(-t/D)$ and $\kappa$ describes the magnitude of the dependence on the energy of the distribution $f$, $t_{\max} = P + \kappa \cdot E$, where $P$ is the time when the intensity reaches a maximum and $E$ is the photon energy. The dashed line shows a distribution for another energy interval that is shifted by an amount of $\Delta t = \kappa \cdot \Delta E$ sketching the shift in time due to quantum gravitational effects.
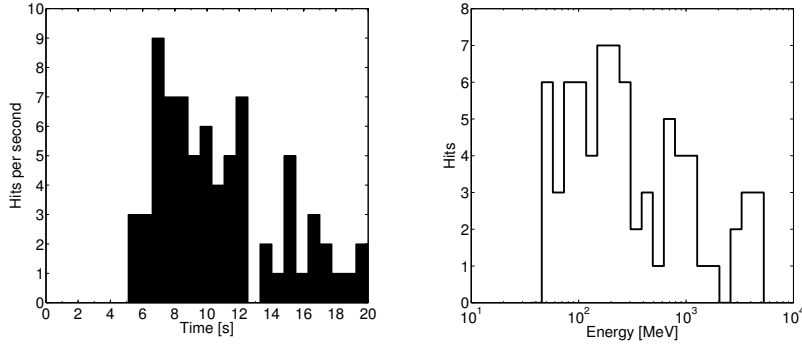
Figure 7.3: *Left panel*: Example of a simulated LAT GRB with *gtobssim* with a total photon number of 74. The burst starts at $t_0 = 5$ s and has a decay time of the order of 10 seconds. *Right panel*: Spectrum of the same GRB as simulated by *gtobssim* for LAT. The first detected photons have an energy of roughly 30 MeV. We choose the high energy exponent $\beta = 2$ (see Eq. (7.3)) and a background with exponent $\gamma = 2.1$

### 7.1.2 Spectrum of the GRBs

As described in the previous section we also need to simulate the energy of the photons. Normally a typical energy distribution of GRBs follows the pattern of the so-called Band function [22] given by the following equation:

$$
\begin{aligned}
N_E(E) \ = \ & A \left( \frac{E}{100 \text{ keV}} \right)^\alpha \exp \left( -\frac{E}{E_0} \right), \\
& \hspace{4cm} (\alpha - \beta)E_0 \geq E, \\
= \ & A \left[ \frac{(\alpha - \beta)E_0}{100 \text{ keV}} \right]^{\alpha - \beta} \left( \frac{E}{100 \text{ keV}} \right)^\beta \exp(\beta - \alpha), \\
& \hspace{4cm} (\alpha - \beta)E_0 \leq E, \hspace{1cm} (7.3)
\end{aligned}
$$

where $\alpha$ is the low-energy exponent, $\beta$ the high-energy one and $E_0$ the break energy. As LAT starts measuring at 30 MeV and the break energy is around 500 keV we shall only be interested in the high-energy behavior of the Band function. However, LAT will open a new window on the spectrum where little is known, therefore there is no certainty whether the Band function is still valid throughout the energy range of LAT.

In order to make the simulations as realistic as possible we used *gtobssim*. As described in the previous section we simulated a GRB with photons following a FRED distribution together with an isotropic background. Since we are only interested in the detection of a possible Lorentz violation we used the same FRED distribution for all GRBs, i.e. with a raise time of the order of a second and a decay time around 10 seconds (see Fig. 7.3). In order to get a feeling of the uncertainty we varied the flux of the burst and only selected the bursts which got about the same number of hits in the detector. We then introduced a Lorentz violating term with the following relation (see Fig. 7.5):

$$\Delta t = \kappa \times E_\gamma, \hspace{1cm} (7.4)$$

where $E_\gamma$ is the energy of the detected photon in MeV and $\Delta t$ is the time delay in seconds caused by quantum gravity given by the relation $t_1 = t_0 + \Delta t$. The parameter $\kappa$ describes

the effect of a Lorentz violation and is given by the following relation:

$$\kappa = \frac{H_0^{-1}}{M_{\mathrm{QG}}c^2} \int_0^z \frac{1+z'}{\sqrt{\Omega_\Lambda + \Omega_m(1+z')^3}} dz' =: \frac{H_0^{-1}}{M_{\mathrm{QG}}c^2} I(z),$$

where $M_{\mathrm{QG}}$ is the mass scale where the Lorentz symmerty breaks down. Henceforth we shall take the most conservative scale and set $M_{\mathrm{QG}} = M_P \approx 1.2 \times 10^{19}$ GeV.

As can be seen in Fig. 7.4 typical values for $\kappa$ lie between $10^{-5}$ and $10^{-4}$ s/MeV. In the Monte Carlo simulations we used a value of $\kappa = 4 \times 10^{-5}$ corresponding to a redshift of $z = 1$.
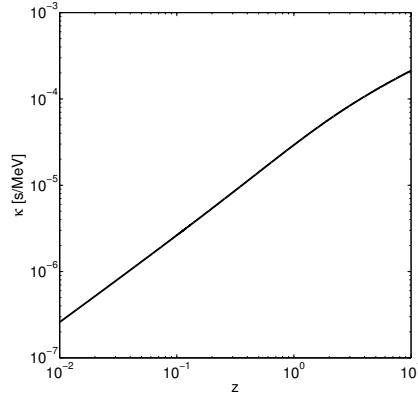


Figure 7.4: The Lorentz violation parameter $\kappa$ as a function of the redshift. As we shall see below, a value of $\kappa = 10^{-4}$ s/MeV could even be measured without requiring a bright burst (see Table 7.1).

We studied two models: one simple one with only the time delays caused by quantum gravity and a more realistic one where we perturbed the energy and the arrival time according to the scheme shown in Fig. 7.5 in order to take into account the energy and time resolution of the LAT. For a given event at time $t_0$ with energy $E_0$ obtained with *gtobssim* we read the energy uncertainty $\sigma_{E_0}/E_0$ from Fig. 7.1 and perturbed this energy with a Gaussian with maximum at $E_0$ and standard deviation $\sigma_{E_0}$. The next step is to take the corrected time $t_1$ and perturb it with a Gaussian with maximum at $t = 0$ and standard deviation $\sigma_t = 10$ $\mu$s so that we get the perturbed arrival time $t_2$.

### 7.1.3 Results

In the previous section we explained how we constructed a burst with photons and perturbed their energies and arrival times to account for Lorentz violation and finite energy and time resolution of LAT. The question is now whether it is possible to get back the value of $\kappa$ parameterizing the Lorentz violating term despite the perturbation of both the energy and arrival time. In [65] we found an exponential dependence between the standard deviation $\sigma_\kappa$ and the number of detected photons $N$ with an exponent of -0.617. However, we only perturbed the arrival time and not the energy.

The final step is to search for $\bar{\kappa}$ which minimizes the likelihood Eq. (7.1). For a single burst we scanned through a large range of $\kappa$ in order to find the global (and not just a local) minimum of the likelihood. We performed 100 Monte Carlo simulations for different luminosities of the burst, i.e. different numbers of total events $N$ (see Table 7.1).
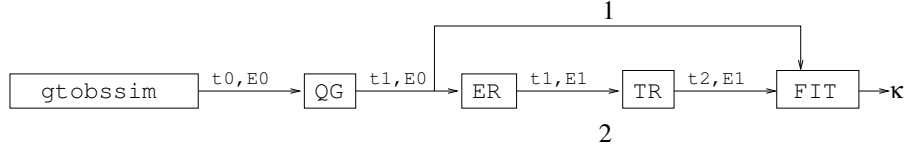
Figure 7.5: Setup of the simulation process. The software *gtobssim* gives as output the arrival time $t_0$ and the energy $E_0$ of a photon. The arrival time is then corrected by means of the relation (7.4) from $t_0$ to $t_1$ (box QG). The simpler case with only QG effects is shown by the arrow number 1. In the second case, the energy of the photon was perturbed from $E_0$ to $E_1$ with a Gaussian distribution with standard deviation according to Fig. 7.1 (box ER). Furthermore, the arrival time was perturbed a second time from $t_1$ to $t_2$ with a Gaussian distribution with standard deviation of 10 $\mu$s corresponding to the time resolution of LAT (box TR). The photon with arrival time $t_2$ and energy $E_1$ is then given to the fitter (box FIT) to get a value for the QG corresponding to $\kappa$.

| | | unperturbed (1.) | | perturbed (2.) | |
|---|---|---|---|---|---|
| N | flux [s$^{-1}$m$^{-2}$] | $\bar{\kappa}$ [s/MeV] | $\sigma_\kappa$ [s/MeV] | $\bar{\kappa}$ [s/MeV] | $\sigma_\kappa$ [s/MeV] |
| 20 | 10 | $1.2 \times 10^{-4}$ | $2.0 \times 10^{-3}$ | $3.9 \times 10^{-4}$ | $1.7 \times 10^{-3}$ |
| 50 | 28 | $9.5 \times 10^{-5}$ | $9.5 \times 10^{-4}$ | $6.4 \times 10^{-5}$ | $7.8 \times 10^{-4}$ |
| 75 | 46 | $8.5 \times 10^{-5}$ | $5.3 \times 10^{-4}$ | $1.4 \times 10^{-4}$ | $2.4 \times 10^{-4}$ |
| 100 | 60 | $6.5 \times 10^{-5}$ | $4.3 \times 10^{-4}$ | $8.4 \times 10^{-5}$ | $3.7 \times 10^{-4}$ |
| 150 | 96 | $4.2 \times 10^{-5}$ | $2.2 \times 10^{-4}$ | $4.6 \times 10^{-5}$ | $3.3 \times 10^{-4}$ |
| 200 | 128 | $5.3 \times 10^{-6}$ | $2.1 \times 10^{-4}$ | $3.7 \times 10^{-5}$ | $2.4 \times 10^{-4}$ |
| 500 | 330 | $2.9 \times 10^{-5}$ | $6.6 \times 10^{-5}$ | $1.4 \times 10^{-5}$ | $6.6 \times 10^{-5}$ |
| 1000 | 660 | $2.3 \times 10^{-5}$ | $5.1 \times 10^{-5}$ | $2.9 \times 10^{-5}$ | $4.3 \times 10^{-5}$ |

Table 7.1: Results of 100 Monte Carlo simulations. The first column shows the number of photons detected by LAT, the second one the approximate flux in m$^{-2}$s$^{-1}$. The third column shows the mean value of $\bar{\kappa}$ for the unperturbed system (1.) and the fourth one its standard deviation. The last two columns are the same as the third and fourth ones, except for the fact that the arrival times and energies were perturbed with a Gaussian distribution (see Sec. 7.1.2).

Fig. 7.6 shows a comparison between the standard deviation of the perturbed and unperturbed system. The fit of the unperturbed system is given by

$$\sigma_\kappa = (2.5 \times 10^{-2}) \cdot N^{-0.93}$$

and the fit of the perturbed system by

$$\sigma_\kappa = (6.0 \times 10^{-2}) \cdot N^{-1.07}. \tag{7.5}$$

The results described above allows us to simulate a full set of GRBs with different redshifts $z$ and time shifts $\kappa$. Fig. 7.7 shows a set of 100 GRBs with redshifts between 0 and 10, where we used the results from [80] and [79] in order to get a rough estimate of the expected number of GRBs detected by Fermi as a function of the number of detected photons and the redshift. Each value for $\kappa$ has been perturbed with a Gaussian with a standard deviation given by Eq. (7.5). Considering a linear approximation to quantum
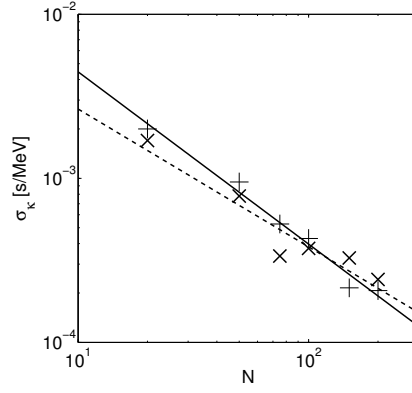
Figure 7.6: Comparison between the standard deviations $\sigma_\kappa$ of the unperturbed and perturbed system. The vertical crosses show the values for the unperturbed system together with the solid line as its fit. The inclined crosses show the values for the system with perturbed arrival times and energies.

gravitational effects we have the relation [41, 42]:

$$\kappa = aI(z) + b(1+z), \tag{7.6}$$

where $a$ and $b$ are fitted coefficients. The constant $b$ parameterizes time lags in the frame of the source caused by unknown internal processes of the GRBs, $a$ describes the expected Lorentz violating effects through

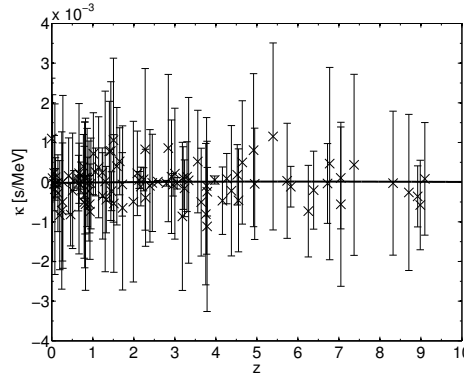$$a_{\text{th}} = \frac{H_0^{-1}}{M_P c^2} \approx 2.56 \times 10^{-5} \ \text{s/MeV}. \tag{7.7}$$



Figure 7.7: Simulation of 100 GRBs where $\kappa$ has been perturbed with a Gaussian according to the relation Eq. (7.5). The error bars show the $1\sigma$ deviation given by Eq. (7.5). The distribution of the GRBs and the luminosity has been computed using results from [80, 79] where a histogram of the number of GRBs as a function of either the redshift or the luminosity is given. The solid line shows the fit given by Eq. (7.8). Note that no systematic errors have been incorporated.

A fit of the 100 GRBs shown in Fig. 7.7 gives

$$\kappa = (2.6 \pm 3.1) \times 10^{-5} \cdot I(z) - (1.9 \pm 2.5) \times 10^{-5} \cdot (1+z). \tag{7.8}$$

We see that the Lorentz violating term is well compatible with the theoretical value $a_{\text{th}}$ while the second term is less than one $\sigma$ off the input values $b_{\text{th}} = 0$ (see Table 7.2). Considering the fact that LAT should see around 500 GRBs each year it might be tantalizing to conclude that only after a couple of months the question whether the Lorentz symmetry is broken might be answered. However, we would like to stress the fact that we did not consider systematic errors caused by the lack of knowledge of the internal processes leading to photon emissions. As these systematic errors were the main problem past works [41, 42, 43, 65] had to deal with, this oversimplified analysis must be taken with precaution. Moreover, a known redshift of the bursts is also needed, thus reducing the number of usable bursts.

| $N$ | $a$ [s/MeV] | $b$ [s/MeV] |
|---|---|---|
| 10 | $(1.7 \pm 5.6) \times 10^{-5}$ | $(-1.8 \pm 3.3) \times 10^{-5}$ |
| 20 | $(2.6 \pm 3.6) \times 10^{-5}$ | $(-1.8 \pm 2.8) \times 10^{-5}$ |
| 50 | $(2.6 \pm 3.2) \times 10^{-5}$ | $(-1.9 \pm 2.6) \times 10^{-5}$ |
| 100 | $(2.6 \pm 3.1) \times 10^{-5}$ | $(-1.9 \pm 2.5) \times 10^{-5}$ |

Table 7.2: Results of the fit Eq. (7.6) for a variable number of bursts. The first column shows the number of bursts considered for the fit, the second one shows the value of $a$ describing the Lorentz violating effects and the third one the value of $b$ parameterizing the time lags caused by unknown internal processes. The theoretical value of $a$ is given by Eq. (7.7). The error on $a$ and $b$ only reduces considerably between $N = 10$ and $N = 20$.

### 7.1.4   Quadradic corrections

In this subsection we are concerned with quadratic corrections, i.e. $(\Delta E)^2$, given by [55]

$$\Delta t = \pm \frac{3}{2} H_0^{-1} \left( \frac{\Delta E}{E_{\text{QG}}} \right)^2 \int_0^z \frac{(1 + z')^2}{\sqrt{\Omega_\Lambda + \Omega_M (1 + z')^3}} dz'. \tag{7.9}$$

Such corrections may be interesting in view of the fact that previous works have already put stringent constraints on linear corrections to the speed of light [2, 43, 46, 56]. To get a rough estimate of the sensitivity of Fermi to quadratic corrections we must first get a bound on the time difference that should be detectable by Fermi. With Eq. (7.4) we see that for $\sigma_\kappa \sim 5 \times 10^{-4}$ s/MeV (see Table 7.1) and $\Delta E \sim 10^3$ MeV we get a bound on the time difference of $\sigma_{\Delta t} \sim 5 \times 10^{-1}$ s. Solving Eq. (7.9) for the mass scale and inserting these results we get a mass scale of

$$M_{\text{quadratic}} \gtrsim 2 \times 10^9 \text{ GeV}.$$

for $z = 1$ up to which Fermi should be sensitive for a *single* burst. This bound may probably be raised by a couple of orders of magnitude with better statistics. However, we do not think that Fermi will be able to detect a quadratic correction if the QG scale is at the Planck scale.

The above estimate may seem very crude. We therefore checked it with results obtained in the literature and found a good agreement between this estimate and a more rigorous statistical analysis. For example, taking $M_L > 7 \times 10^{15}$ GeV obtained in Eq. (36) in [41] together with $\Delta E \sim 100$ keV and $\sigma_{\Delta t} \sim 5 \times 10^{-3}$ s for BATSE we get a bound on the quadratic correction of $M_Q \gtrsim 0.8 \times 10^6$ GeV, which corresponds more or less to the result $M_Q > 3 \times 10^6$ GeV obtained in [41] with a rigorous analysis.

### 7.1.5 Other distributions

Until now we only considered FRED distributions for GRBs. However, despite the fact that these distributions may describe a large number of GRBs, we also have to consider other burst shapes in order to get an estimate for the validity of our likelihood method with non-FRED distributions. We studied two other shapes, a linearly raising and falling distribution and a double-peak distribution (see Fig. 7.8). We then applied the likelihood method to these peaks with 200 photons and compared the results with Table 7.1 for $N = 200$. For the linear peak (see left panel in Fig. 7.8) we found a value $\bar{\kappa} = 1.7 \times 10^{-6}$ s/MeV and a standard deviation of $\sigma_\kappa = 1.6 \times 10^{-4}$ s/MeV. Comparing this value with the perturbed system for $N = 200$ (see Table 7.1) we see that the likelihood method gives a slightly better results for the linear peak. We also studied the double peak (see fight panel in Fig. 7.8) and found a value of $\bar{\kappa} = 2.0 \times 10^{-6}$ s/MeV with a standard deviation of $\sigma_\kappa = 1.6 \times 10^{-4}$. Thus the results of both cases lead to the conclusion that our likelihood method is also able to deal with non-FRED distributions.

We fixed the duration time of the simulated GRBs to about 20 seconds, which seems quite arbitrary. However, we expect the likelihood to get better as the duration of the burst gets shorter (as long as the total number of photons remains constant). The reason is that, while $\kappa$ is independent of the duration, the ratios $\kappa/R$ and $\kappa/D$ (see Fig. 7.2) are inverse proportional to $t_1 - t_0$. We checked this claim for bursts with a duration time of about 6 seconds, 200 photons and FRED-distributed. We found a value $\kappa = 2.6 \times 10^{-5}$ s/MeV with a standard deviation of $\sigma_\kappa = 3.7 \times 10^{-5}$ s/MeV. Comparing this value with Table 7.1 we see that the likelihood is able to recover the Lorentz violating term with a precision of about one order of magnitude better. On the other hand, the convergence of the likelihood decreases with the duration time of the bursts, thus narrowing the study of short bursts to the brighter ones.
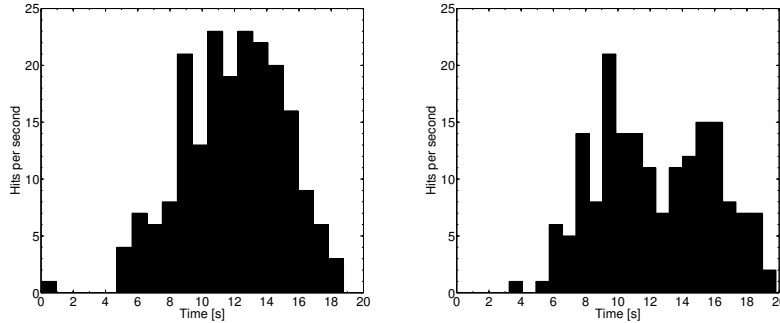


Figure 7.8: *Left panel*: Example of a simulated LAT GRB with a linear raise and linear decay. *Right panel*: Example of a simulated LAT GRB with a double-peak shape.

# Chapter 8

# Conclusion

We first described a method that is able to analyze unbinned data of GRBs detected by INTEGRAL. We introduced a maximum likelihood function following a Fast Raise and Exponential Decay behavior with a parameter describing time lags of photons for different energies. In order to know which minimum time lags are measurable with INTEGRAL, we performed Monte Carlo simulations and varied the total photon number.

We had 11 GRBs with known redshift at our disposal and were able to get 17 measurements of time lags. We used these measurements to fit a nonlinear relation depending on the redshift. This relation has a term that describes possible quantum gravitational effects and one that accounts for intrinsic time lags of the GRB. By using a likelihood function we made a $\chi^2$ analysis of the data and showed that there is a strong minimum of $\chi^2$ around $4 \times 10^{11}$ GeV, which apparently would disfavor a quantum gravitational scale around the Planck mass. However, as shown by our Monte Carlo simulations in Section 6.3 it is obvious that it is impossible to obtain the required sensitivity with the presently available statistics of GRB data, especially when only 11 GRBs are at disposal. Correcting for intrisinc time lags [48, 78, 77] dramatically increases this lower bound to $1.5 \cdot 10^{14}$ GeV, but this method stands on shaky ground.

Then we studied possible Lorentz violations with special focus on the Large Array Telescope (LAT) of Fermi, where we concentrated on models with linear corrections to the speed of light. We simulated bursts and introduced a Lorentz violating term in the arrival times of the photons. We further perturbed these arrival times and energies with a Gaussian distribution corresponding to the time resp. energy resolution of Fermi. We then varied the photon flux in order to derive a relation between the photon number and the standard deviation of the Lorentz violating term. We concluded with the fact that our maximum likelihood method is able to make a statement whether Nature breaks the Lorentz symmetry if the number of bursts with known redshifts is of the order of 100. However, the systematic errors caused by unknown mechanisms for photon emission were not considered despite the fact that these errors should be the main obstacle to detecting Lorentz violations.

Yet we had to make a couple of assumptions. The most important one was that we had to assume that the BAND function is still valid at LAT energies, implying that photons with energies above 10 GeV are extremely rare. But Fermi detected a photon from GRB 090510 with an energy of about 30 GeV with no sign of any Lorentz violation. Of course, one GRB is not sufficient to exclude an (linear) energy-dependent speed of light as internal emission processes are still not well understood. A couple of bursts emitting such energetic photons may be sufficient to definitively settle the question whether Einstein was right.

# Appendix A

# Symmetry Reduction of Connections

In this section we shall repeat the complete analysis introduced in [59, 30, 25] in order to see the impact of a compact topology on a connection. Our strategy is to find an invariant connection on the covering space $\tilde{M}$ and then restrict it to the compact space $M$ by means of the covering map (2.2). In the following section, when referring to the covering space, we shall use a tilde. The results of this appendix are used in Section 2.4.

## A.1   Invariant Connections

Let $\tilde{P}(\tilde{M}, SU(2), \pi)$ be a principal fiber bundle over $\tilde{M}$ with structure group $SU(2)$ and projection $\pi : \tilde{P} \to \tilde{M}$. We require that there be a symmetry group $\tilde{S} \subset \mathrm{Aut}(\tilde{P})$ of bundle automorphisms which acts transitively on $\tilde{M}$. Furthermore, for Bianchi I models $\tilde{S}$ does not have a non-trivial isotropy subgroup $\tilde{F}$ so that the base manifold is isomorphic to the symmetry group $\tilde{S}$, i.e. $\tilde{M}/\tilde{S} = \{x_0\}$ is represented by a single point that can be chosen arbitrarily in $\tilde{M}$. Since the isotropy group $\tilde{F}$ is trivial the coset space $\tilde{S}/\tilde{F} \cong \tilde{S}$ is reductive with a decomposition of the Lie algebra of $\tilde{S}$ according to $\mathcal{L}\tilde{S} = \mathcal{L}\tilde{F} \oplus \mathcal{L}\tilde{F}_\perp = \mathcal{L}\tilde{F}_\perp$ together with the trivial condition $\mathrm{Ad}_{\tilde{F}}\mathcal{L}\tilde{F}_\perp \subset \mathcal{L}\tilde{F}_\perp$. Here, $\mathcal{L}S$ is the orthogonal complement of $\mathcal{L}S$ with respect to the Cartan-Killing metric on $\mathcal{L}S$. This allows us to use the general framework described in [30, 25, 59].

Since the isotropy group plays an important role in classifying symmetric bundles and invariant connections we describe the general case of a general isotropy group $\tilde{F}$. Fixing a point $x \in \tilde{M}$, the action of $\tilde{F}$ yields a map $\tilde{F} : \pi^{-1}(x) \to \pi^{-1}(x)$ of the fiber over $x$. To each point $p \in \pi^{-1}(x)$ in the fiber we assign a group homomorphism $\lambda_p : \tilde{F} \to G = SU(2)$ defined by $f(p) =: p \cdot \lambda_p(f), \forall f \in \tilde{F}$. As this homomorphism transforms by conjugation $\lambda_{p \cdot g} = \mathrm{Ad}_{g^{-1}} \circ \lambda_p$ only the conjugacy class $[\lambda]$ of a given homomorphism matters. In fact, it can be shown [59] that an $\tilde{S}$-symmetric principal bundle $P(\tilde{M}, G, \pi)$ with isotropy subgroup $\tilde{F} \subseteq \tilde{S}$ is uniquely characterized by a conjugacy class $[\lambda]$ of homomorphisms $\lambda : \tilde{F} \to G$ together with a reduced bundle $Q(\tilde{M}/\tilde{S}, Z_G(\lambda(\tilde{F})), \pi_Q)$, where $Z_G(\lambda(\tilde{F}))$ is the centralizer of $\lambda(\tilde{F})$ in $G$. In our case, since $\tilde{F} = \{1\}$ all homomorphisms $\lambda : \tilde{F} \to G = SU(2)$ are given by $1 \mapsto 1_G$.

After having classified the $\tilde{S}$-symmetric fiber bundle $\tilde{P}$ we seek a $[\lambda]$-invariant connection on $\tilde{P}$. We use the following general result [34]:

**Theorem 2** (Generalized Wang theorem)**.** *Let $\tilde{P}$ be an $\tilde{S}$-symmetric principal bundle classified by $([\lambda], Q)$ and let $\tilde{\omega}$ be a connection in $\tilde{P}$ which is invariant under the action of $\tilde{S}$. Then $\tilde{\omega}$ is classified by a connection $\tilde{\omega}_Q$ in $Q$ and a scalar field (usually called the Higgs*

*field)* $\phi : Q \times \mathcal{L}\tilde{F}_\perp \to \mathcal{L}G$ *obeying the condition*

$$\phi(\mathrm{Ad}_f(X)) = \mathrm{Ad}_{\lambda(f)}\phi(X), \quad \forall f \in \tilde{F}, \ X \in \mathcal{L}\tilde{F}_\perp. \tag{A.1}$$

The connection $\tilde{\omega}$ can be reconstructed from its classsifying structure as follows. According to the decomposition $\tilde{M} \cong \tilde{M}/\tilde{S} \times \tilde{S}/\tilde{F}$ we have $\tilde{\omega} = \tilde{\omega}_Q + \tilde{\omega}_{\tilde{S}/\tilde{F}}$ with $\tilde{\omega}_{\tilde{S}/\tilde{F}} = \phi \circ \iota^* \tilde{\theta}_{\mathrm{MC}}$, where $\iota : \tilde{S}/\tilde{F} \hookrightarrow \tilde{S}$ is a local embedding and $\tilde{\theta}_{\mathrm{MC}}$ is the Maurer-Cartan form on $\tilde{S}$. The structure group $G$ acts on $\phi$ by conjugation, whereas the solution space of Eq. (A.1) is only invariant with respect to the reduced structure group $Z_G(\lambda(\tilde{F}))$. This fact leads to a partial gauge fixing since the connection form $\tilde{\omega}_{\tilde{S}/\tilde{F}}$ is a $Z_G(\lambda(\tilde{F}))$-connection which explicitly depends on $\lambda$. We then break down the structure group from $G$ to $Z_G(\lambda(\tilde{F}))$ by fixing a $\lambda \in [\lambda]$.

In our case, the embedding $\iota : \tilde{S} \to \tilde{S}$ is the identity and the base manifold $\tilde{M}/\tilde{S} = \{x_0\}$ of the orbit bundle is represented by a single point so that the invariant connection is given by

$$\tilde{A} = \phi \circ \tilde{\theta}_{\mathrm{MC}}.$$

The three generators of $\mathcal{L}\tilde{S}$ are given by $T_I$, $1 \leq I \leq 3$, with the relation $[T_I, T_J] = 0$ for Bianchi I models. The Maurer-Cartan form is given by $\tilde{\theta}_{\mathrm{MC}} = \tilde{\omega}^I T_I$ where $\tilde{\omega}^I$ are the left invariant one-forms on $\tilde{S}$. The condition (A.1) is empty so that the Higgs field is given by $\phi : \mathcal{L}\tilde{S} \to \mathcal{L}G$, $T_I \mapsto \phi(T_I) =: \phi_I{}^i \tau_i$, where the matrices $\tau_j = -i\sigma_j/2$, $1 \leq j \leq 3$, generate $\mathcal{L}G$, where $\sigma_j$ are the standard Pauli matrices. In summary the invariant connection is given by

$$\tilde{A} = \phi_I{}^i \tau_i d\tilde{\omega}^I. \tag{A.2}$$

In order to restrict this invariant connection we define the invariant connection $A$ on $\mathbb{T}^3$ with the pullback given by the covering map (2.2). The generators of the Teichmüller space (see Eq. (2.3)) allow us to write $A$ as:

$$A_a^i := \bar{\phi}_I{}^i \omega_a^I, \quad (\bar{\phi}_I{}^i) = \begin{pmatrix} \bar{\phi}_1{}^1 & \bar{\phi}_2{}^1 & \bar{\phi}_3{}^1 \\ 0 & \bar{\phi}_2{}^2 & \bar{\phi}_3{}^2 \\ 0 & 0 & \bar{\phi}_3{}^3 \end{pmatrix}. \tag{A.3}$$

# Appendix B

# Kasner Solutions

In Section 2.3.2 we introduce a scalar field in order to allow for an isotropic expansion of the universe. In this appendix we will explain the reason for this choice by considering a homogeneous vacuum solution of Einstein's equations known as the Kasner solution and show that it doesn't admit an isotropic expansion. We shall only give a short overview on this topic and refer the reader to [108] for further details.

**Definition 7.** *A Lorentzian manifold is a vacuum solution to the Einstein's field equations if its corresponding Einstein tensor $G_{\mu\nu} = R_{\mu\nu} - \frac{1}{2}Rg_{\mu\nu}$ vanishes, or equivalently, the Ricci tensor $R_{\mu\nu}$ vanishes.*

We would like to find all spatially flat and homogeneous vacuum solutions with $G = \mathbb{R}^3$ as Lie group acting transitively on the spatial manifold, i.e. we seek vacuum solutions for a Bianchi type I model (see Section 2.2.3). It can be shown that these are given by the following metric

$$ds^2 = -dt^2 + t^{2p_1}(\omega^1)^2 + t^{2p_2}(\omega^2)^2 + t^{2p_3}(\omega^3)^2, \tag{B.1}$$

where $\omega^i$ are the left-invariant one-forms and the constants $p_i$ the so-called Kasner exponents. This metric describes a spacetime whose spatial slices are flat but expanding or contracting at different rates in different regions. Moreover, it is an exact solution to Einstein's equation if and only if the Kasner exponents satisfy the Kasner conditions

$$p_1 + p_2 + p_3 = 1 = (p_1)^2 + (p_2)^2 + (p_3)^3.$$

The first condition defines a plane and the second one a sphere. In a isotropically expanding universe all Kasner exponents would be equal, i.e. $p_i = 1/3$ but the second Kasner condition would not be satisfied since $(p_1)^2 + (p_2)^2 + (p_3)^3 = 1/3 \neq 1$. We thus conclude that isotropic expansion or contraction is not allowed. Moreover at least one Kasner exponent is always negative (except when one single exponent is equal to one and the two others 0). Since the volume of the spatial slice is given by

$$\sqrt{|g|} = t^{p_1+p_2+p_3} = t,$$

it increases (decreases) like $t$ despite the fact that at least one direction is contracting (expanding).

What about the (isotropic) Friedmann-Robertson metric? The important point is that only in presence of matter can space expand or contract isotropically. This is the reason why we added matter to gravity to compute the evolution of a torus given in (see Section 2.3.2).

# Appendix C

# Representation Theory and Weyl Algebra

In this section we are interested in a few general considerations which are important to understand the difference between loop quantum cosmology and 'standard' quantization of cosmology à la Wheeler-DeWitt. We will introduce the Stone-von Neumann theorem and explain why there is a difference between these two quantum cosmologies. Further details can be found in e.g. [24, 33, 88].

## C.1    General Considerations

We would like to introduce the general concepts leading to a general construction of a Hilbert space. The starting point is the following definition:

**Definition 8.**

1. *An algebra $\mathcal{A}$ is a vector space together with a multiplication map $\mathcal{A} \times \mathcal{A} \to \mathcal{A}$; $(a, a') \mapsto aa'$ which is associative and distributive.*

2. *An algebra $\mathcal{A}$ is Abelian if all elements commute with each other and unital if it has a unit element.*

3. *An involution on $\mathcal{A}$ is a map $* : \mathcal{A} \to \mathcal{A}$;    $a \mapsto a^*$ satisfying*

    - *$(za + z'b)^* = \bar{z}a^* + \bar{z}'b^*$,*
    - *$(ab)^* = b^*a^*$ and*
    - *$(a^*)^* = a$*

    *for all $a, b \in \mathcal{A}$, $z, z' \in \mathbb{C}$.*

4. *An algebra with an involution is called a $*-$algebra.*

5. *A normed algebra $\mathcal{A}$ is equipped with a norm $\|.\| : \mathcal{A} \to \mathbb{R}^+$ satisfying $\|ab\| \leq \|a\|\|b\|$, for all $a, b \in \mathcal{A}$. If $\mathcal{A}$ has an involution we require that $\|a^*\| = \|a\|$ and if it is unital we demand that $\|1\| = 1$.*

6. *A norm induces a metric $d(a, b) = \|a - b\|$ and an algebra $\mathcal{A}$ is called Banach if every Cauchy sequence converges.*

7. *A $C^*-$algebra $\mathcal{A}$ is a Banach algebra with involution and $\|a^*a\| = \|a\|^2$.*

Note that for example $\mathbb{C}$ is a unital, Abelian $C^*$-algebra in the usual metric topology of $\mathbb{R}^2$.

**Definition 9.**

1. *The spectrum $\Delta(\mathcal{A})$ of a $C^*-$algebra is defined as the set of all non-zero *-homomorphisms $\rho : \mathcal{A} \to \mathbb{C}$ satisfying $\rho(ab) = \rho(a)\rho(b)$ and $\rho(a)^{-1} = \rho(a^{-1})$.*

2. *The Gel'fand transform is defined by*

$$\bigvee : \mathcal{A} \to \Delta(\mathcal{A})'$$
$$a \mapsto \check{a}(\rho) := \rho(a),$$

   *where $\Delta(\mathcal{A})'$ is the space of continuous linear functionals on $\Delta(\mathcal{A})$.*

This allows us to use the following theorem

**Theorem 3.** *Every unital abelean $C^*$-algebra $\mathcal{A}$ is isometric isomorph to the space of continous functions $C(\Delta(\mathcal{A}))$. Moreover the spectrum of the algebra is a compact Hausdorff space.*

The spectrum is compact w.r.t. the weak *-topology on $\Delta(\mathcal{A})$, i.e. every net $(\rho^\alpha(a))$ in $\Delta(\mathcal{A})$ converges to $\rho(a)$, for all $a \in \mathcal{A}$. Furthermore, a topological space is Hausdorff if any two distinct points possess disjoint neighborhoods.

Every compact Hausdorff space is also locally compact. This fact allows us to use the following theorem

**Theorem 4** (Riesz-Markov). *Let $X$ be a locally compact Hausdorff space. For any positive linear functional $\Lambda : C_0(X) \to \mathbb{C}$ there is a unique regular measure $\mu$ on $X$ such that*

$$\Lambda(f) = \int_X f(x)d\mu(x),$$

*for all $f \in C_0(X)$.*

Here a positive linear functional $\omega$ is a linear map $\omega : \mathcal{A} \to \mathbb{C}$ which satisfies $\omega(a^*a) \geq 0$ for every $a \in \mathcal{A}$ and is unital if $\omega(e) = 1$, where $e$ is the unit element of $\mathcal{A}$. Such a functional is called a state and can be used to define a sesquilinear form

$$\langle a, b \rangle := \omega(a^*b),$$

for all $a, b \in \mathcal{A}$. In general this sesquilinear form is not necessarily positive definite. However, as we are interested in LQC we will assume that $\langle \cdot, \cdot \rangle$ is positive definite.

**Definition 10.** *A representation of $\mathcal{A}$ is a pair $(\mathcal{H}, \pi)$ consisting of a Hilbert space $\mathcal{H}$ and a *-homomorphism $\pi : \mathcal{A} \to L(\mathcal{H})$ into the algebra of linear operators on $\mathcal{H}$ satisfying $\pi(za + z'b) = z\pi(a) + z'\pi(b)$, $\pi(ab) = \pi(a)\pi(b)$ and $\pi(a^*) = [\pi(a)]^\dagger$ where $^\dagger$ denotes the adjoint in $\mathcal{H}$. The representation is faithful if $Ker(\pi) = \{0\}$, non-degenerate if $\pi(a)\psi = 0$ implies $\psi = 0$, for all $a \in \mathcal{A}$, and cyclic if there exists a normed vector $\Omega \in \mathcal{H}$ such that $\pi(a)\Omega$ is dense in $\mathcal{H}$.*

Now, the key result is a construction named after Gel'fand, Naimark and Segal (GNS):

**Theorem 5** (GNS construction). *Let $\omega$ be a state on a unital \*-algebra $\mathcal{A}$. Then there are GNS data $(\mathcal{H}_\omega, \pi_\omega, \Omega_\omega)$ consisting of a Hilbert space $\mathcal{H}_\omega$, a cyclic representation $\pi_\omega$ of $\mathcal{A}$ and a normed, cyclic vector $\Omega_\omega \in \mathcal{H}_\omega$ such that*

$$\omega(a) = \langle \Omega_\omega, \pi_\omega(a)\Omega_\omega \rangle_{\mathcal{H}_\omega}. \tag{C.1}$$

*Moreover the GNS data are uniquely determined by Eq. (C.1) up to unitary equivalence, i.e. if $(\mathcal{H}'_\omega, \pi'_\omega, \Omega'_\omega)$ are another GNS data then the operator $U : \mathcal{H}_\omega \to \mathcal{H}'_\omega$ defined by $U\pi_\omega(a)\Omega_\omega = \pi'_\omega(a)\Omega'_\omega$ is unitary.*

## C.2   Weyl Algebra

The general considerations of the last section are a powerful tool to build a cyclic representation from a state on a \*-algebra. On the other hand there are (in general) infinitely many states such that additional physical assumptions have to be made. For example let us consider the Weyl algebra of quantum mechanics generated by $(a, b \in \mathbb{R})$:

$$U(a) := \exp(iaq/\hbar) \quad \text{and} \quad V(b) = \exp(-ibp/\hbar) \tag{C.2}$$

satisfying

$$U(a)U(a') = U(a + a'), \quad V(b)V(b') = V(b + b'), \quad V(b)U(a) = e^{iab/\hbar}U(a)V(b),$$
$$U(a)^* = U(a^\dagger) \quad \text{and} \quad V(b)^* = V(b^\dagger).$$

We need the following definition

**Definition 11.** *Let $x_n$ be a sequence in a topological vector space $X$. Then $x_n$ converges weakly to $x$ or $x_n \xrightarrow{w} x$ if*

$$\phi(x_n) \xrightarrow{(n\to\infty)} \phi(x)$$

*for all $\phi \in X^*$.*

In order to study the uniqueness of representations of the Weyl algebra we need the following theorem

**Theorem 6** (Stone-von Neumann). *The only irreducible and weakly continuous representation of the Weyl algebra (C.2) is the Schrödinger representation on $\mathcal{H} := L^2(\mathbb{R}, dx)$ defined by*

$$[\pi(U(a))\psi](x) = \exp(iaq/\hbar)\psi(x) \quad \text{and} \quad [\pi(V(b))\psi](x) = \psi(x + b).$$

*Irreducible means that every vector $\psi$ is cyclic.*

In this specific case weak continuity means that $\lim_{a\to 0}\langle \psi, \pi(U(a))\psi' \rangle = \langle \psi, \psi' \rangle$ for all $\psi, \psi' \in \mathcal{H}$. The last theorem states for instance that the Schrödinger representation is unitarily equivalent to the Heisenberg representation.

Given a finite number of degrees of freedom, is it possible to construct an inequivalent representation? The answer is affirmative if we drop the assumption of weak continuity. Define a non-separable Hilbert space $\mathcal{H}_{\text{NS}}$ with the uncountable basis $T_x$, $x \in \mathbb{R}$, and set $\pi(U(a))T_x = T_{x+a}$ and $\pi(V(b))T_x = \exp(ibx)T_x$. The representation $\pi(U(a))$ fails to be weakly continuous because $\lim_{a\to 0}\langle T_x, \pi(U(a))T_x \rangle = \lim_{a\to 0} \delta_{x,x+a} = 0 \neq \langle T_x, T_x \rangle = 1$.

**Definition 12.** *$U(t)$ is a weakly continuous, one-parameter group of unitary operators if*

- *For each $t \in \mathbb{R}$ $U(t)$ is a unitary,*

- *$U(s)U(t) = U(s+t)$, for all $s, t \in \mathbb{R}$,*

- *$\lim_{t \to 0} \langle \psi, U(t)\psi' \rangle = \langle \psi, \psi' \rangle$, for all $\psi, \psi' \in \mathcal{H}$.*

**Theorem 7** (Stone). *Let $U(t)$ be a weakly continuous, one-parameter group of unitary operators. Then there exists a self-adjoint operator $\hat{A}$ such that $U(t) = \exp(it\hat{A})$ called the infinitesimal generator of the group.*
*Conversely, let $\hat{A}$ be a self-adjoint operator. Then $U(t) = \exp(it\hat{A})$, $t \in \mathbb{R}$, is a strongly continuous one-parameter family of unitary operators.*

The implication of this theorem is that no such self-adjoint operator exists if the one-parameter group is not weakly continuous. In the example given above where the representation $\pi(U(a))$ failed to be weakly continuous there is no well defined operator $\hat{x}$ on $\mathcal{H}_{\mathrm{NS}}$.

The construction given in this appendix is very important for the rest of this thesis because one representation of the Weyl operators in LQC also fails to be weakly continuous such that a unitarity inequivalent representation is found. *The physical reason behind this is that space in LQG is quantized so there is no infinitesimal generator of translations.* Such representations are also called polymer representations to stress the discrete character of space. A neat example of a polymer quantization of simple systems such as the free particle or the oscillator can be found in [37]. In such a case dynamics is governed by a difference operator rather than a differential operator.

# Appendix D

# Almost Periodic Functions and the Bohr Compactification

**Definition 13.**

1. *Let $n \in \mathbb{Z}$. A trigonometric polynomial of degree $N \in \mathbb{N}$ is defined as*

$$T(x) = \sum_{n=-N}^{N} a_n e^{inx}; \quad x \in \mathbb{R}.$$

*Let $Trig(\mathbb{R})$ be the \*-algebra of trigonometric polynomials.*

2. *Let $k \in \mathbb{R}$ and define the periodic functions of period $2\pi/k$ by*

$$T_k : \mathbb{R} \to \mathcal{C}; \quad x \mapsto \exp(ikx).$$

*The algebra $\mathcal{C}$ of almost periodic functions is the finite complex linear space of the functions $T_k$:*

$$f = \sum_{I=1}^{N} z_I T_{k_I}, \quad k_I \in \mathbb{R} \quad \text{and} \quad z_I \in \mathbb{C}.$$

*They form a \*$-$algebra since $T_k T_{k'} = T_{k+k'}$ and $\overline{T_k} = T_{-k}$.*

3. *Let $\bar{\mathcal{C}}$ be the closure of $\mathcal{C}$ in the supremum norm, which is an Abelian $C^*-$algebra.*

Since $\mathbb{Q}$ is dense in $\mathbb{R}$ for every $\epsilon > 0$ and $f = \sum_{I=1}^{N} z_I T_{k_I}$ as defined in Definition 13 there is a $q_I = m_I/n_I$, $0 \neq n_I, m_I \in \mathbb{Z}$ such that $|k_I - q_I| < \epsilon$ and such that $f$ behaves as if it were periodic with period $2\pi n_1 \ldots n_N$ for sufficiently small range of $x$. It is only truly periodic if the $k_I$ are rationally dependend, i.e. $\sum_{I=1}^{N} q_I k_I = 0$ implies $q_1 = \ldots = q_N = 0$ for $q_I \in \mathbb{Q}$. Figure D.1 shows the almost periodic function $f = \exp(i\sqrt{2}x) + \exp(2ix)$ for $\epsilon = 0.1$ (left panel) and $\epsilon = 0.05$ (right panel). This function is clearly not periodic because it has the value 2 only for $x = 0$.

Thus, the functions $\mathcal{N}_\mu(c)$, $\mu \in \mathbb{R}$, form an Abelian, unital $C^*$-algebra (upon completion in the supremum norm). This allows us to use the powerfull tools described in Appendix C. Thus, applied to the almost periodic functions we have

**Definition 14.** *The Bohr compactification $\bar{\mathbb{R}}_B$ of the real line $\mathbb{R}$ is defined as the spectrum of the abelean unital $C^*$-algebra $\bar{\mathcal{C}}$, i.e. $\bar{\mathbb{R}}_B := \Delta(\bar{\mathcal{C}})$.*
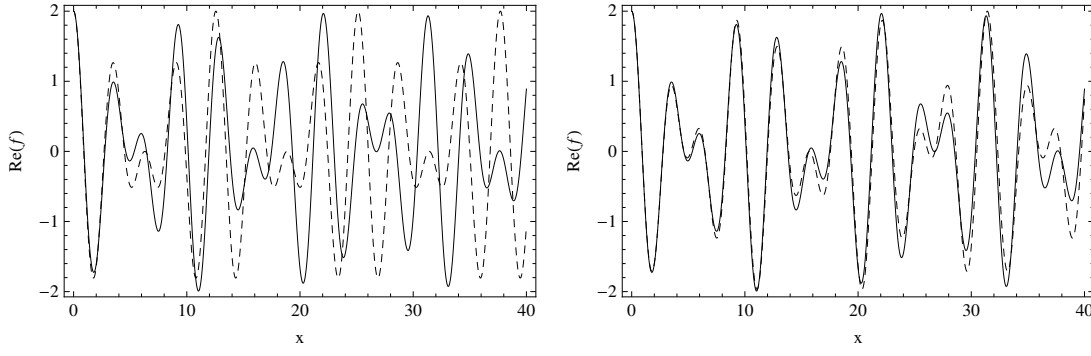
Figure D.1: Comparison between an almost periodic function given by $f = \exp(i\sqrt{2}x) + \exp(2ix)$ (solid line) and its periodic approximation (dashed line). Notice that contrary to the periodic approximations $f$ only reaches the value 2 once at $x = 0$. *Left panel*: The required precision is $\epsilon = 0.1$ such that $q = 3/2$ or $|\sqrt{2} - 3/2| = 0.086 < \epsilon$. The period of the approximation is $4\pi$. *Right panel*: The required precision is $\epsilon = 0.05$ such that $q = 7/5$, the period is $10\pi$.

As such, the space $\bar{\mathbb{R}}_B$ can be seen as the quantum configuration space (point 2 in Section 3.2) with the homomorphisms $\rho : \bar{\mathcal{C}} \to \mathbb{C}$; $T_k \mapsto \rho(T_k)$ as elements. In order to see that this space is much larger than the classical configuration space $\mathbb{R}$ let us rewrite $\rho$ as $X(k) = \rho(T_k)$. Since $\rho$ is an homomorphism $X$ fulfills the conditions

$$X(k)X(k') = X(k + k'), \quad \overline{X(k)} = X(-k) \tag{D.1}$$

and $|X(k)|^2 = 1$. Thus $X$ is an homomorphism from $\mathbb{R}$ to the group $U(1)$, i.e. $X \in \mathrm{Hom}(\mathbb{R}, U(1))$ which doesn't need to be continuous. However, if $X$ is once differentiable a differentiation of the first condition in Eq. (D.1) with $k' = 0$ leads to the differential equation $X'(k) = X'(0)X(k)$ with solution $X(k) = \exp(ikx)$ for some $x \in \mathbb{R}$. Thus if we write $X(k) = g_k(x)$ we see that $\mathbb{R} \subset \bar{\mathbb{R}}_B$.

A general element $X(k) \in \mathrm{Hom}(\mathbb{R}, U(1))$ is given by $X(k) = \exp(if(x))$ where (modulo $2\pi$)

$$f(k + k') = f(k) + f(k') \quad \text{and} \quad f(-k) = -f(k).$$

However this requirement lacks the scalar multiplication $f(\lambda k) = \lambda f(k)$ in order for $f(k)$ to be a linear function. This is the reason why it allows for the construction of functions $f(k)$ which are discontinuous on a dense subset of $\mathbb{R}$ (see [104] for an explicit example). We conclude that $\bar{\mathbb{R}}_B$ is much larger than $\mathbb{R}$ with typical elements consisting of everywhere discontinuous homomorphisms $\mathbb{R} \to U(1)$. On the other hand the image of $\mathbb{R}$ in $\bar{\mathbb{R}}_B$ consists only of smooth homomorphisms.

From Theorem 3 we conclude that the space $\bar{\mathbb{R}}_B$ is a compact Hausdorff space and every elements $\check{T}_k$ is continuous. Furthermore Theorem 4 ensures that, given a positive linear functional $\Lambda \in C(\bar{\mathbb{R}}_B)$, there exists a regular measure $\mu_0$ such that

$$\Lambda(\check{T}_k) = \delta_{\mu,0}, \tag{D.2}$$

where $\delta$ is the Kronecker delta. This functional defines a scalar product via:

$$\langle \check{T}_k, \check{T}_{k'} \rangle := \Lambda(\overline{\check{T}_k}\check{T}_{k'}) = \Lambda(\check{T}_{k'-k}) = \delta_{k'-k,0} = \delta_{k,k'} \tag{D.3}$$

and a norm

$$\|f\|_{L^2} := \sqrt{\langle f, f \rangle}.$$

A Cauchy completion with this norm leads to the Hilbert space $L^2(\bar{\mathbb{R}}_B, d\mu_0)$ where the measure is defined by Eq. (D.2). The meaning of Eq. (D.3) is that the elements $\check{T}_k$ form an orthonormal basis in $L^2(\bar{\mathbb{R}}_B, d\mu_0)$. Furthermore it can be proven that the measure $\mu_0$ can also be considered as a Haar measure on $\mathbb{R}$ via

$$\mu_B(f) := \lim_{T \to \infty} \frac{1}{2T} \int_{-T}^{T} f(x)dx,$$

where $f$ is an element of the $^*$−algebra $\mathcal{C}$ (see [104] for further details).

**Theorem 8.** *An almost periodic function is bounded i.e., there exists a constant $C = C(f)$ such that*

$$|f(x)| \le C \quad \text{for} \quad x \in \mathbb{R}.$$

As a consequence of this theorem, if $f(x)$ is almost periodic, so is $(f(x))^2$ and if $|f(x)| > 0$ for all $x \in \mathbb{R}$, then $1/f(x)$ is also almost periodic. Furthermore, as $\mathcal{C}$ is an algebra, a product and a sum of almost periodic functions is almost periodic.

## D.1   Differential Operators in Spaces of Almost Periodic Functions

In this section we give a brief review of the main results given in [94, 95]. We need the following definintion:

**Definition 15.** *The Sobolev space $H^1(\bar{\mathbb{R}}_B)$ is given by the completion of the space of trigonometric polynomials $\mathrm{Trig}(\mathbb{R})$ (see Definition 13) in the Sobolev norm*

$$\|f\|_{H^1}^2 = \|f\|_{L^2(\bar{\mathbb{R}}_B)}^2 + \|f'\|_{L^2(\bar{\mathbb{R}}_B)}^2$$

.

In other words, $H^1(\bar{\mathbb{R}}_B)$ consists of all almost periodic functions $f \in \mathcal{C}$ such that $f' \in \mathcal{C}$.

**Theorem 9.** *Let the differential operator $\hat{p} := -i\frac{d}{d\xi}$ on $L^2(\bar{\mathbb{R}}_B)$ have the domain of definition $\mathrm{Trig}(\mathbb{R})$. Then its closure has the domain $H^1(\bar{\mathbb{R}}_B)$. The adjoint operator to $\hat{p}$ on $L^2(\bar{\mathbb{R}}_B)$ has also the domain $H^1(\bar{\mathbb{R}}_B)$ and coincides with $\hat{p}^+$ on it. Since $\hat{p} = \hat{p}^+$, $\hat{p}$ is essentially self-adjoint on $\mathrm{Trig}(\mathbb{R})$ [94, 95].*

A proof can be found in [95].

# Appendix E

# Solutions of Eq. $(3.22)$

In this Appendix we show that the functions $f_\lambda$ (see Eq. (3.28)) solve the partial differential equation (3.22).

We first note that the function $\Omega_1(\sin\theta\tan(\xi/2))$ is annihilated by $\hat{A}$ because

$$-i\cos\theta\frac{\partial\Omega_1}{\partial\xi} + i\frac{\sin\theta}{\sin\xi}\frac{\partial\Omega_1}{\partial\theta} \equiv 0$$

for any $\Omega_1 \in C^1$. Furthermore, $\sqrt{\tan(\xi/2)}$ is also annihilated by $\hat{A}$ because

$$-i\cos\theta\frac{\partial\sqrt{\tan(\xi/2)}}{\partial\xi} + \frac{i}{2}\frac{\cos\theta}{\sin\xi}\sqrt{\tan(\xi/2)} \equiv 0.$$

The problem is therefore reduced to showing that

$$-i\cos\theta\frac{\partial F(\xi,\theta)}{\partial\xi} + i\frac{\sin\theta}{\sin\xi}\frac{\partial F(\xi,\theta)}{\partial\theta} = \lambda F(\xi,\theta), \tag{E.1}$$

where

$$F(\xi,\theta) = \sqrt{2}\left(i\cos\theta\sin(\xi/2) + \cos(\xi/2)\alpha\right)^{\frac{2\lambda}{\alpha}},$$

where $\alpha = \sqrt{1 + \sin^2\theta\tan^2(\xi/2)}$. The derivation of $F$ along $\xi$ is given by

$$\partial_\xi F = 2\lambda F\left[ -\frac{\log(\sqrt{2}i\cos\theta\sin(\xi/2) + \sqrt{2}\cos(\xi/2)\alpha)\partial_\xi\alpha}{\alpha^2} \right.$$
$$\left. +\frac{\frac{i\cos\theta\cos(\xi/2)}{\sqrt{2}} - \frac{\sin(\xi/2)\alpha}{\sqrt{2}} + \sqrt{2}\cos(\xi/2)\partial_\xi\alpha}{\sqrt{2}\alpha(i\cos\theta\sin(\xi/2) + \cos(\xi/2)\alpha)} \right]$$

and along $\theta$ by

$$\partial_\theta F = 2\lambda F\left[ -\frac{\log(\sqrt{2}i\cos\theta\sin(\xi/2) + \sqrt{2}\cos(\xi/2)\alpha)\partial_\theta\alpha}{\alpha^2} \right.$$
$$\left. +\frac{-i\sin\theta\sin(\xi/2) + \cos(\xi/2)\partial_\theta\alpha}{\alpha(i\cos\theta\sin(\xi/2) + \cos(\xi/2)\alpha)} \right]$$

Upon insertion of the last two equations into Eq. (E.1) we see that the first term in the square brackets of $\partial_\xi F$ cancels the first term of $\partial_\theta F$ because $\partial_\xi\alpha = \frac{\tan\theta}{\sin\xi}\partial_\theta\alpha$. Thus the

left-hand side of Eq. (E.1) simplifies to

$$\lambda F \frac{\cos^2\theta \cos(\xi/2) + \frac{\sin^2\theta}{\cos(\xi/2)} + i\cos\theta \sin(\xi/2)\alpha}{\alpha(i\cos\theta \sin(\xi/2) + \cos(\xi/2)\alpha)},$$

which, upon insertion of the definition of $\alpha$, reduces to

$$\lambda F(\xi, \theta).$$

We have thus shown that $F(\xi, \theta)$ solves Eq. (E.1) and that

$$\hat{A}f_\lambda = \lambda f_\lambda$$

as

$$f_\lambda = \sqrt{\tan(\xi/2)} F(\xi, \theta)\Omega_1(\sin\theta \tan(\xi/2)).$$

$\square$

# Bibliography

[1] Abdo A A *et al.* A limit on the variation of the speed of light arising from quantum gravity effects. *Nature*, 461:1176, 2009.

[2] Albert J *et al.* Probing quantum gravity using photons from a Mkn 501 flare observed by MAGIC. 2007, arXiv:astro-ph/0708.2889.

[3] Amelino-Camelia G. Enlarged bound on the measurability of distances and quantum $\kappa$-Poincaré group. *Phys. Lett. B*, 392:283, 1997.

[4] Amelino-Camelia G. Relativity in spacetimes with short-distance structure governed by an observer-independent (Planckian) length scale. *Int. J. Mod. Phys. D*, 11:35, 2002.

[5] Amelino-Camelia G. Proposal of a second generation of quantum-gravity-motivated Lorentz-symmetry tests: Sensitivity to effects suppressed quadratically by the Planck scale. *Int. J. Mod. Phys. D*, 12:1633, 2003.

[6] Amelino-Camelia G, Ellis J, Mavromatos N E, Nanopoulos D V, and Sarkar S. Tests of quantum gravity from observations of big gamma-ray bursts. *Nature*, 393:763, 1998.

[7] Arnowitt R, Deser S, and Misner CW. *Gravitation: An introduction to current research*. New York: Wiley, 1962.

[8] Ashtekar A. New variables for classical and quantum gravity. *Phys. Rev. Lett.*, 57:2244, 1986.

[9] Ashtekar A. New Hamiltonian formulation of general relativity. *Phys. Rev. D*, 36:1587, 1987.

[10] Ashtekar A and Bojowald M. Quantum geometry and the Schwarzschild singularity. *Class. Quantum Grav.*, 23:391, 2006.

[11] Ashtekar A, Bojowald M, and Lewandowski J. Mathematical structure of loop quantum cosmology. *Adv. Theor. Math. Phys.*, 7:233, 2003.

[12] Ashtekar A and Lewandowski J. Background independent quantum gravity: A status report. *Class. Quantum Grav.*, 21:R53, 2004.

[13] Ashtekar A, Pawlowski T, and Singh P. Quantum nature of the Big Bang: An analytical and numerical investigation. *Phys. Rev. D*, 73:124038, 2006.

[14] Ashtekar A, Pawlowski T, and Singh P. Quantum nature of the Big Bang: Improved dynamics. *Phys.Rev. D*, 74:084003, 2006.

[15] Ashtekar A and Samuel J. Bianchi cosmologies: the role of spatial topology. *Class. Quantum Grav.*, 8:2191, 1991.

[16] Aurich R. A spatial correlation analysis for a toroidal universe. *Class. Quantum Grav.*, 25:225017, 2008.

[17] Aurich R, Janzer H S, Lustig S, and Steiner F. Do we live in a 'small universe'. *Class. Quantum Grav.*, 25:125006, 2008.

[18] Aurich R, Lustig S, and Steiner F. CMB anisotropy of spherical spaces. *Class. Quantum Grav.*, 22:3443, 2005.

[19] Aurich R, Lustig S, and Steiner F. CMB anisotropy of the Poincaré dodecahedron. *Class. Quantum Grav.*, 22:2061, 2005.

[20] Aurich R, Lustig S, and Steiner F. Hot pixel contamination in the CMB correlation function. 2009, arXiv:0903.3133.

[21] Baez J and Muniain J P. *Gauge fields, knots and gravity.* Singapore: World Scientific, 1994.

[22] Band D L *et al.* BATSE observations of gamma-ray burst spectra. i - spectral diversity. *ApJ*, 413:281, 1993.

[23] Band D L *et al.* Analysis of burst observations by GLAST's LAT detector. *American Institute of Physics Conference Series*, 727:692, 2004.

[24] Blackadar B. *Operator Algebras.* Berlin: Springer-Verlag, 2006.

[25] Bojowald M. Loop quantum cosmology i: Kinematics. *Class. Quantum Grav.*, 17:1489, 2000.

[26] Bojowald M. Loop quantum cosmology ii: Volume operator. *Class. Quantum Grav.*, 17:1509, 2000.

[27] Bojowald M. Isotropic loop quantum cosmology. *Class. Quantum Grav.*, 19:2717, 2002.

[28] Bojowald M. Homogeneous loop quantum cosmology. *Class. Quantum Grav.*, 20:2595, 2003.

[29] Bojowald M. Loop quantum cosmology. *Living Re. Relativity*, 11:4, 2008.

[30] Bojowald M and Kastrup H A. Symmetry reduction for quantized diffeomorphism-invariant theories of connections. *Class. Quantum Grav.*, 17:3009, 2000.

[31] Bojowald M and Swiderski R. The volume operator in spherically symmetric quantum geometry. *Class. Quantum Grav.*, 21:4881, 2004.

[32] Bolmont J, Jacholkowska A, Atteia J, Piron F, and Pizzichini G. Study of time lags in HETE-2 gamma-ray bursts with redshift: search for astrophysical effects and quantum gravity signature. *ApJ*, 676:523, 2008.

[33] Bratelli O and Robinson D W. *Operator Algebras and Quantum Statistical Mechanics.* New York: Springer, 1979.

98

[34] Brodbeck O. On symmetric gauge fields for arbitrary gauge and symmetry groups. *Helv. Phys. Acta*, 69:321, 1996.

[35] Caillerie S *et al.* A new analysis of the Poincaré dodecahedral space model. *A & A*, 476:691C, 2007.

[36] Chiou D-W. Loop quantum cosmology in bianchi type i models: Analytical investigation. *Phys.Rev. D*, 75:024029, 2007.

[37] Corichi A, Vukasinac T, and Zapata J A. Polymer quantum mechanics and its continuum limit. *Phys.Rev. D*, 76:044016, 2007.

[38] D'Avanzo P *et al.* Discovery of the optical afterglow of XRF 040812: VLT and Chandra observations. *Nuovo Cimento B*, 121:1467, 2006.

[39] de Luca A *et al.* XMM-Newton and VLT observations of the afterglow of GRB 040827. *A & A*, 440:85, 2005.

[40] Ellis J, Farakos K, Mavromatos N E, Mitsou V A, and Nanopoulos D V. Astrophysical probes of the constancy of the velocity of light. *ApJ*, 535:139, 2000.

[41] Ellis J, Mavromatos N E, Nanopoulos D V, and Sakharov A S. Quantum-gravity analysis of gamma-ray bursts using wavelets. *A & A*, 402:409, 2003.

[42] Ellis J, Mavromatos N E, Nanopoulos D V, Sakharov A S, and Sarkisyan E K G. Robust limits on Lorentz violation from gamma-ray bursts. *Astropart. Phys.*, 25:402, 2006.

[43] Ellis J, Mavromatos N E, Nanopoulos D V, Sakharov A S, and Sarkisyan E K G. Erratum (astro-ph/0510172): Robust limits on Lorentz violation from gamma-ray bursts. 2007, arXiv:astro-ph/0712.2781.

[44] Fagundes H V. Relativistic cosmologies with closed, locally homogeneous spatial sections. *Phys. Rev. Lett.*, 54:1200, 1985.

[45] Fagundes H V. Closed spaces in cosmology. *Gen. Rel. Grav.*, 24:199, 1992.

[46] Fan Y-Z, Wei D-M, and Xu D. Gamma-ray burst UV / optical afterglow polarimetry as a probe of quantum gravity. *Mon. Not. Roy. Astron. Soc.*, 376:1857, 2007.

[47] Fatkhullin T A, Sokolov V V, Castro-Tirado A J, Komarova V N, and Lebedev V S. Early-time spectroscopy of the GRB 041218 optical transient with 6-m telescope. *www.ioffe.ru/astro/NS2005/ABSTRACTS/fatkhullin.ps*, 2005.

[48] Fenimore E E, in't Zand J J M, Norris J P, Bonnell J T, and Nemiroff R J. Gamma-ray burst peak duration as a function of energy. *ApJL*, 448:L101, 1995.

[49] Fermi Science Support Center. *http://fermi.gsfc.nasa.gov/ssc/data/access/*.

[50] Barbero G. Real Ashtekar variables for Lorentzian signature space-times. *Phys. Rev. D*, 51:5507, 1995.

[51] Geroch R. The domain of dependence. *Journ. Math. Phys.*, 11:437, 1970.

[52] GLAST LAT Performance. *http://www-glast.slac.stanford.edu/software/IS/glast_lat_performance.htm*.

[53] GLAST Science Support Center. *http://glast.gsfc.nasa.gov/gssc*.

[54] Immirzi G. Real and complex connections for canonical gravity. *Class. Quantum Grav.*, 14:L177, 1987.

[55] Jacob U and Piran T. Lorentz-violation-induced arrival delays of cosmological particles. *J. Cosmol. Astropart. Phys.*, 2008.

[56] Jacobson T, Liberati S, and Mattingly D. A strong astrophysical constraint on the violation of special relativity by quantum gravity. *Nature*, 424:1019, 2003.

[57] Jakobsson P *et al.* GRB coordinates network. *GRB Coordinates Network*, 4015, 2005.

[58] Kamke E. *Diffenrentialgleichungen, Lösungsmethoden und Lösungen*, volume 2. Stuttgart: B.G. Teubner, 1979.

[59] Kobayashi S and Nomizu K. *Foundations of Differential Geometry*, volume 2. John Wiley & Sons, New York, 1963.

[60] Koike T, Tanimoto M, and Hosoya A. Compact homogeneous universes. *J. Math. Phys.*, 35:4855, 1994.

[61] Komatsu E *et al.* Five-year Wilkinson Microwave Anisotropy Probe (WMAP) observations: Cosmological interpretation. 2008, arXiv:0803.0547.

[62] Kowalski-Glikman J. *Towards Quantum Gravity*. Berlin: Springer Verlag, 2005.

[63] Kowalski-Glikman J and Nowak S. Doubly special relativity theories as different bases of $\kappa$–Poincaré algebra. *Phys. Lett. B*, 539:126, 2002.

[64] Lamon R. GLAST and Lorentz violation. *J. Cosmol. Astropart. Phys.*, JCAP08:022, 2008.

[65] Lamon R, Produit N, and Steiner F. Study of lorentz violation in INTEGRAL gamma-ray bursts. *Gen. Rel. Grav.*, 40:1731, 2008.

[66] Lebrun F *et al.* ISGRI: The INTEGRAL Soft Gamma-Ray Imager. *A & A*, 411:L141, 2003.

[67] Magueijo J and Smolin L. Generalized Lorentz invariance with an invariant energy scale. *Phys. Rev. D*, 67:044017, 2002.

[68] Magueijo J and Smolin L. Lorentz invariance with an invariant energy scale. *Phys. Rev. Lett.*, 88:190403, 2002.

[69] McGlynn S *et al.* INTEGRAL and XMM-Newton observations of the low-luminosity and X-ray-rich burst GRB 040223. *Nuovo Cimento C*, 28:481, 2005.

[70] Modesto L. Disappearance of black hole singularity in quantum gravity. *Phys. Rev. D*, 70:124009, 2004.

[71] Modesto L. The Kantowski-Sachs space-time in loop quantum gravity. *Int. J. Theor. Phys.*, 45:2235, 2006.

[72] Modesto L. Loop quantum black hole. *Class. Quantum Grav.*, 23:5587, 2006.

100

[73] Moran L *et al.* INTEGRAL and XMM-Newton observations of GRB 040106. *A & A*, 432:467, 2005.

[74] Nakahara M. *Geometry, topology and physics.* Bristol: Institute of Physics Publishing, 2003.

[75] Nash C and Senn S. *Topology and geometry for physicists.* Academic Press, 1983.

[76] Norris J P, Bonnell J T, Marani G F, and Scargle J D. GLAST, GRBs and quantum gravity. *International Cosmic Ray Conference*, 4:20, 1999.

[77] Norris J P, Marani G F, and Bonnell J T. Connection between energy-dependent lags and peak luminosity in gamma-ray bursts. *ApJ*, 534:248, 2000.

[78] Norris J P *et al.* Attributes of pulses in long bright gamma-ray bursts. *ApJ*, 459:393, 1996.

[79] Omedei N and GLAST/LAT GRB Science Group. The GLAST mission, LAT and GRBs. 2006, arXiv:astro-ph/0603762.

[80] Omodei N *et al.* GRB simulations in GLAST. *American Institute of Physics Conference Series*, 906:1, 2007.

[81] Pelangeon A and Atteia J-L. *GRB Coordinates Network*, 4704:1, 2006.

[82] Perelman G. The entropy formula for the Ricci flow and its geometric applications. 2002, arXiv:math.DG/0211159.

[83] Perelman G. Finite extinction time for the solutions to the Ricci flow on certain three-manifolds. 2003, arXiv:math.DG/0307245.

[84] Perelman G. Ricci flow with surgery on three-manifolds. 2003, arXiv:math.DG/0303109.

[85] Piran T. Gamma ray bursts as probes of quantum gravity. 2004, arXiv:astro-ph/0407462v1.

[86] Prochaska J X, Chen H-W, Bloom J S, and Stephens A. *GRB Coordinates Network*, 2005.

[87] Prochaska J X, Ellison S, Foley R J, Bloom J S, and Chen H-W. *GRB Coordinates Network*, 2005.

[88] Reed S and Simon B. *Functional Analysis*, volume I. San Diego: Academic Press, 1980.

[89] Roberts J E. *J. Math. Phys.*, 7:1097, 1966.

[90] Roberts J E. *Commun. Math. Phys.*, 3:98, 1966.

[91] Rovelli C. *Quantum Gravity.* Cambridge: Cambridge University Press, 2004.

[92] Ryan M P and Shepley L C. *Homogeneous Relativistic Cosmologies.* Princeton: Princeton University Press, 1975.

[93] Scott P. The geometries of 3-manifolds. *Bull. London Math. Soc.*, 15:401, 1983.

[94] Shubin M A. Differential and pseudodifferential operators in spaces of almost periodic functions. *Math. USSR Sbornik*, 24:547, 1974.

[95] Shubin M A. Almost periodic functions and partial differential operators. *Russian Math. Surveys*, 33:1, 1978.

[96] Singer I M. Infinitesimally homogeneous spaces. *Comm. Pure Appl. Math.*, 13:685, 1960.

[97] Straumann N. *General Relativity: With Applications to Astrophysics*. Springer-Verlag, 2004.

[98] Straumann N. *Relativistische Quantentheorie*. Springer-Verlag, 2005.

[99] 't Hooft G. A property of electric and magnetic flux in non-abelian gauge theories. *Nucl. Phys. B*, 153:141, 1979.

[100] Tanimoto M, Koike T, and Hosoya A. Dynamics of compact homogeneous universes. *J. Math. Phys.*, 38:350, 1997.

[101] Thiemann T. Anomaly-free formulation of non-perturbative, four-dimensional Lorentzian quantum gravity. *Phys. Lett. B*, 380:257, 1998.

[102] Thiemann T. Qsd v: Quantum gravity as the natural regulator of matter quantum field theories. *Class. Quantum Grav.*, 15:1281, 1998.

[103] Thiemann T. Quantum spin dynamics (qsd). *Class. Quantum Grav.*, 15:839, 1998.

[104] Thiemann T. *Modern Canonical Quantum General Relativity*. Cambridge: Cambridge University Press, 2007.

[105] Thurston W. Three-dimensional manifolds, Kleinian groups and hyperbolic geometry. *Bull. Amer. Math. Soc.*, 6(3):357, 1982.

[106] Thurston W. *Three-dimensional geometry and topology*, volume 1. Princeton: Princeton University Press, 1997.

[107] Velhinho J M. The quantum configuration space of loop quantum cosmology. *Class. Quantum Grav.*, 24:3745, 2007.

[108] Wald R M. *General relativity*. Chicago: The University of Chicago Press, 1984.

[109] Watson D, Reeves J N, Hjorth J, Jakobsson P, and Pedersen K. Delayed soft X-ray emission lines in the afterglow of GRB 030227. *ApJL*, 595:L29, 2003.

[110] Watson D *et al.* A very low luminosity x-ray flash: XMM-Newton observations of GRB 031203. *ApJL*, 605:L101, 2004.

[111] Winkler C *et al.* The INTEGRAL mission. *A & A*, 411:L1, 2003.

[112] Wolf J A. *Spaces of Constant Curvature*. Boston: Publish Or Perish, 1974.

[113] Yao W-M *et al.* Review of particle physics. *J. Phys. G*, 33:1, 2006.

[114] Zeidler E. *Quantum Field Theory II*. Springer-Verlag, 2009.

# Publication List

- Lamon R and Woehr A, Quintessence and (Anti-)Chaplygin Gas in Loop Quantum Cosmology, *Phys. Rev. D* 81:024026, 2010

- Lamon R, Loop Quantum Cosmology on a Torus, `arXiv:0909.2578`, 2009.

- Lamon R, Glast and Lorentz Violation, *JCAP* 0808:022, 2008.

- Lamon R, Produit N and Steiner F, Study of Lorentz violation in INTEGRAL gamma-ray bursts, *Gen. Rel. Grav.* 40:1731, 2008.

- Lamon R and Durrer R, Constraining Gravitino Dark Matter with the Cosmic Microwave Background, *Phys. Rev. D* 73:023507, 2006.

# Talks & Posters

| | |
|---|---|
| 2004 | Talk at the ETHZ on spontaneous symmetry breaking and the Higgs mechanism |
| 2004 | Talk at the ETHZ on path integrals and decoherence |
| 2004 | Talk at the ETHZ on root systems and Dynkin diagrams |
| 2006 | Talk at the University of Ulm on gravitino dark matter and the CMB |
| 2007 | Attended the conference of the German Physical Society in Heidelberg, Germany |
| 2007 | Invited talk at the INTEGRAL Science Data Center in Versoix, Switzerland |
| 2008 | Three lectures on loop quantum cosmology at Ulm University |
| 2008 | Talk at the conference of the German Physical Society in Freiburg, Germany |
| 2009 | Talk at the Promotionskolleg of Ulm University |
| 2009 | Talk at the conference Loops09 in Beijing, China |
| 2010 | Poster at the Annual Meeting of the Graduate School in Blaubeuren |

# Curriculum Vitae

## Persönliche Informationen

| | |
|---|---|
| Name: | Raphaël Lamon |
| Geburtsdatum: | 7. Januar, 1982 in Caracas, Venezuela |
| Addresse: | Langweid 1 |
| | 6333 Hünenberg-See |
| | Schweiz |
| E-mail: | raphael.lamon82@googlemail.com |

## Ausbildung

| | |
|---|---|
| ab 2006 | Doktorand an der Universität Ulm, |
| | Institut für Theoretische Physik, Ulm, Deutschland |
| 2005 | Forschungsassistent an der Université de Genève, |
| | Institut de Physique Théorique, Genève, Schweiz |
| 2004-2005 | Diplomarbeit an der Université de Genève, |
| | Institut de Physique Théorique, Genève, Schweiz |
| 2000-2005 | Diplom in Physik an der ETH Zurich, |
| | Departement Physik, Zürich, Schweiz |
| 1998-2000 | Matura an der Kantonsschule Zug, Zug, Schweiz |
| 1990-1998 | Primar- und Sekundarschule in der Schweiz |

## Auszeichnung

| | |
|---|---|
| 2008 | Teilnahme an der 58th Meeting of Nobel Laureates in Lindau |

# Acknowledgment

I would like to thank Prof. Dr. Frank Steiner for giving me the opportunity to work on this thesis, for many helpful discussions, corrections and his support as well. Moreover I'm very thankful for the freedom he gave me to choose any topic related to quantum gravity and also for the pressureless atmosphere which was necessary to learn the difficult mathematical and physical tools in order to generalize loop quantum cosmology to toroidal topologies.

I thank Dr. Nicolas Produit for his help, comments and corrections and also for inviting me to the INTEGRAL Science Data Center in Versoix near Geneva.

I'm also indebted to thank Prof. Dr. Jens Bolte who thoroughly corrected my thesis and asked for more mathematical rigor. I would like to thank Prof. Dr. Wolfgang Arendt for discussions and corrections and Prof. Dr. Martin Plenio for hospitality.

Furthermore I'm thankful to the graduate school "Analysis of Complexity, Information and Evolution" of the Land Baden-Württemberg for the funding of the trip to the conference Loops09 in Beijing and to the conference 'Beyond Einstein' in Mainz.

I would like to thank Ralf Aurich, Martin Bojowald, Sebastian Endres, Holger Janzer, Sven Lustig, Robin Nittka, Eric Sträng and Andreas Wöhr for many fruitful discussions, comments and corrections.

Last but not least I would like to thank my parents Ursula and Paul-Henri, my brother Christophe and my girlfriend Reyna for all their support.

# Erklärung

Ich erkläre hiermit, dass ich die voliegende Dissertation selbstständig verfasst und keine anderen als die angegebenen Quellen und Hilfsmittel verwendet habe.

Ulm, November 2009

Raphaël Lamon